



January 2015

Developing A Heterotypic Cell Culture Model To Determine Vegf Action Of Neural Stem Cell Fate Choice

Stephanie Snyder

[How does access to this work benefit you? Let us know!](#)

Follow this and additional works at: <https://commons.und.edu/theses>

Recommended Citation

Snyder, Stephanie, "Developing A Heterotypic Cell Culture Model To Determine Vegf Action Of Neural Stem Cell Fate Choice" (2015). *Theses and Dissertations*. 1836.
<https://commons.und.edu/theses/1836>

This Thesis is brought to you for free and open access by the Theses, Dissertations, and Senior Projects at UND Scholarly Commons. It has been accepted for inclusion in Theses and Dissertations by an authorized administrator of UND Scholarly Commons. For more information, please contact und.common@library.und.edu.

DEVELOPING A HETEROTYPIC CELL CULTURE MODEL TO DETERMINE
VEGF ACTION ON NEURAL STEM CELL FATE CHOICE

by

Stephanie Danielle Snyder
Bachelor of Arts, Gustavus Adolphus College, 2011
Master of Science, University of North Dakota, 2015

A Thesis
Submitted to the Graduate Faculty

of the

University of North Dakota


In partial fulfillment of the requirements

for the degree of

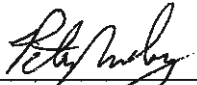
Master of Science in Biology

Grand Forks, North Dakota
August 2015


This thesis, submitted by Stephanie Danielle Snyder in partial fulfillment of the requirements for the Master of Science from the University of North Dakota, has been read by the Faculty Advisory Committee under whom the work has been done, and is hereby approved.



Diane C. Darland, Ph.D




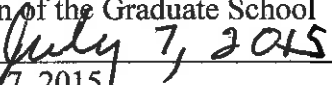
Peter Meberg, Ph.D



Tristan Darland, Ph.D

This thesis is being submitted by the appointed advisory committee as having met all of the requirements of the Graduate School at the University of North Dakota and is hereby approved.



Wayne Swisher
Dean of the Graduate School


July 7, 2015

Copyright 2015 Stephanie Snyder

PERMISSION

Title Developing a heterotypic cell culture model to determine Vegf action on neural stem cell fate choice

Department Biology

Degree Master of Science

In presenting this thesis in partial fulfillment of the requirements for a graduate degree from the University of North Dakota, I agree that the library of this University shall make it freely available for inspection. I further agree that permission for extensive copying for scholarly purposes may be granted by the professor who supervised my thesis work, or in her absence, by the Chairperson of the department of the dean of the Graduate School. It is understood that any copying or publication or other use of this thesis of part thereof for financial gain shall not be allowed without my written permission. It is also understood that due recognition shall be given to me and to the University of North Dakota in any scholarly use which may be made of any material in my thesis.

Stephanie Danielle Snyder
July 7, 2015

TABLE OF CONTENTS

LIST OF FIGURES.....	v
LIST OF TABLES.....	viii
ACKNOWLEDGEMENTS.....	ix
ABSTRACT.....	x
CHAPTER	
I. INTRODUCTION.....	1
II. METHODS.....	19
III. RESULT.....	43
Immortalized neural epithelial cells display comparable morphological features and gene expression to native neural epithelial cells	43
Vascular cells influence gene expression pattern in immortalized neural epithelial cells.....	54
The influence of vascular cells on neural epithelial cells differs with an altered Vegf isoform profile.....	71
DNA methylation in neural stem cell fate choice <i>in vivo</i> and <i>in vitro</i>	88
IV. DISCUSSION.....	105
APPENDICES.....	126
REFERENCES.....	141

LISTS OF FIGURES

Figure	Page
1. Vessel formation via vasculogenesis and angiogenesis.....	3
2. The exon composition of Vegf isoforms leads to differences in protein structure, features, and location in the microenvironment.....	5
3. Angiogenesis of the cortex occurs in a ventral to dorsal fashion correlated with expression of neural transcription factors.....	10
4. Diagram depicting cell division and primitive layer formation from embryonic day 9.5 to 13.5 in mice.....	14
5. Isolation of SSEA-1-enriched NSCs from E13.5 embryonic forebrain.....	23
6. Heterotypic cell culture model used to determine the influence of vascular cells on neural stem cell fate choice.....	28
7. Native and Immortalized SSEA-1-enriched neural epithelial cells display similar gene expression patterns.....	44
8. Immortalized neural epithelial cells exhibit comparable growth patterns and morphology relative to native neural epithelial cells.....	46
9. Wild type immortalized neural epithelial cell populations consist primarily of neural stem cells.....	49
10. SSEA-1 enriched neural epithelial cells exhibit a similar morphology to native neural epithelial cells in coculture with MEFs.....	51
11. Neural stem cells extend processes through porous membrane and can establish contact with MEFs.....	53
12. Immortalized SSEA-1-enriched neural epithelial cells display a shift in gene expression patterns when cocultured with vascular cells.....	55
13. The presence of vascular cells leads to an increase in the mitotic profile displayed by neural epithelial cells.....	56

14. Wild type SSEA-1-enriched neural epithelial cocultured with vascular cells display shifts in expression of genes associated with neural stem cell fate choice.....	59
15. Wild type neural epithelial cells cultured in contacting coculture display a disruption in correlation between Pax6 and Sox2 gene expression	61
16. Contact with vascular cells disrupts the correlation of Pax6 and Id1 in WT neural epithelial cells in contacting coculture.....	63
17. Wild type neural epithelial cells cultured in contacting coculture display a disruption in correlation between Pax6 and Tbr2 gene expression.....	65
18. Wild type neural epithelial cells cocultured with MEFs express all three Vegf isoforms.....	68
19. Vascular cells and immortalized neural epithelial cells display distinct Vegf isoform expression when cocultured.....	70
20. Immortalized neural epithelium derived from Vegf isoform mice show a similar neural stem cell gene expression profile compared to WT.....	72
21. Comparison from a gene-specific perspective reveals clear patterns of NSC genes across genotypes.....	75
22. Native and immortalized neural epithelial cells exhibit distinct Vegf isoform expression profiles.....	78
23. Wild type and Vegf isoform NSCs* exhibit increased migration when cocultured with MEFs.....	80
24. Coculture with MEFs leads to a difference in NSC* total nuclei profiles that varies with Vegf isoform profiles.....	82
25. Expression of Pax6 and Tbr2 correlate in Vegf isoform neural epithelial cultures grown in contact with vascular cells.....	87
26. Wild type and Vegf isoform neural epithelial cells cultured with vascular cells display a positive correlation between Pax6 and Tbr1 gene expression.....	89
27. The proportion of methylation and hydroxymethylation differs in embryonic forebrains with an altered Vegf profile <i>in vivo</i>	91

28. <i>In vivo</i> Pax6 and Id1 gene expression correlates with changes in DNA promoter methylation.....	94
29. Wild type mice display an expanded range of Suz12 positive cells compared to Vegf isoform mice <i>in vivo</i>	97
30. Global methylation and hydroxymethylation was detected <i>in vitro</i> utilizing E13.5 immortalized SSEA-1 enriched neural epithelial cells.....	99
31. Changes in DNA promoter methylation correlate with Pax6 and Id1 gene expression <i>in vitro</i>	101
32. A positive correlation exists between Pax6 and Suz12 in WT and Vegf isoform neural epithelial cells.....	104
33. The <i>in vitro</i> system recaptured the microenvironment present during different stages in cortical development.....	117
34. Vegf isoform neural epithelial cells cultured in contact with vascular cells exhibit a correlation between Pax6 and Sox2 gene expression.....	132
35. Expression of Pax6 and Id1 correlates in Vegf isoform neural epithelial cells grown in contacting coculture with vascular cells.....	133
36. Vegf120 SSEA-1-enriched neural epithelial cells display shifts in expression of genes associated with neural stem cell fate choice when cocultured with vascular cells.....	138
37. Vegf188 SSEA-1-enriched neural epithelial cells cocultured with vascular cells display shifts in expression of genes associated with neural stem cell fate choice.....	139
38. Vegf120/188 SSEA-1-enriched neural epithelial cells cocultured with vascular cells display shifts in expression of genes associated with neural stem cell fate choice.....	140

LIST OF TABLES

Table	Page
1. WT and Vegf isoform neural epithelial cells grown in contacting coculture with vascular cells display expression correlation between Pax6 and genes associated with neural stem and progenitor cells.....	85
2. Sequence for forward and reverse primers used for genotype, qualitative, and quantitative PCRs.....	128
3. Standard PCR protocol for Vegf120 genotyping.....	130
4. Standard PCR protocol for Vegf188 genotyping.....	131
5. The results of an analysis of correlation between Pax6 and Sox2 for immortalized SSEA-1-enriched WT and Vegf isoform neural epithelial cells.....	134
6. The results for an analysis of correlation between Pax6 and Id1 for immortalized SSEA-1-enriched WT and Vegf isoform neural epithelial cells.....	135
7. The results of an analysis of correlation between Pax6 and Tbr2 for immortalized SSEA-1-enriched WT and Vegf isoform neural epithelial cells.	136
8. The results of an analysis of correlation between Pax6 and Tbr1 for immortalized SSEA-1-enriched WT and Vegf isoform neural epithelial cells.....	137

ACKNOWLEDGEMENTS

I wish to express my sincere appreciation to the members of my advisory committee for their guidance and support during my time in the Master's program at the University of North Dakota.

To my mom and dad, who have supported me through it all!

ABSTRACT

Brain development requires tight cell and molecular regulation for proper neural stem cell (NSC) proliferation and differentiation. Increasing interest in NSCs has arisen due to the flexibility inherent within their proliferative capacity and their ability to generate multiple neuronal cell types. Our main focus is on the cortex, the primary integrator for higher order brain function. Cortical NSC proliferation and differentiation occur in concert with blood vessel ingression into the primitive cortex to vascularize the neuroepithelium. One potential influence derived from vascular cells is Vascular endothelial growth factor A (Vegf). Vegf has the ability to regulate both neurogenesis and angiogenesis making it an attractive candidate for a role in regulating NSC fate choice. My hypothesis is that NSCs require vascular cells and Vegf isoforms to regulate their transition from NSC to differentiated neurons and this regulation occurs through epigenetic mechanisms. To address this hypothesis a triculture assay system was used to recapitulate the microenvironment of the early cortical neuroepithelium. I have immortalized neuroepithelium and explored their potential cell fate based on the influence of microvascular cells. The results indicate that NSCs in contact with the microvasculature express neural stem cell (Pax6 & Sox2), neural progenitor (Id1 & Tbr2), and neuron (Tbr1) genes. Also, the presence of microvascular cells leads to a significant increase in NSC proliferation. Furthermore transgenic mice expressing modified Vegf isoform profiles were used to test the hypothesis that Vegf isoforms have distinct regulatory potential in the early cortical microenvironment. In order to

determine if vascular cells and Vegf isoforms are influencing NSC fate choice through epigenetic mechanisms I investigated promoter methylation of *Pax6* and *ID1* as well as global methylation and hydroxymethylation. These investigations are important not only for understanding normal neural developmental, but also for clarifying the potential role of NSC in neural degenerative disorders.

CHAPTER I

INTRODUCTION

Vasculogenesis and Angiogenesis

The vascular system is the earliest functioning system within developing organisms and is indispensable for embryonic development. Blood vessels serve as a primary system-wide transport “conduit” that brings resources such as oxygen, hormones, signaling molecules to specific tissues, and removes waste. A defect during formation of this system can lead to impaired tissue function or even prenatal death. The vascular system forms via two main mechanisms: vasculogenesis and angiogenesis.

Vasculogenesis is the process of *de novo* blood vessel formation which begins with the formation of blood islands (reviewed in ^{1,2}). Blood islands consist of aggregates of pluripotent mesenchymal cells that have differentiated into hemangiogenic stem cells.

Hemangiogenic stem cells on the periphery of the aggregate will differentiate into angioblasts and form a tube-like structure around the group of remaining stem cells (Figure 1) (reviewed in ³). Angioblasts will eventually differentiate into endothelial cells while the remaining hemangiogenic cells are slated to differentiate into red blood cells.

Angioblasts/endothelial cells will continue to establish vasculature by forming cord-like structures (reviewed in ¹). These structures will eventually give rise to the primary vascular network. In order to generate a complex vascular network, angiogenesis must be utilized in combination with vasculogenesis. Angiogenesis is the formation of blood vessels from preexisting vessels. This occurs when an endothelial cell within a blood

vessel is signaled by cues from the microenvironment to become a tip cell, a polarized cell with numerous filopodia⁴. The tip cell along with the supporting stalk cells will migrate away from the preexisting vessel and establish a new vessel within the tissue.

These initial vessels will continue to develop and mature in order to generate a functioning vascular system. One process involved with vessel maturation is the formation of a lumen. During vasculogenesis, angioblasts will adhere to one another creating a tube-like structure that will develop into a lumen (Figure 1)^{reviewed in 5}. While lumen formation during vasculogenesis occurs primarily through one mechanism, two mechanisms are used during angiogenesis. The first method involves an aggregate of endothelial cells that undergo exocytosis of vesicles into the center of the aggregate^{6 (and reviewed in 5)}. These vesicles will combine to form the lumen. The second method includes a single line of endothelial cells aligning vesicles along the center of each cell. Those vesicles will fuse together within the cell and with vesicles from adjacent cells to form a lumen⁷. Vessel maturation continues with the association of pericytes with endothelial cells. Pericyte processes wrap around endothelial cells with the soma, generally located at the endothelial cell junctions in the vasculature^{1 (and reviewed in 2)}. The presence of pericytes in conjunction with bovine aortic endothelial cells leads to an increase in Vegf expression which is essential for endothelial cell survival³. However, when pericytes are not present it leads to irregular diameters of blood vessels, endothelial hyperplasia, and crowding of endothelial cells within the microvessel wall⁴. These studies indicate that pericytes play a role in regulating endothelial cell proliferation, maturation, and survival and are, therefore, critical for vessel function and stability. The combination of endothelial cells and pericytes comprise the primary vascular cells present in developing

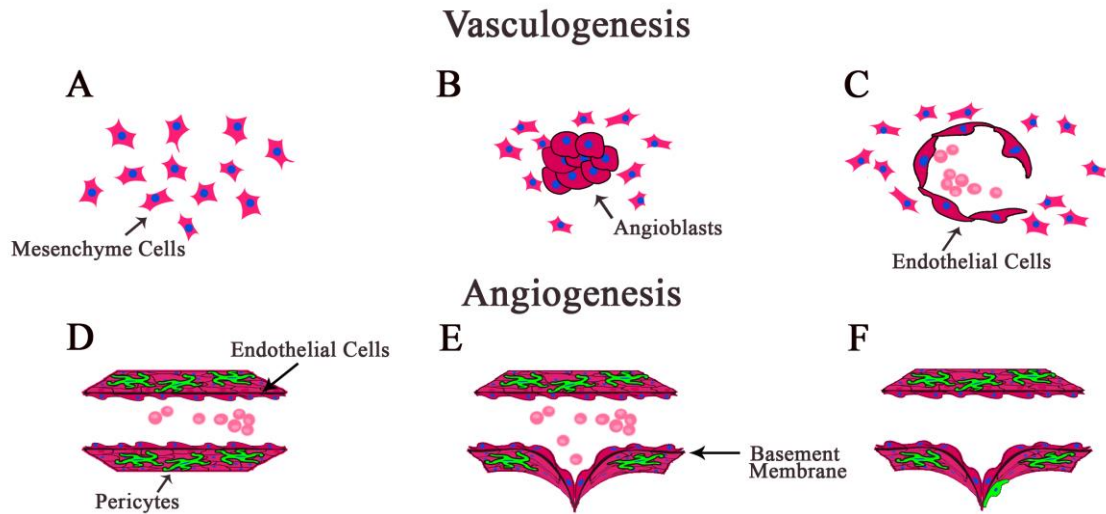


Figure 1: Vessel formation via vasculogenesis and angiogenesis. Vasculogenesis is the process of forming vessels *de novo* (A-C). It first begins (A) when mesenchymal cells (fibroblast-like cells) form aggregates and then (B) differentiate into angioblasts (round red cells with blue nuclei). (C) Angioblasts on the periphery of the cluster will differentiate into endothelial cells and will encompass the remaining cells ^{reviewed in 8}. The cells present in the initial vessel structure will differentiate and give rise to the future red blood cells (small pink cells). The early vessel structure will be used to generate additional vasculature through branching, also known as angiogenesis (D-F). The vessels are established (D) by endothelial cells (flat red cells) within the vessel sprouting and migrating away from the current vessel. The migration of endothelial cells into a new section of tissue will generate a new vascular plexus (E). During vasculogenesis and angiogenesis, pericytes (green cells) will be recruited (F) to the growing vascular structure. The pericytes can influence endothelial cell maturation, proliferation, and survival, directly impacting vessel stability ⁹.

and adult organisms. While an initial vascular network is formed before basic tissue and organ structures are fully developed, the vascular tree continues to be refined as development progresses.

Vascular endothelial growth factor and receptors

The vascular network, established early in development, utilizes and requires the presence of Vascular endothelial growth factor (Vegf). Vegf is a member of a homodimeric glycoprotein family which is related to the platelet-derived growth factor family. Members that comprise this family are Vegf-A, Vegf-B, Vegf-C, Vegf-D and Vegf-E, but the focus of this study deals solely with Vegf-A, referred to as Vegf for this document. Vegf is comprised of multiple isoforms generated by alternative splicing of heteronuclear RNA during RNA processing/maturation stage (Figure 2). Vegf isoforms that are commonly associated with angiogenesis and cortical development are Vegf120, Vegf164, and Vegf188, where the number correlates to the amino acid sequence¹⁰. These isoforms all contain exons 1-5 and 8 with an altered composition with regard to exon 6 and 7¹⁰. The alteration in exon presence has led to the postulation that there is a difference in the bioavailability of the isoforms in the microenvironment due to a heparin binding domain coded for by exons 6 and 7^{10,11}. Vegf binds to heparan sulfate proteoglycans in the extracellular matrix and cellular environment as well as binding to heparin columns *in vitro*¹¹ (and reviewed in¹²). Exon 7 is present in both Vegf164 and Vegf188 leading to both Vegf isoforms having an affinity for heparan sulfate proteoglycans. This affinity leads to an increase in the probability for these Vegf isoforms to be localized to the cell surface or surrounding extracellular matrix. Since Vegf164 only has exon 7 present, the protein it codes for has moderate affinity for heparan sulfate

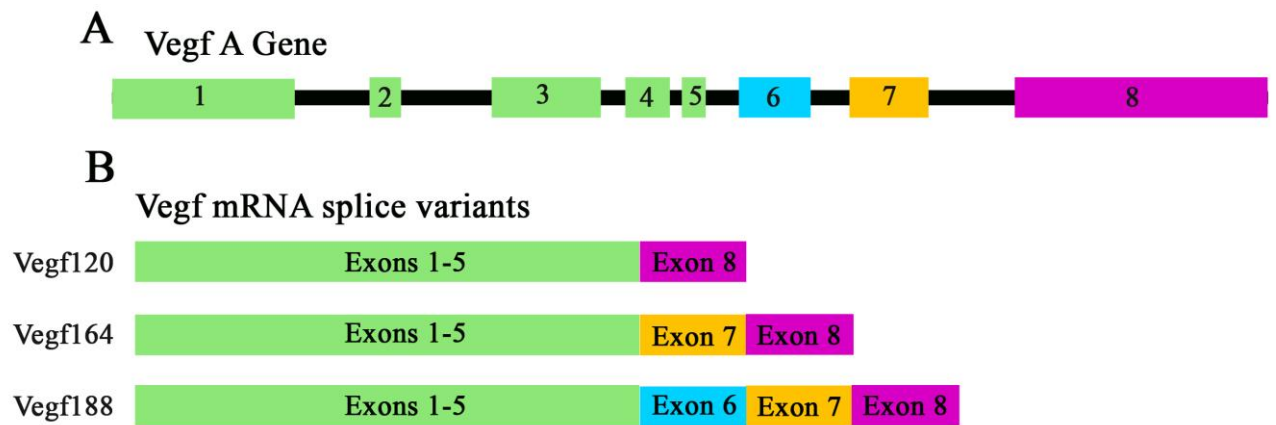


Figure 2: The exon composition of Vegf isoforms leads to differences in protein structure, features, and location in the microenvironment. (A) Vegf isoforms are generated from alternative splicing of the heteronuclear, genomic DNA. Black bars indicate intronic sequence. (B) All three isoforms contain exons 1-5 (green) and 8 (purple) but differ in the composition regarding exons 6 (blue) and 7 (gold). Vegf188 consists of all 8 exons whereas Vegf164 lacks exon 6 and Vegf120 lacks exons 6 and 7.

The Vegf isoforms are hypothesized to differ in their availability in the microenvironment due to the presence of a heparan sulfate proteoglycan binding domain coded for by exons 6 and 7. The presence of the heparan sulfate proteoglycan binding domain likely leads to the Vegf isoforms being locally retained (Vegf164 and Vegf188) while the absence of one or both of these exons allows the isoform to diffuse into the microenvironment (Vegf120 and Vegf164).

proteoglycans, which allows Vegf164 to diffuse into the microenvironment and be locally retained. Vegf120 has neither exon 6 nor 7 present which allows the protein to diffuse fully into the microenvironment¹¹. The differences in biochemical properties the Vegf isoforms may lead to a gradient of Vegf isoforms in the microenvironment, which is essential for proper vascular development. Mouse embryos only expressing Vegf120 displayed a dose-dependent decrease in vessel branch formation during angiogenesis¹³. In contrast, when only locally retained Vegf188 is present it causes formation of long, thin microvessels¹³. These results suggest that a Vegf gradient including both diffusible and locally retained Vegf isoforms are required for proper vascular development. Alternatively, the isoforms may have distinct differences in the outcome of their ligand-receptor interactions.

Vegf isoforms signal through Vegf receptors and neuropilins with a variety of effects on cell survival, proliferation, and migration (reviewed in¹⁴). There are three tyrosine kinase Vegf receptors that bind and respond to Vegf: VEGFR1 (FMS-Related Tyrosine Kinase 1; Flt-1), VEGFR2 (Kinase Insert Domain Receptor; Flk-1), and VEGFR3 (FMS-Related Tyrosine Kinase 4; Flt-4); all three are located on endothelial cell membranes¹⁵ (and reviewed in¹⁶). There is evidence to support that both VEGFR1 and VEGFR2 are involved with the formation of the vascular network while VEGFR3 is primarily involved with lymphendothelial development^{17, 18} (and reviewed in¹⁹). VEGFR1 and VEGFR2 are required for vascular development but they differ in the role within this system. Mice deficient in VEGFR1 exhibited an outgrowth of angioblasts during blood island formation¹⁸. This outgrowth is believed to be caused by a change in VEGFR2 activation. The change in VEGFR2 activation indicates that VEGFR1 may be

involved with regulating VEGFR2 activation in endothelial cells indirectly through sequestration of Vegf^{18,20}. The proposed mechanism is that VEGFR1 has a higher binding affinity for Vegf compared to VEGFR2²¹ (and reviewed in¹⁶). This idea is further supported by the fact that porcine aortic cells transfected with VEGFR1 has a reduced kinase activity resulting in a weaker signaling cascade compared to VEGFR2 porcine aortic cells²¹. In contrast to VEGFR1, VEGFR2 has multiple phosphorylation sites which can elicit varying responses in endothelial cells (reviewed in¹⁹).

Phosphorylation of Y1175 on VEGFR2 initiates DNA synthesis which is required for bovine aortic endothelial cell proliferation²². Whereas phosphorylation of Y1214 on VEGFR2, by Vegf, triggers formation of stress fibers which influences cell migration in both human umbilical vein endothelial cells (HUVEC) and porcine aortic endothelial cells (PAE)²³. The ability to induce multiple responses leads to VEGFR2 being one of the main Vegf receptors for endothelial cells. While the current role of VEGFR1 does not appear as influential as VEGFR2 in vasculogenesis and angiogenesis it does not negate the fact that it is important for proper development. During development VEGFR2 is involved in regulating angioblasts/endothelial cell migration, proliferation, and maturation²⁴. Mice lacking VEGFR2 display a disruption in blood island formation due to a failure in mouse embryonic endothelial cell migration and proliferation^{20,25}. The failure in cell migration and proliferation could be a result of a Vegf not being able to activate specific signaling pathways, such as the Ras pathway. The Ras pathway is responsible for regulation genes involved with cell growth, differentiation, and survival. When Vegf signaling is inhibited it leads to a decrease in Ras activation which in turn results in a decrease in HUVEC migration and proliferation²⁶. Knocking out either

VEGFR1 or VEGFR2 it leads to embryonic death. Mice deficit in VEGFR1 display enlarged vascular structures which contribute to a disorganized vascular network, thus resulting in embryonic death by embryonic day 9 (E9)¹⁸. Whereas knocking out VEGFR2 in mice causes a failure in blood island formation resulting in embryonic death at E8.5²⁵. These results indicate that both receptors are required for development of the vascular system. While both receptors bind Vegf isoforms the responses elicited from the Vegf isoforms can differ. Binding of Vegf164 to VEGFR2 in PAE cells exhibit more phosphorylation of Y1173 (VEGFR2 tyrosine phosphorylation site) compared to when Vegf120 is bound to VEGFR2²⁷. The difference in phosphorylation patterns could result in different cellular responses. This has been seen with Vegf164 which induces sprouting in differentiating mouse embryonic stem cells compared to no sprouting with the presence of Vegf120²⁷. Difference in phosphorylation patterns and cellular responses have not been assessed with Vegf188 due to a recombinant Vegf188 not being commercially available until recently. All this information with Vegf isoforms and receptors highlights the range of Vegf signaling which can be further modified through dimerization of Vegf receptors.

Vegf signaling can be regulated and refined by Vegf receptors forming homodimers and heterodimers. VEGFR1 and VEGFR2 can homodimerize and heterodimerize with one another in PAE cells²⁸ (and reviewed in¹²). VEGFR2 can also heterodimerize with neuropilin transmembrane proteins, which is mediated by Vegf165 (human recombinant Vegf)²⁹. Neuropilins are highly conserved membrane proteins found across vertebrate species and are located on multiple cell types, such as endothelial and neural cells³⁰ (and reviewed in³¹). There are two neuropilin (NRP) receptors, NRP1

and NRP2, through which Neuropilin-1 is capable of binding different Vegf isoforms. Vegf164 and Vegf188 are able to bind to NRP1 due to the presence of exon 7 which codes for a sequence of amino acid that bind NRP1. In contrast, Vegf120 is able to bind to VEGFR2 but is not able to bridge to NRP1 due to its lack of exon 7²⁹. NRP1 has been shown to enhance the binding of Vegf164 to VEGFR2 leading to an increase in PAE cell migration³². NRP1 does not elicit similar responses when present by itself, leading to the idea that NRP1 acts primarily as a co-receptor for VEGFR1 and VEGFR2³². What is clear is Vegf has the capability to induce multiple responses within cells which is essential for a developing organisms.

Vasculature, Organogenesis, and the Cortex

Organogenesis is the process of forming organs during development, which occurs in concert with, and is dependent upon, angiogenesis. A key step in organogenesis is the specification and commitment of cells to undergo cellular differentiation at the right time and place. The continued differentiation and development of these cells, in many cases, requires the presence of endothelial cells and a forming vasculature (reviewed in³³). An example of this is during liver bud formation (reviewed in³⁴). The initial specification of hepatic cells can occur without the presence of endothelial cells, but for the continued growth and maturation of the liver bud it requires the presence of endothelial cells³⁵. Endothelial cells have the capability to influence specific cell sources within the developing organ, as seen with liver. In addition to endothelial cells, growth factors and other signaling cues that are released by vascular cells can be used for communication between cell types. For example, liver epithelial cells produce Vegf and

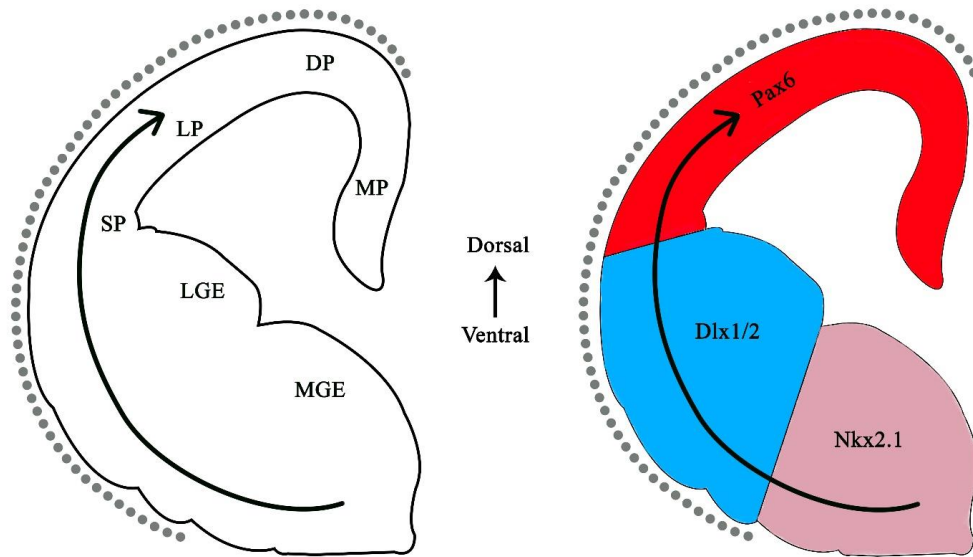


Figure 3: Angiogenesis of the cortex occurs in a ventral to dorsal fashion correlated with expression of neural transcription factors. (A) Angiogenesis of the telencephalon occurs by 1) invasion from pial vessels and 2) expansion of existing plexi. By E9 in mice, the pial surface is encompassed with vasculature (grey dotted line, left). At this time point blood vessels are being generated through angiogenesis in the ventral region of the telencephalon. These blood vessels establish a lattice network that expands from the ventral region towards the dorsal region (solid black arrow). At the same time blood vessels expand in a caudal to rostral fashion within the cortex. (B) The pattern of angiogenesis corresponds to regional transcription factor expression associated with neural progenitor cells (right). Within the ventral region, transcription factors Nkx2-1 (medial ganglionic eminence) and Dlx1/2 (ventral progenitor cells) are present while Pax6 (neural stem cells) is expressed in the dorsal region. Abbreviations are MGE: medial ganglionic eminence, LGE: lateral ganglionic eminence, SP: subpallium, LP: lateral pallium, DP: dorsal pallium, and medial pallium.

secrete it into the microenvironment which signals arterial vasculogenesis into that region thereby initiating vascular plexus formation³⁶. While stem cells can produce Vegf to attract blood vessels, these cells can also require the presence of Vegf for their own development. The predominant Vegf isoform expressed in the lung is Vegf188, followed closely by Vegf164. Very little Vegf120 is normally expressed in developing or adult lung³⁷. During lung development type II cells, part of the pulmonary epithelium, produce and secrete Vegf188. When Vegf188 is not present during lung development it leads to pulmonary and microvascular defects³⁸. Indicating that Vegf as well as specific Vegf isoforms can mediate interactions between two systems which is essential for a functioning organism. This example highlights the complex and dynamic relationship that occurs with a developing organ and the investing vasculature. These complex interactions have been primarily studied in organ systems that arise initially through budding (pancreas, liver, and kidney)^{34, 35} (and reviewed in³⁹). While these studies are important on their own, they also lay the ground work for studying the role of vascular and neural interactions during cortical development.

The cortex is vascularized by a preprogrammed patterning system that relies both on vascular and neural derived cells. Vascularization of the cortex begins with the localization of blood islands to the head region. These blood islands lead to the development of two main types of blood vessels found within the cortex: pial and periventricular vessels². The pial vessels are restricted to the periphery of the cortex and the periventricular vessels are the main source of vasculature within the cortex. An initial vascular foundation is established before embryonic day 9 (E9) in mice, with the pial vessels encompassing the brain along with the generation of early periventricular vessels

⁴⁰. However, at this stage no vessels are present within the neuroepithelium; oxygen and metabolic waste exchange occur via diffusion ⁴⁰. The periventricular vessels are generated by branching from the basal vessel located in the basal ganglia. While the pial vessels have surrounded the brain by E9, the periventricular vessels are still primarily restricted to the ventral region of the cortex. In order to establish a vascular network, the cells within the periventricular vessels migrate and branch in a ventral-dorsal and caudal to rostral pattern (Figure 3). By E10, the periventricular vessels have established a network within the ventral telencephalon and are beginning to infringe on the lateral pallium⁴⁰. Around E11, the periventricular vessels have established a lattice network within the dorsal telencephalon, roughly 20µm thick and parallel to the pial and ventricular surfaces². In addition, the periventricular vessels have connected to the pial plexus by forming and extending narrow branches. This vascular network established in the cortex corresponds with transcription factors expressed in neural epithelial cells. These transcription factors form boundaries and generate regional specification within the cortex. The transcription factors present in the ventral region of the telencephalon are Nkx2-1 (medial ganglionic eminence) and Dlx1/2 (distal-less homeobox 1; ventral progenitor cells) while Pax6 (paired box protein; neural stem cells) is expressed in the dorsal region (Figure 3) ⁴⁰. All three transcription factors are involved with cortical development ⁴¹ (and reviewed in ⁴²). When a defect in expression of any of these three transcription factors occurs it leads to a region-specific defect in endothelial cell proliferation and migration. A defect within either system (vascular or cortical) has a profound impact on the other system, reflecting the intricate and interdependent nature of these two systems.

Cortical Development

Development of the cortex is a complex process that requires the proliferation, migration, and differentiation of neural epithelial cells. Expansion and development of the cortex begins around E9.5 in the neuroepithelium of the telencephalon, consisting primarily of Pax6 positive (Pax6⁺) neural stem cells (Figure 4) ⁴¹. During this time, neural stem cells are undergoing symmetric division generating two daughter neural stem cells. This type of division leads to an increase in the neural stem cell population, setting the foundation for cortical expansion. Rapid expansion of the cortex begins around E10.5 where neural stem cells begin to undergo asymmetric division in addition to symmetric division⁴³. At roughly E11.5 asymmetric division generates a neural stem cell and a Tbr2 (T-box brain protein 2)-positive (Tbr2⁺) neural intermediate progenitor cell⁴⁴. The neural stem cell will stay within the ventricular zone while the intermediate progenitor cell will migrate to the subventricular zone⁴³. In the subventricular zone the progenitor cell will divide symmetrically producing two neural progenitor cells⁴³ (and reviewed in ⁴⁵). This generates two cell populations within the neuroepithelium: neural stem cells and neural progenitor cells that are present by E11.5. Differentiating neural progenitor cells will migrate towards the pial surface generating a new population of Tbr1 (T-box brain protein 1)-positive (Tbr1⁺) early lineage neural cells (E13.5) ⁴⁶. These early lineage cells will differentiate into the neurons that comprise the different layers of the cortex. Radial glial cells are an additional cell source present in the neuroepithelium during the rapid expansion. Glia span the cortex with “endfeet” imbedded in the vasculature located at the pial surface which allows them to act as scaffolding for migrating neural precursor cells

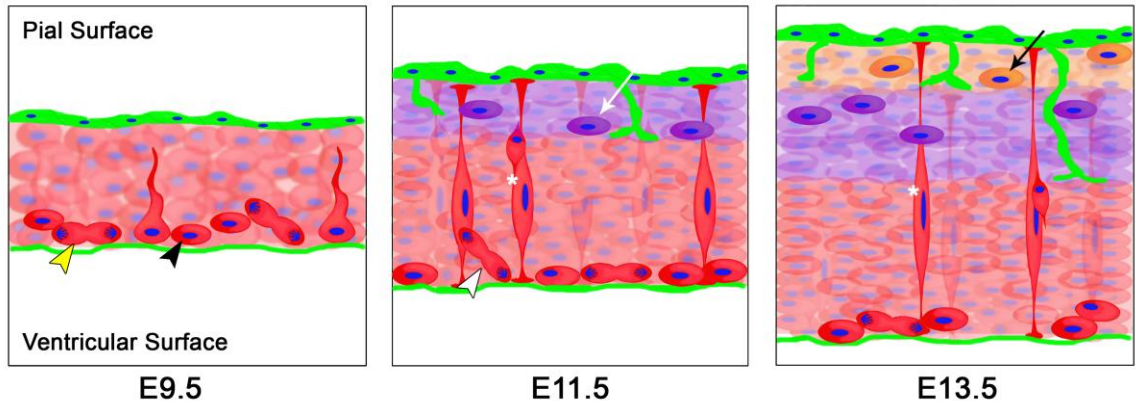


Figure 4: Diagram depicting cell division and primitive layer formation from embryonic day 9.5 to 13.5 in mice. At embryonic day 9.5 (E9.5; mid-gestation) the neural epithelium consists primarily of neural stem cells (black arrowhead and red cells). These cells are dividing symmetrically (yellow arrowhead), producing two daughter stem cells as well as asymmetrically (white arrowhead), producing both a stem and a progenitor cell. Blood vessels (green) are restricted to the pial surface. At E11.5, neural stem cells continue to divide symmetrically as well as asymmetrically which contributes to the growing neural progenitor cell population (white arrow and purple cell). In parallel, blood vessels begin to ingress into the cortex, vascularizing the neuroepithelium. Beginning just after E11.5, radial glial cells (white asterisk) are formed and span the neuroepithelium with the soma located at or near the ventricular surface and the endfeet imbedded in the extracellular matrix at the pial surface. As the neuroepithelium continues to expand, a population of early lineage neurons (black arrow and orange cells) becomes apparent beginning at E13.5, while both neural stem and progenitor populations are still present. As these early cortical layers form, there is a concomitant elaboration in the vasculature investing the neural epithelium.

^{47, 48}. Radial glial cells also contribute to the expansion of the cortex through asymmetric division which creates neural progenitor cells^{49, 50}.

Vegf and the Nervous System

Vascular endothelial growth factor is required for the vascularization of the early neural epithelium as well as the development of a subset of neural epithelial cells. Vegf is expressed in early mouse forebrain development, produced in both the neural epithelial cells and in the perivascular cells^{9, 51}. The expression of Vegf isoforms generates a gradient in the neuroepithelium which is essential for vascularization of the cortex. By establishing this gradient it induces endothelial cell migration and vessel branching into non-vascularized tissue¹³. In addition, the gradient acts as a migrational cue for neural epithelial cells. For example, cerebellar granule cells utilize the Vegf gradient to migrate from the external granule cell layer towards the Purkinje cell layer⁵². While Vegf may influence cell migration it can also mediate axon guidance. When Vegf is added to cultures containing superior cervical ganglion neurons (SCG) it leads to these cells exhibiting axonal outgrowth⁵³. This outgrowth can be direction mediated towards a localized Vegf source indicating Vegf can be used as a guidance cue for axon growth⁵⁴. While Vegf can act as a guidance cue, it can also influence neural epithelial cell survival. Neural stem cells isolated from an adult Fischer rat displayed an increase in neural stem cell survival and expansion when cultured with Vegf⁵⁵. Also, the presence of Vegf increases the survival of embryonic cortical neural cell *in vitro* as well as retinal neurons by decreasing cell apoptosis^{56, 57}. Coupled to this, Vegf also promotes proliferation of cortical cultures isolated from E16 mouse embryos⁵⁸. While studies have shown the

influence of Vegf, as a whole, on neural epithelial cells, the precise influence of each Vegf isoform is still unclear.

Recapturing the Neural-Vascular Environment

This study aims to determine the influence of vascular cells on neural stem cell fate choice with particular emphasis on the cellular microenvironment and the influence of the Vegf isoforms. During cortical development neural stem cells require multiple cues from the microenvironment in order to regulate cell fate choices. For example, the presence of bone morphogenetic protein 4 (BMP-4) promotes primary human neural precursor cells to display neural and glial markers. Whereas the presence of Notch ligands will induce these cells to express neural progenitor cell characteristics⁵⁹. Many of these cues are derived from the basement membrane as well as the extracellular matrix (ECM). The basement membrane is generated by extracellular matrix proteins and is involved with separating cell types, tissue regions, and most notably epithelial cell layers. The ECM protein, laminin, a key component in the basement membrane, provides cues for proper development of neural cells. Laminin is able to induce cell proliferation in neural precursor cells, isolated from postnatal day 1 forebrains in mice, through integrin signaling⁶⁰. This influence laminin has on neural cells can be dependent on characteristics of the laminin matrix. An acid laminin matrix leads to an increase in neural outgrowth whereas a neutral matrix leads to an increase in proliferation of primary cerebral cortex neurons⁶¹. In addition to providing signaling cues, laminin can be used to anchor neural cells in the correct location within the cortex. As an example, glial cells will anchor their endfeet in the basement membrane through integrin-laminin interaction. Failure to anchor endfeet to laminin leads to a defect in migration of neural cells that

require glial cells as scaffolding^{62, 63}. While laminin is involved with cell adhesion there are other components within the ECM, such as heparan sulfate proteoglycans, that are capable of anchoring different growth factors. The presence of growth factors in the ECM and basement membrane leads to an increase probability that cells will be exposed and influenced by these growth factors. This is the case with epidermal growth factor (EGF) and fibroblast growth factor (FGF) where they have been shown to promote self-renewal in adult mice neural stem cells.

In order to effectively study neural stem cell fate choice *in vitro*, we developed a culture system that will allow recapitulation of cell sources and extracellular components present in the developing cortical microenvironment. A heterotypic tri-culture system provides the ability to recapitulate the microenvironment *in vitro*. This experimental model system provides a manageable, simple model that includes multiple components (neural cells, vascular cells, ECM proteins, growth factors, heparan sulfate proteoglycans bound factors) but at the same time allows for the ability to distinguish between these specific inducing factors. In order to establish this system, Transwell™ inserts will be used to culture three cell sources in one environment. This system contains a porous membrane that allows cells to establish contact by the extension of cellular process through the membrane pores. These pores also permit the movement of soluble factors within the system. In addition, the porous membrane can be coated with substrates such as poly-l-lysine and laminin (poly-l-lysine is required to promote efficient laminin attachment to the membrane) to provide a matrix similar to the basement membrane and ECM present *in vivo*. There are other ECM proteins in the basement membrane but laminin appears to be the primary player for neural progenitor and neural cells during

development (reviewed in ⁶⁴). The matrix will provide neural stem cells a support system required for neural epithelial cell attachment, migration, proliferation, survival, and differentiation. While previous research has used similar methods to mimic the neurovascular environment they did not incorporate pericytes, which in combination with endothelial cells comprise the vasculature present *in vivo*^{65, 66}. The presence of pericytes is critical due to 1) they produce Vegf isoforms, 2) stabilize the vasculature, and 3) provide “stem” factors ^{9, 67}. Although this study lays the ground work for examining the neurovascular environment, our system allows a more comprehensive examination of the effects of the vasculature on neural stem cell fate choice. Using this system we will address the hypothesis that neural stem cells require vascular cells (endothelial cells and pericytes) and Vegf isoforms to regulate their transition from NSC to differentiated neurons.

CHAPTER II

METHODS

Animal Husbandry, timed pregnancies, and genotyping

Mice utilized in this study are from the C57 Black 6 (C57Bl6) strain and were housed in a temperature-humidity controlled room in filter-top Techniplast cages. The mice were maintained on a 12 hour light/dark cycle and checked daily. Every cage was situated with a nestlet, housing unit, and woodchips to provide an enriched environment and sufficient bedding material. Food, water, and cage/bedding were changed when needed, every 4-6 days. Mice within the colony were ear tagged and tracked through identification numbers. Male mice were assigned an even number and females were assigned odd numbers. Littermates of the same gender were assigned the same initial number but ear punching of the right ear, designating a number 0-4, was used to specify individual mice. Male mice were caged separately except during breeding or time pregnancy set ups. In general, females were housed at densities of 2-3 mice per cage. The handling and euthanasia followed NIH guidelines and were approved by the University of North Dakota Institutional Animal Care and Use Committee (IACUC protocol #1204-3c and Animal Welfare Assurance #A3917-01). Additional wild type (WT) mice were obtained, as needed, for annual outbreeding (Harlan Labs, Indianapolis, Indiana).

The mouse colony consists of wild type and transgenic mouse lines: Vegf120, Vegf188, and Vegf120/188, all which have been previously described^{37, 68}. Vegf120

mice were generated by homologous recombination leading to the removal of exons 6 and 7⁶⁸. Homozygous Vegf120 mice are early post natal lethal therefore, the Vegf120 line is maintained as heterozygotes. The generation of Vegf188 mice occurred through allelic recombination by replacing the genomic sequence with a cDNA construct consisting of fused exons 4-8³⁸. The fusion of exons prevents alternative splicing of the transcript. The Vegf120/188 mice were generated by crossing either heterozygous or homozygous Vegf188 mice with heterozygous Vegf120 mice. Mice expressing only Vegf164 are not maintained in the colony. Embryos at embryonic days E9.5 and E13.5 were generated through timed pregnancies (plug date, day 0.5) with pregnancy confirmed by weight gain. Embryo extraction is described under cell source and microdissection.

Genotype was determined by collecting genomic DNA from adult and embryonic tails. Tail samples were digested in 180µl lysis buffer and 20µl proteinase K (20 mg/ml stock) and incubated in a VorTemp 56 (Labnet, Woodbridge, NJ) overnight at 55°C with constant shaking at 25 rpm. The DNA was precipitated by adding 200µl isopropanol and incubating at -80°C for ≥ 4 hours. Samples were then centrifuged at 16,000rpm for 8 minutes and the supernatant was removed by careful pipetting that did not disturb the pellet. Genomic DNA was washed with 70% ethanol, centrifuged, and then the ethanol supernatant was removed. The DNA pellet was air dried for 30 minutes until the pellet became translucent. Genomic DNA was resuspended in 30µl TE at 4°C overnight. Genotype was assessed using standard PCR to amplify Vegf120 and Vegf188 isoforms from genomic DNA. Either one or both PCRs were conducted depending on the genotype of the parental cross. Genomic DNA (0.5µl) was combined with 0.25µl Vegf forward primer, 0.25µl Vegf isoform specific reverse primer and 9µl PCR super mix (Table 2 in

appendix). The PCR protocol for Vegf120 PCR and Vegf188 PCR is listed in Appendix Table 2. PCR products were run on a 1.2% agarose gel and visualized using a BioSpectrum 510 (UVP, Upland, CA). Genotype was confirmed based on product size and pattern.

Cell Culture

Cell Sources and Microdissection

Neural stem cell (NSC) populations. Neural epithelial cells were obtained by microdissecting embryonic day (E) 13.5 forebrains. Embryos were extracted using clean surgical technique from the dual uterine horns. Adipose debris and extra tissue were removed and individual placentae were placed in Dulbecco's phosphate buffered saline (DPBS; HyClone, Logan, Utah) solution without calcium (Ca^{+2}) and magnesium (Mg^{+2}) containing additional Pen Strep (penicillin 5000 units/mL, streptomycin 5000 $\mu\text{g}/\text{mL}$; Life technologies Grand Island, NY). Embryos were transferred to an EdgeGARD Hood (The Baker Company Inc, Sanford, ME) for further dissection. Embryonic dorsal anterior forebrain was removed according to the dissection region indicated in Figure 5. The posterior margin of the cut was at the sulcus anterior to the diencephalon. Tissue was placed into 15ml conical tubes containing trypsin with 0.5% ethylenediaminetetraacetic acid (trypsin-EDTA; Life technologies) and transferred to NuAire bio safety level II sterile hood (NuAire, Plymouth, MN). A single cell suspension was generated after a 10 minute incubation with trypsin-EDTA (Life technologies) and triturating with a blunt pipette. Trypsin was inactivated by adding an equivalent amount of complete neural basal media [50 ml Neurobasal media (Life technologies), B27 Supplement without Vitamin A (from 50X stock; Life technologies), N2 Supplement

(from 100X stock; Life technologies), GlutaMAX (from 100X stock; Life technologies), Pen Strep, and 20ng/ml recombinant mouse Epidermal growth factor (EGF; Life technologies); cNBM].

The cell suspension was enriched for neural stem cells using a two-step process that included antibody-based sub-population enrichment of the initial heterogeneous cell suspension. The antibody-coated plate was prepared by adding 50µl of SSEA-1 [Fucosyltransferase 4 (Alpha (1,3) Fucosyltransferase, Myeloid-Specific), 0.5mg/ml stock and 0.001mg/ml in well, neural stem cell marker; BD Biosciences, San Jose, CA] diluted in sodium bicarbonate coating buffer (0.5mg/ml stock) to 10 wells on a 48 well plate and incubated overnight for 4°C. The plate was washed 2 X 5 minutes at room temperature (RT) with wash buffer [Dulbeccos' phosphate buffered saline with Ca²⁺ and Mg²⁺ (PBS) with 0.1% BSA] before plating the cell suspension. The cells were placed in a Beckman CS-15R Centrifuge (GMI, Ramsey, MN) and spun at 2100 rpm for 5 minutes at RT. Trypsin and cNBM were removed without disruption of the cell pellet and the cells were resuspended in 1 ml of cNBM. Cells were visually inspected with an inverted Olympus CK2 scope to ensure that they were disaggregated prior to being plated in a 48 well plate that had been pre-coated with SSEA-1 IgM antibody. For step one (Figure 5), cells were incubated on the SSEA-1 plate in an AutoFlow NU-4850 Humidity Control Water Jacket CO₂ Incubator (NuAire) in conditions of 37°C, 5% CO₂, & 93% humidity, for 1.5 hours. After incubation, the media and non-adherent cells were removed and attached cells were washed with DPBS. Cells were incubated with trypsin for 10 minutes and then inactivated with cNBM. The single cell suspension was spun down at 2100 rpm for 5 minutes and the media was removed, ensuring that the cell pellet remained intact.

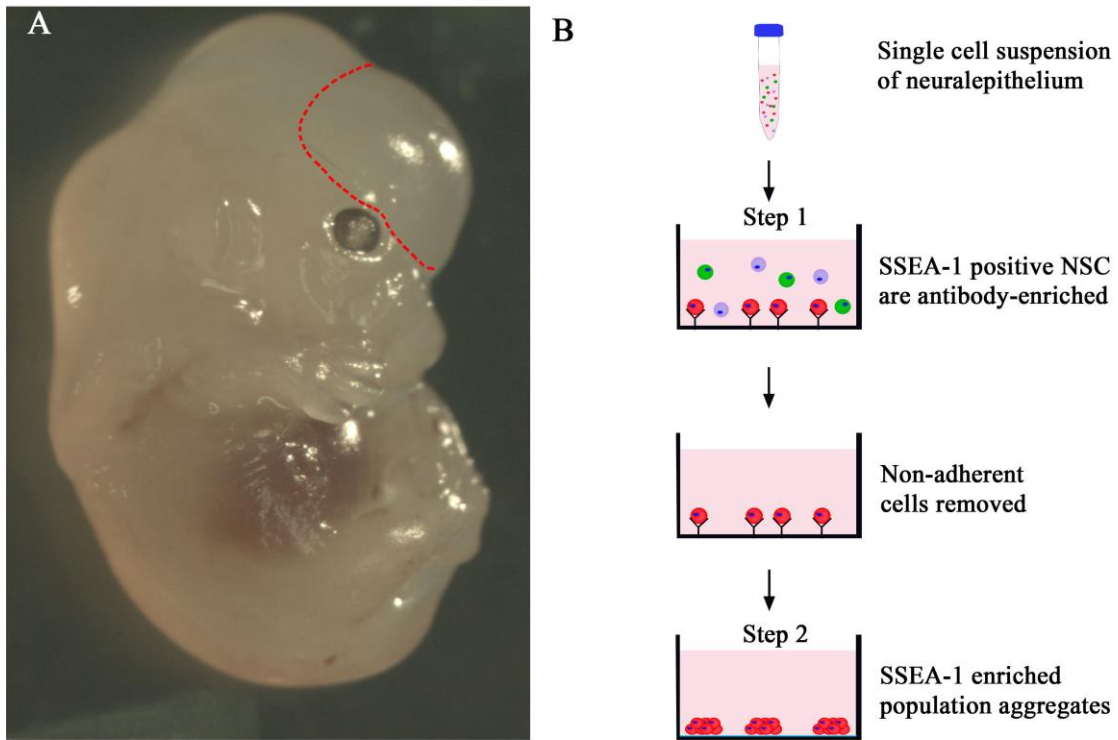


Figure 5: Isolation of SSEA-1-enriched NSCs from E13.5 embryonic forebrain.

Neural epithelial cells were dissected from the dorsal anterior of an E13.5 embryo forebrain (A, indicated by the red dashed line). Once the tissue was dissected from the embryo, SSEA-1-enriched NSCs were isolated through antibody-based cell isolation (B). A single cell suspension was generated and neural epithelial cells were incubated in wells with SSEA-1 antibody bound to the well. SSEA-1-positive neural cells (red cells) attached to SSEA-1 antibodies while non-attached cells (green and purple cells) were removed (reverse panning). SSEA-1-enriched neural epithelial cells were transferred to wells coated with poly-lysine and laminin (light blue) where NSCs proliferated and migrated to form clusters (aggregates) of neural cells.

For step two (Figure 5), the SSEA-1 enriched cells were resuspended in cNBM and plated onto a well coated with poly-lysine (0.05mg/μl; Sigma-Aldrich, St. Louis, MO) and laminin (0.05mg/μl; Sigma-Aldrich). Coating occurred two hours before plating cells by incubating 50μl of poly-lysine at room temperature for an hour followed by an hour incubation of 50μl laminin, both substrates were diluted in Neurobasal media without additives.

Vascular endothelial cells and pericytes. Mouse embryonic fibroblasts (MEFs) were generated from the body of a WT E13.5 embryo. The head was removed from the body to collect neural epithelium cells and the body was used to generate MEFs. All major internal organs and the spinal cord (including dorsal root ganglia) were dissected away from the body. The remaining tissue consisted primarily of skin, primitive limb buds, and muscle fascia. The body was then incubated in trypsin for 10 minutes and the entire slurry placed into a 3 ml syringe. To generate a single cell suspension the body was passed through an 18 gauge needle and the trypsin was inactivated with Dulbecco's Modified Eagle Medium (DMEM; Life technologies) containing Pen Strep and 10% heat inactivated fetal bovine serum (HI FBS; Sigma-Aldrich). Cells were spun down at 2100 rpm for 4 minutes and resuspended in 3 ml of DMEM. The heterogeneous cell mixture was plated in a 6 well plate and incubated for 2 hours at 37°C to allow the rapidly adhering fibroblast cells to settle. The media and non-adherent cells were then removed leaving an enriched populations of fibroblasts in the wells. Bovine aortic endothelial cells (BAEs) were obtained as primary cultures (purified by D. Darland) from bovine aortic tissue via direct trypsinization and scarping of the aortic intimal wall. The homogeneity of the population was confirmed by uptake of DiI-acetylated low-density lipoprotein

(Biomedical Technologies, Stoughton, MA). Cells were collected by serial trypsinization and DPBS wash similar to the primary cell population described above. Frozen cells were shipped from Boston, MA (D'Amore Lab, Schepens Eye Research Institute) and propagated as needed at the University of North Dakota. BAE populations were used between passages 1-10 with consistent results. Vascular cells utilized for experiments consisted of combining an equal quantity of MEFs and BAEs. The combination of MEFs and BAEs were used for vascular cells due to MEFs forming capillary-like structures in coculture with BAEs and differentiate into pericytes cells that express smooth muscle actin ⁹.

Cell Culture Maintenance

Neural epithelium cells that were SSEA-1-enriched were grown and maintained in a 48 well plate coated with poly-lysine and laminin, with cNBM and incubated in AutoFlow NU-4850 at 37°C, 5% CO₂, & 93% humidity. When individual cultures became 70% confluent with large aggregate populations, they were spilt into 2 wells. This was accomplished by removing the cNBM, washing with DPBS, and incubating in trypsin for 5 minutes. The trypsin was inactivated with cNBM and the cell suspension was transferred to a 15 ml conical tube and spun at 2100 rpm for 4 minutes. Neural stem cells (NSCs) were resuspended in 1 ml cNBM. Five hundred µl of cell suspension was plated into the original well while 500µl were plated in a new pre-coated well. These steps were repeated for each well once it reached 70% confluence.

MEFs were initially cultured in 6 well plate until they reached 70% confluence. At that point, the MEFs were washed with PBS and then incubated in trypsin for 5 minutes. The trypsin was inactivated with complete DMEM and the cells were spun

down at 2100 rpm for 4 minutes. MEFs were resuspended as a single cell suspension (confirmed by inspection) and plated in a T75 flask. Frozen cultures of MEFs and BAEs were generated once a T75 flask became 80-90% confluent. Cells were dissociated from the flask, divided into two 15ml conical tubes, and centrifuged as previously described. Cells in one tube were resuspended in DMEM and plated into a new T75 flask. Cells in the second tube were resuspended in DMEM freezing media (DMEM with Pen Strep, 10% HI FBS, and 10% DMSO), transferred to a cryogenic vial (Nalgene Company, Rochester, NY) and incubated at -20°C for an hour. Frozen vials were transferred to -80°C for one week and then stored in liquid nitrogen, -196°C.

Immortalization

NSCs were cultured between 2-5 days before they underwent the immortalization process. Immortalized NSC were generated using in vitro infection with Lentivirus containing the entire SV40 genome, including the Large and Small T antigens and the capsid proteins, VP1 and VP2 (Capital Bioscience Rockville, MD). To maximize binding of viral particles to the cell membranes of the primary cultures, virus was suspended in polybrene solution to a final concentration of 6 ng of polybrene (from a 0.8 mg/ml stock solution in water) per 250 colony forming units (cfu) of lentivirus. Just prior to infection, cNBM was removed from the NSCs that were designated to be immortalized and 250 µl of Lenti-SV40/Polybrene solution was added to each well. The cell-virus mixture was incubated at 37°C for roughly 12-15 hours at which point 250µl of cNMB was added to the well to dilute the SV40 1:2. After 24 hours from the NSCs' initial exposure to SV40, the cNBM/SV40 solution was removed and replaced with 500µl cNBM. Immortalized neural stem cells are designated as NSCs*. All standard safety precautions associated

with virus handling were followed and these procedures were approved under the Institutional Biosafety Registration number #IBC200806-014 (PI: D. Darland).

Coculture System

Triculture assay system (Transwell™)

For the heterotypic cell culture assay, 12 well Transwell™ (0.4 µm pore size; 1.12 cm²; Corning Incorporated Life Sciences, Tewksbury, MA) were used and the membranes coated with poly-lysine and laminin (coating concentrations and methods stated previously). Vascular cells were plated prior to NSC*. MEFs and BAEs were dissociated from T75 Flasks as previously described. Trypsin was inactivated by adding DMEM and the total volume was brought up to 10ml. All cell counts were obtained by adding 0.5ml of cell suspension to 9.5ml Isoton II Diluent (Beckman Coulter Indianapolis, IN) in a coulter cup. A Beckman Z1 Coulter Particle Counter (Beckman Coulter) was used to calculate the number of cells present in the cell suspension. While the MEFs and BAE cell suspensions were being counted, the 15 ml cell suspensions were centrifuged at 2100 rpm for 4 minutes. MEFs and BAEs were each separately resuspended in DMEM to produce a cell density of 20,000 cells per 50 µl. MEFs and BAE cell suspensions were then combined to generate a mixed population containing 10,000 MEFs and 10,000 BAEs per 100 µl. To generate the contact-based or non-contact vascular cell coculture wells, 8 Transwell™ inserts were removed from a 12 well plate and placed upside down in a large sterile petri dish. One hundred µl of the MEFs/BAE cell suspension was plated either on the underside of 4 Transwell™ membranes or on the bottom of 4 of the wells in the 12 well plate. No vascular cells were plated in the remaining 4 Transwell™ membranes since these wells were used to generate the NSC*

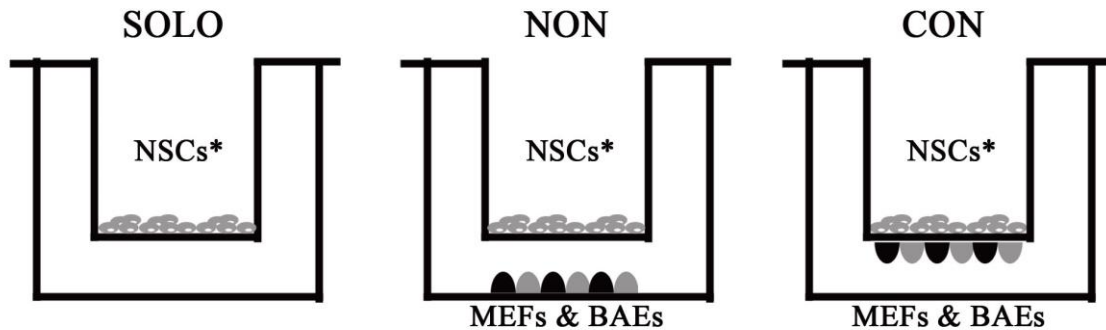


Figure 6: Heterotypic cell culture model used to determine the influence of vascular cells on neural stem cell fate choice. Immortalized SSEA-1-enriched neural epithelial cells (NSCs*) were plated in varying conditions to assess the influence of vascular cells [mouse embryonic fibroblasts (MEFs) and bovine aortic endothelial cells (BAEs)] on neural cell fate choice. The first treatment consisted of plating the NSCs* by themselves on top of the permeable membrane (SOLO) representing neural epithelial cells at the ventricular surface. Second, NSCs* were plated in non-contacting coculture with vascular cells (NON) with the NSCs* being plated on top of the membrane and vascular cells on the bottom of the well, which recapitulates when neural stem and progenitor cells are midway and near the ventricular surface. The third treatment entailed plating the NSCs* in non-contacting coculture with vascular cells (CON) with the vascular cells plated on the underside of the membrane. This represents neural epithelial cells at the pial surface. The difference in contacting and non-contacting coculture allows us to investigate the influence of juxtacrine, autocrine, and contact dependent microenvironment signals on neural stem cell development. The permeable membranes consist of pores with a 0.4 μ m diameter on average, and allow movement of diffusible factors across the membrane as

well as cell process-based contact across the membrane. Cell movement across the membrane is prohibited due to the small pore size. Membranes were pre-coated with poly-lysine and laminin to simulate the ECM microenvironment of the developing cortical neural epithelium.

solo culture condition without vascular cell contact. MEFs and BAEs were returned to the incubator to allow the cells to settle and attach, after which the media and nonattached cells were removed. Transwell™ inserts were placed back into the 12 well plate and 0.5ml cNBM was added to each well. WT, Vegf120, Vegf188, and Vegf120/188 NSC* were prepared by removing media, washing with DPBS, and incubating for 5 minutes in trypsin. NSC* were centrifuged at 2100 rpm for 5 minutes and resuspended to generate a single cell suspension of ~30,000 cells per 200 µl cNBM. Two hundred µl of WT, Vegf120, Vegf188, Vegf120/188 NSCs* were plated into Transwell™ inserts and allowed to settle for 15 minutes. Then an additional 200 µl of cNBM were added to each Transwell™. Variation in plating of MEFs, BAEs, and NSCs* generated solo (no MEFs/BAEs), contacting (MEFs/BAEs plated on underside of membrane), and non-contacting (MEFs/BAEs plated on the bottom of the well) cocultures (Figure 6). Cells were incubated for 5-7 days, at which point total RNA or genomic DNA was collected from NSCs*.

Immunohistochemistry

E13.5 embryos and NSC* were fixed in buffered 4% paraformaldehyde (from a 16% stock, VWR International, Arlington Heights, IL). Embryos were equilibrated through a gradient up to 30% sucrose then embedded in Neg50 (Fisher Scientific) and cut with a Lecia HM550 cryostat at 10 µm section thickness. Sections and NSC* were blocked and permeabilized in blocking solution [3% donkey serum, 2% goat serum (Vector Laboratories, Burlingame, CA), 0.1% Triton X-100, and 2% bovine serum albumin (BSA) in phosphate-buffered saline (PBS)] overnight at 4°C. The primary antibody incubation with suppressor of zeste (Suz12; Santa Cruz Biotechnology Inc.,

Santa Cruz, CA) was overnight at 4°C in a sealed, moist chamber. The absence of primary antibody or the use of species-matched immunoglobulins were used as negative controls. The secondary incubation was for 1 hour at room temperature with a variety of secondary antibodies species-matched to the primary antibody Donkey or Goat anti-mouse or anti-rabbit and conjugated to cy3 or fluorescein isothiocyanate (FITC). Stocks of secondary antibodies were stored long-term as glycerol diluted aliquots and used at 1:200 (Jackson ImmunoResearch Laboratories, West Grove, PA). Nuclei were labeled in the minor groove of DNA with 4',6-diamidino-2-phenylindole (DAPI; Vector Labs) for standard fluorescent microscopy. Directly conjugated fluorescein *Griffonia simplicifolia* lectin (Vector Labs, Burlingame, CA) was incubated with secondary antibody incubation period to visualize blood vessels.

Migration Assay

A modified 24 well Transwell™ system was utilized for a NSC* migration assay. The pore size was 0.8µm across a 0.33cm² area (Corning Incorporated Life Sciences) which permitted cell movement through the membrane pores. MEFs were used as a microenvironment chemoattractant source to induce NSC* migration. The MEFs were dissociated via trypsinization as described previously. The Transwell™ inserts were removed from a 12 well plate and stored upside down in a sterile petri dish while the MEFs adhered to the bottom of the well. The MEFs were counted, plated at a density of ~14,000 cells per well, and allowed to adhere in the incubator. Media and non-adherent cells were removed after 2 hours and the Transwell™ inserts replaced. Each well was given 0.5ml of cNBM, but not inside the Transwell™ inserts themselves. NSCs* derived from WT, Vegf120, Vegf188, and Vegf120/188 were trypsinized and counted as

previously described. A cell suspension of 3,000 NSCs* per 200 μ l was generated and 200 μ l of cell suspension was plated into each Transwell™ insert. NSCs* and MEFs were incubated in AutoFlow NU-4850 incubator for 5 days. NSCs* attached to Transwell™ membranes were fixed in 0.5% glutaraldehyde (Sigma-Aldrich) for 1 hour at RT and then rinsed with PBS. Cells were incubated in blocking solution for 1 hour at RT. Primary labeling incubation occurred for 1.5 hours with biotinylated phalloidin (50 μ g/ml; Sigma-Aldrich) at 1:50. For detection, streptavidin (a bacterial derived protein that binds to biotin at a 5:1 ratio of avidin:biotin, Jackson ImmunoResearch Laboratories) 1:200 and DAPI 1:400 were incubated for 1 hour. Membranes were removed and mounted on slides using Vectashield (Vector Labs, Burlingame, CA). Membranes were visualized using an Olympus BX51WI. A counting paradigm was designed to represent 30% of the total membrane. This consisted of dividing the membrane into 8 sections with a random point used in each section for counting at 40X. The images were counted by two independent investigators to ensure consistency across the counting paradigm. Results were analyzed by two way ANOVA with a Tukey's post hoc using JMP version 11.0 (SAS institute Inc., Cary, NC).

Mitotic Cell Count Assay

The Transwell™ cell culture system was also used to generate mitotic counts in NSC*, with plating protocols similar to that previously described. In brief, MEFs and BAEs were dissociated from the T75 flask and plated at a density of 10,000 cells per 100 μ l for each population, MEFs and BAEs. The combined cultures of MEF and BAE cell suspensions were each moved to a new conical tube. The MEFs were centrifuged so that the cell pellet could be resuspended in the labeling diluent solution for PKH67 dye

(Sigma-Aldrich), an aliphatic cell linker dye with a manufacturer's estimated labeling half-life of 10-12 days. MEFs were labeled with PKH67 green fluorescence by resuspending 40,000 MEFs in 250 μ l Diluent C (Sigma-Aldrich). PKH67 was diluted 1:1000 in Diluent C (0.5 μ l PKH67 stock dye in 250 μ l Diluent C) and combined with MEFs in Diluent C and incubated for 5 minutes at RT to allow the dye to pass through the phospholipid membrane. After incubation, 1ml cNBM was added to the cell/PKH67 solution and mixed. MEFs suspension was slowly layered onto a 5ml bed of heat-inactivated FBS and centrifuged for 5 minutes at 1600rpm. The MEFs in solution passed through the greater density serum layer and pelleted at the bottom of the conical tube. MEFs were resuspended in DMEM to wash away unbound dye and then centrifuged again. The PKH67 labelled MEFs were combined with non-labeled BAEs to generate a cell suspension containing 10,000 MEFs and 10,000 BAEs per 100 μ l DMEM. One hundred μ l of MEFs/BAEs suspension were plated on the underside of three 12 well Transwell™ membranes and on the bottom of 3 wells (same plating methods as in coculture and migration assays). MEFs and BAEs were incubated for 2 hours at 37°C, followed by removal of the media and non-adherent cells. Five hundred μ l cNBM were added to each well and the Transwell™ inserts that were previously removed to allow MEFs/BAEs plating, were placed in the 12 well plate. WT and Vegf isoform NSCs* were dissociated, counted, resuspended, and labeled in the same manner as MEFs. A cell suspension of 32,000 cells per 300 μ l cNBM was generated and 1,800 μ l cell suspension was transferred to a new tube and centrifuged in order to label NSCs*. The same method for labeling MEFs was used to label NSCs* with PKH26 red fluorescent aliphatic dye (Sigma-Aldrich). After NSCs* were labeled, they were plated inside 6 Transwell™

inserts with a cell density of 32,000 NSCs* per well. NSCs*, MEFs and BAEs in solo or coculture conditions were incubated for 5 days.

One replicate set (solo, contacting coculture, and non-contacting coculture) was used to collect RNA from NSCs* and the other replicate was labeled to determine mitotic profiles. The media was removed from inside the Transwell™ inserts and MEFs and BAEs were removed by scraping the Transwell™ insert on a kimwipe (Kimberly-Clark Professional, Roswell, GA) to remove cells on the underside of the membrane. The total RNA was extracted and isolated from NSCs* using an Arcturus PicoPur RNA Isolation Kit (Applied Biosystems, Foster City, CA) following the manufacturer's directions and the details provided in the RNA purification and Reverse Transcription-PCR methods below.

The mitotic profile of NSCs* were determined by removing cNBM from each Transwell™ insert and the well and fixing cells with 3.7% paraformaldehyde for 15 minutes at RT. NSCs* were washed gently twice with PBS for 5 minutes each and then blocked and permeabilized in blocking solution for 1 hour. The cells were incubated with DAPI (1:1000) and then washed twice with PBS. Membranes were removed and mounted on slides using Vectashield (Vector Labs) and a round coverslip. Membranes were visualized using an Olympus BX51WI and 5 representative images at 40X were captured per membrane using a MBF CX 9000 camera (MBF bioscience, Williston, VT) and Picture Frame software (MBF bioscience). Images were used to count the number of NSCs* exhibiting mitotic profiles compared to cells in interphase (Figure 13B depicts example of mitotic profiles). An one way ANOVA with a Tukey's post hoc was used to investigate statistical difference in the proportion of mitotic profiles for WT samples and

total nuclei for both WT and Vegf isoform samples by using JMP version 11.0 (SAS Institute Inc.).

RNA purification and Reverse Transcription-PCR

Total RNA was collected from E13.5 WT and Vegf isoform NSCs* and E9.5 forebrains. Arcturus PicoPur RNA Isolation Kit (Applied Biosystems) was used to extract, isolate and purify RNA following the manufacturer's instructions. In brief, the RNA was extracted by adding 50µl extraction buffer into a well containing NSCs* after the media had been removed. The extraction buffer was mixed with a pipette tip, and then transferred into a 1.5ml tube. This was repeated with an additional 50µl extraction buffer. The extraction lysate was incubated at 42°C for 30 minutes in Dry Bath Incubator (Fisher Scientific, Pittsburgh, PA). After incubation, an equivalent amount of 70% ethanol was added to each sample and transferred to a purification column. Wash Buffer I was added to the column and centrifuged to wash the RNA. Next, the RNA purification column was treated with DNase for 15 minutes to eliminate genomic DNA contamination. The purification column was washed twice with Wash Buffer II to remove unbound material, excess salts, and protein and the total RNA was eluted using TE elution buffer. Total RNA was quantified using a Nanodrop DS Spectrophotometer (DeNovix Wilmington, DE) and quality inferred via the ratio of the absorbance of the RNA at 260nm/280nm.

The cDNA was generated via reverse transcription of 400ng of total RNA using the GeneAmp RNA PCR Core Kit (Applied Biosystems). This was accomplished by incubating RNA with Murine Leukemia Virus (MuLV)-derived Reverse Transcriptase (50U/µl), RNase Inhibitor (20U/µl), PCR Buffer II (500mM KCL and 100mM Tris-HCl),

MgCl₂ (25mM), Random Hexomers (50μM), Oligo d(T) (50μM), dATP (100μM), dTTP (100μM), dGTP (100μM), dCTP (100μM), and nuclease-free water in a PTC 200 Thermal Cycler (GMI) at 42°C for 15 minutes followed by 5 minutes at 99°C. The cDNA synthesis was quality confirmed by conducting a PCR to amplify the 18S gene and then running the PCR product on a 1.2% agarose gel (Sigma-Aldrich). If a band was detected at the correct size (129bp for 18S, for example) it validated the cDNA quality for further use.

Quantitative Real Time PCR (qPCR)

Amplicon Generation and Subcloning

Amplicons for qPCR standard curves were generated with forward and reverse primers designed using Integrated DNA Technologies (IDT; Coralville, IA) and NCBI Primer-BLAST. Primers were designed to have the following features: GC content between 40-50%, a fragment dimer melting range from 50-60°C, and minimal hairpin and self-dimerization characteristics. The initial primer product was amplified by standard PCR using 1μl cDNA, 0.5μM each of forward and reverse primers (0.5μl of a 10μM stock), and 8μl of PCR Supermix (Invitrogen/Life technologies). A standard cycling profile (PTC 200 Thermal Cycler (GMI) was used with 30 cycles of 95°C melting temperature for 30 seconds, 50-60°C annealing temperature for 30 seconds, and 72°C extension temperature for 30 seconds. Primer specific annealing temperatures and GeneBank sources are indicated in appendix Table 2. The source cDNAs were from a variety of embryo ages and cell culture experiments to ensure that primers were able to amplify a product effectively. Products of the PCR reaction were run on a 1.2% agarose (Sigma-Aldrich) gel and visualized on a BioSpectrum 510 (UVP) to determine if the size

of the product matched the size of the gene of interest based on a 100 bp DNA ladder (New England BioLabs Inc., Ipswich, MA). If the product size was appropriate to the predicted Amplicon size the PCR product was subcloned using the TOPO TA Cloning Kit (Invitrogen/Life technologies). The PCR product was cloned into the TOPO-TA cloning vector (Invitrogen/Life technologies) based on the amplification chemistry that results in a “hanging” A nucleotide base on the open 5’ and 3’ ends of the amplicon. The TOPO-TA vector is commercially available as a linearized double-stranded plasmid with “hanging” T bases inserted on both ends of the multiple cloning site. The ligation step included adding 2µl of PCR product, 1µl of salt solution, 2.5µl water, and 0.5µl TOPO-TA vector. The post-PCR ligation step was conducted for 5-minute incubation at RT that incorporated the gene of interest into the plasmid without regard to orientation. After a 5 minute incubation on ice, the plasmid was then transformed into *E. coli* TOP10 chemically-competent cells (Invitrogen/Life technologies) with a 30 second heat shock at 42°C. The bacteria were allowed to recover in Super Optimal Broth with catabolic repression (SOC) medium for 1 hour, shaking at 37°C in an Innova 4000 (New Brunswick, Ramsey, MN). Agar plates were made by dissolving one LB tablet of Luria Broth (LB) agar (Sigma Aldrich) into 500mL of H₂O and autoclaving to dissolve. Once the liquid cooled, ampicillin was added to a concentration of 100µg/mL (known as LB-amp agar plates) and then poured into petri plates once it cooled to 55°C and. After the bacteria recovered, they were plated on LB-amp agar plates with X-gal for blue-white colony screening and incubated overnight at 37°C in a Blue M B-2730-Q incubator (Thermal Product Solution, Riverside, MI) for 15-18 hours. Plates were inspected the following morning, wrapped with parafilm, and placed at 4°C for temporary storage.

Plasmid Purification and Sequence Validation

To generate sufficient purified plasmid, small-scale liquid bacteria cultures were established by selecting a single white bacteria colony using a toothpick and inoculating 3ml of LB with 50 μ g Ampicillin (Sigma-Aldrich) and incubated shaking at 37°C overnight. The next day, liquid bacteria cultures were transferred to 1.5ml tubes in three increments, centrifuging the suspension at 8,000 relative centrifugal force (rcf) for 4 minutes in an Eppendorf 5417R Centrifuge (Eppendorf, Hauppauge, NY), removing supernatant between increments. The bacterial pellet was resuspended in 1X lysis buffer (Zyppy Kit, Zymo Research Corporation, Irvine, CA) and mixed to ensure complete lysis. The lysis buffer was inactivated by adding cold neutralization buffer and mixing. The samples were centrifuged at 11,000rcf for 3 minutes and the supernatant, containing the plasmid, was transferred to a column collection tube. The column tube was spun at 11,000rcf for 15 seconds and then the plasmid was washed with endo-wash buffer and Zyppy wash buffer, centrifuging at 11,000rcf for 15 and 30 seconds respectively, between washes. The plasmid was eluted into a clean 1.5ml microcentrifuge tube by incubating 50 μ l Zyppy Tris ethylenediaminetetraacetic acid (Tris-EDTA) elution buffer on the column for 10 minutes and then centrifuging at 8,000rpm for 15 seconds. The TOPO-TA vector contains M13 sequencing sites, so M13-specific primers were used to amplify product from the plasmid and size-checked on a standard agarose gel as previously described. Once the plasmid was sized confirmed it was amplified by using BigDye Terminator v3.1 Cycle Sequencing Kit (Life technologies) and M13-specific primers. Unincorporated dye was separated from the product using the Dye Spin 2.0 (Qiagen). The purified product was then sequenced using 3100 Genetic Analyzer

(Applied Biosystems), and third it was analyzed using BioEdit (Ibis Bioscience, Carlsbad, CA). All amplicons in plasmids were sequence confirmed using NCBI BLAST program prior to being used in quantitative real time PCR (qPCR). Amplicons for qPCR standard curves were generated by amplifying the gene of interest using standard PCR and M13 primers. The PCR mix was brought to 200 μ l with 18 mega-Ohm (m Ω) water and the product was precipitated from the reaction mix using a 10% volume of 3M sodium acetate (pH 5.2) and 2.5X volume of 100% ethanol (molecular grade). After an overnight incubation at -20°C to precipitate the amplicon. The solution was centrifuged at 8,000rcf for 10 minutes and the supernatant was removed. The pellet was washed with cold 70% ethanol, centrifuging at 8,000rcf for 10 minutes and the residual supernatant was removed. The pellet was air dried for 10 minutes and then resuspended in 30 μ l TE. Amplicons were stored at -20°C with minimal freeze/thaws prior to use in generating standard curves (see below).

Quantitative real time PCR (qPCR)

The relative concentration of specific gene transcripts of interest from WT mice, Vegf isoform mice, and experimental treatments was determined using qPCR. A 8-point log standard curve was generated for each qPCR run for each primer set. The unknown samples were determined from the standard curve based on the formula: $y=mx + b$ where y is \log_2 of the C_t value, m is slope of the standard curve and b is the intercept. Primer efficiencies were based on the standard curve using the formula: $-1/m$ where m is slope of the standard curve. Amplicons (produced from the subcloning procedure) were diluted in TE in a 1:10 serial dilution to generate the standard curve. Amplicons used for qPCR were small ribosomal subunit (18S), sex determining region Y box-2 (Sox2), paired box

6 (Pax6), inhibitor of DNA binding 1 (Id1), T-box brain 2 (Tbr2), and T-box brain 1 (Tbr1). The cDNA samples were diluted in TE, 1:18 for 18S and 1:4 for all the other genes. Diluted cDNA samples were plated in a 96 well plate and stored at -20°C with a plastic seal. Standard curve samples and cDNA samples were combined with Absolute Blue qPCR SYBR Green with ROX (Thermo Fisher Scientific, Waltham, MA), forward and reverse primers (Appendix Table 2), and water in a 96 well plate. The plate was centrifuged at 1000rpm for 1 minute and then was placed in a StepOnePlus™ Real-Time PCR System (Applied Biosystems). The preprogramed SYBR Green cycling procedure was conducted with modifications to the initial activation which was increase to 15 minutes and the second step during the melt curve was shortened to 30 seconds. JMP software (SAS institute Inc.) was used to conduct a one way ANOVA with a Tukey's post hoc to analyze significant differences between samples as well as conduct correlation analyses on n=5-7 samples for each analysis.

Epigenetics

Genomic DNA purification for methylation analysis

Genomic DNA was isolated from the E9.5 dorsal anterior telencephalon and E13.5 NSCs* in vitro. Genomic DNA isolation methods were previously described above. After isolation, DNA was quantified by Nanodrop DS Spectrophotometer (DeNovix) and good quality DNA samples with a 260/280 ration in the range of 1.9-2.1 were further processed using the QIAamp genomic DNA kit (Qiagen, Germantown, MD) following the manufacturer's instructions. In brief, the kit components AW1 and AW2 were added to the genomic DNA sample. The solution was transferred to a QIAamp MinElute column and centrifuged at 6,000rcf for 1 minute. The column was washed with

AW2 and centrifuged at 6,000rcf for 1 minute to allow unbound material to flow through. The membrane was dried, the DNA was eluted with 30µl Buffer AE added to the column and the column unit was centrifuged at 20,000rcf for 1 minute. The genomic DNA eluate was stored at -20°C until it was used in methylation analysis.

Global methylation and hydroxymethylation

Genomic DNA isolated from E9.5 forebrains and E13.5 NSCs* was used in the EpiGentek MethylFlash and HydroxymethylFlash kits (EpiGentek, Farmingdale, NY) according to the manufacturer's instructions. A concentration of 175ng of DNA was used in both the MethylFlash and HydroxymethylFlash kits. DNA was incubated in the binding solution in the pre-coated wells at 37°C for 90 minutes. Next, the DNA was incubated with the capture antibody (1µg/ml) for 60 minutes, the detection antibody (0.2µg/ml) for 30 minutes, and the enhancer solution for 30 minutes. After each incubation, the DNA was washed three times with wash buffer (provided in the kit). The signal detection of methylated and hydroxymethylated DNA was achieved by incubating the DNA in the developer solution for 10 minutes followed by adding an equal amount of the stop solution. An Epoch Spectrophotometer (BioTek, Winooski, VT) was used to read the absorbance at 450nm. Absorbency readings of samples, a negative control, and positive controls generating a standard curve, were used to calculate the proportion of methylated and hydroxymethylated DNA from the *in vivo* (E9.5 forebrain-derived) and *in vitro* (E13.5 NSCs*) genomic DNA samples. Statistical analysis was conducted using a one way ANOVA with a Tukey's post hoc (JMP, SAS Institute Inc.).

DNA promoter methylation

Genomic DNA isolated from E9.5 forebrains and E13.5 NSCs* was used in the Methyl II DNA Restriction Kit (Qiagen) following manufacturer's directions to determine DNA promoter methylation of Pax6, Id1, and Suz12 (polycomb protein). For each genomic DNA sample, 250ng of genomic DNA was combined with the restriction digestion buffer and water and then divided equally between four, 0.2ml centrifuge tubes. Varying combinations of methylation-sensitive restriction enzymes, methylated-dependent restriction enzymes and water were added to the 0.2ml tubes to digest both methylated and non-methylated DNA. The DNA and restriction enzymes were incubated at 37°C for 6 hours in a PTC 200 Thermal Cycler (GMI) and the reaction was stopped by incubating the samples at 65°C for 20 minutes. DNA promoter methylation was determined by amplifying the digested and non-digested DNA using qPCR and primers for Pax6, ID1, and SUZ12 (Qiagen). The primers target specific regions that have been previously identified to be responsive to direct DNA methylation. The qPCR reaction was conducted on CFX384 Real Time System (Bio-RAD, Hercules, CA) using a modified cycling protocol that entailed adding a melt curve with SYBR green fluorescence detection. DNA promoter methylation was assessed using Ct values from the qPCR results. The Ct values were entered into a pre-programed methylated data analysis template provided by Qiagen which automatically calculated proportion of DNA methylation. Values were expressed as percentage of methylation for graphing purposes and human methylation controls (Qiagen) were used to assess enzyme activity.

CHAPTER III

RESULTS

Immortalized neural epithelial cells display comparable morphological features and gene expression to native neural epithelial cells

In order to obtain a renewable population of neural epithelial derived stem cells, we established an immortalized population from primary neural epithelial using Lenti SV40 large T antigen (TA_g) virus. To determine if our immortalized cell population retained similar features compared to the SSEA-1-enriched native neural epithelial cells, we did a qualitative gene expression assessment for key genes (Figure 7) and basic morphological features (Figure 8) over a short culture time frame. Native and immortalized neural epithelial cells exhibit similar expression patterns for 18S ribosomal RNA and neural stem cell transcription factor Pax6, with an absence of the differentiated-induced neuronal transcription factor Tbr1 (Figure 7). We observed that both native and immortalized neural epithelial cells have similar expression patterns for these 3 genes. We also compared expression of Vegf isoforms; Vegf164, Vegf120, and Vegf188. The expression levels for the immortalized neural epithelial cells looks similar to *in vivo* samples collect from E9.5 dorsal forebrain^{37, 69} (and unpublished data). The similarity in gene expression indicates that immortalized neural epithelial cells have a similar pattern in gene expression compared to native neural epithelial cells.

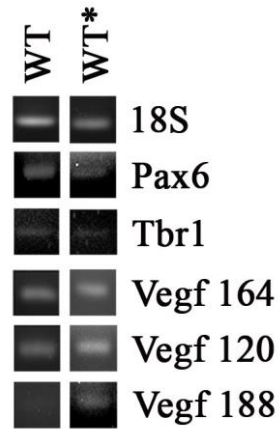


Figure 7: Native and Immortalized SSEA-1-enriched neural epithelial cells display similar gene expression patterns. Total RNA was collected from both native and immortalized (*) NSC that were enriched for neural stem cells using SSEA-1 reverse antibody panning. The RNA was reverse transcribed to cDNA and qualitative gene-specific expression determined with standard PCR. Expression of 18S, the small ribosomal subunit, was used as a reference gene. Expression of Pax6, a marker of neural stem populations, and Tbr1, a transcription factor expressed in post-mitotic neural lineages, were compared in both populations. Expression of the individual Vegf isoforms was determined in parallel for both source populations. Expression of each target gene was detected in both the native and immortalized cells, suggesting a similar composition in the populations.

While gene expression patterns for native and immortalized neural epithelial cells were similar, they exhibited comparable morphological features. SSEA-1-enriched native and immortalized neural epithelial populations were plated on poly-lysine/laminin coated 48 well plates in cNBM. Cultures were visualized over the course of the first 96 hours in culture based off cell loss in native neural epithelial cells that occurs ~7 days after primary plating. After 24 hours in culture, native and immortalized neural epithelial cells form varying sizes of aggregates (Figure 8). The majority of the aggregates are less than 25 μ m in diameter; red arrows indicate representative cell aggregates from each population. In some cases, cells form large aggregates, between 25-40 μ m, indicated with white arrow heads for both populations. At 48 hours native neural epithelial cell aggregates are similar in size compared to those observed at 24 hours (25 μ m), indicating that these cell aggregates are not growing or that the rate of proliferation and cell death are equal. Cultures were not fed between 24 and 96 hours so the loss of individual cells was due to death and not due to loss by media replacement. In contrast, the immortalized neural epithelial cells at 48 hours exhibited an increase in aggregate size (>40 μ m) indicating cell proliferation, coalescing migration, or both. Immortalized cells within the large aggregates are extending processes (black arrow) towards other aggregates as well as nearby individual cells. After 96 hours, there is a decrease in individual cells and aggregates in the native neural epithelial cell population indicating cell death (black arrow head). In contrast, immortalized neural epithelial cells have formed cell aggregates >50 μ m with clear processes extending away from the cell aggregates (yellow arrow) to

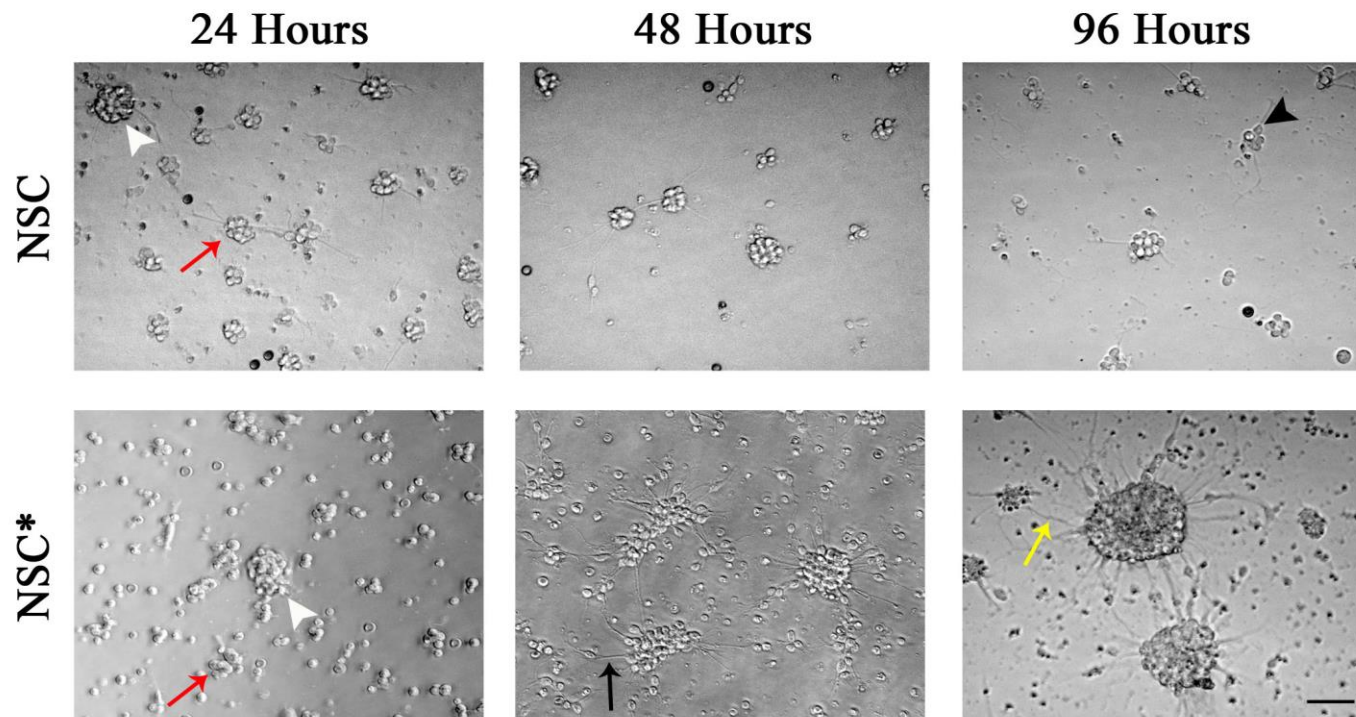


Figure 8: Immortalized neural epithelial cells exhibit comparable growth patterns and morphology relative to native neural epithelial cells. Neural epithelial cells were isolated from E13.5 WT forebrains and enriched for neural stem cells using SSEA-1 based reverse antibody panning. Neural epithelial cells of comparable plating density were either cultured directly after enrichment (NSC) or were immortalized with Lenti-SV40 Large T Antigen (NSC*). Both types of neural cells were cultured for 96 hours with images collected at 24 hour intervals. At 24 hours, cell aggregates ranging from $< 25\mu\text{m}$ (red arrow) to between $25\text{-}40\mu\text{m}$ (white

arrowhead) were apparent in both cultures. After 48 hours, small aggregates remained in the NSC while the immortalized cells had developed numerous cellular processes (black arrow) and significantly larger aggregates. Cell death and degradation (black arrowhead) were readily apparent in native cultures at 96 hours with only a few viable aggregates with short processes remaining. In contrast, the immortalized cell aggregates had continued to grow, achieving diameters in excess of 100 μm in some cases, and had established extensive process connections with neighboring aggregates and small cell clusters. This type of basic comparison was repeated for each WT collection with consistent results, Representative images are shown. Scale bar equals 25 μm .

contact with nearby cells and aggregates. These results indicate that immortalized neural epithelial cells exhibit an increase in proliferation during the initial 96 hours while native neural cells begin to die after 96 hours.

In order to determine the cell composition of immortalized SSEA-1-enriched neural epithelial populations, we looked at expression patterns of genes associated with neural epithelium development within these populations. Total RNA was collected from WT immortalized neural epithelial cells and reverse transcribed to cDNA which was then utilized in qPCR. WT immortalized neural epithelial cells express neural stem cell transcription factors Pax6, Sox2, and Id1 (Figure 9). While there are differences in the concentration between Pax6, Sox2, and Id1, these results indicate that the SSEA-1 immortalized neural epithelial cells consist primarily of neural stem cells. Expression of Tbr2, a neural progenitor cell marker, was significantly lower than the neural stem cell markers (Pax6, Sox2, and Id1; Tukey's *post hoc* $p < 0.00001$), suggesting that the number of neural progenitor cells was significantly smaller than the neural stem cell population or that the per cell expression was low for Tbr2. Expression for early lineage neuronal cells, Tbr1, was barely detectable relative to the neural stem cell genes, which suggests that very few differentiated neurons have developed in the immortalized SSEA-1-enriched neural epithelial populations ($p < 0.00001$, respectfully). Expression of Tbr2 was significantly higher than Tbr1 (Tukey's *post hoc* $p = 0.003$) although still lower than neural stem cell genes, indicating that neural progenitor cells are more prevalent than differentiated neural cells in the neural epithelial cultures. These results suggest that the majority of the SSEA-1-enriched neural epithelial cells collected and immortalized

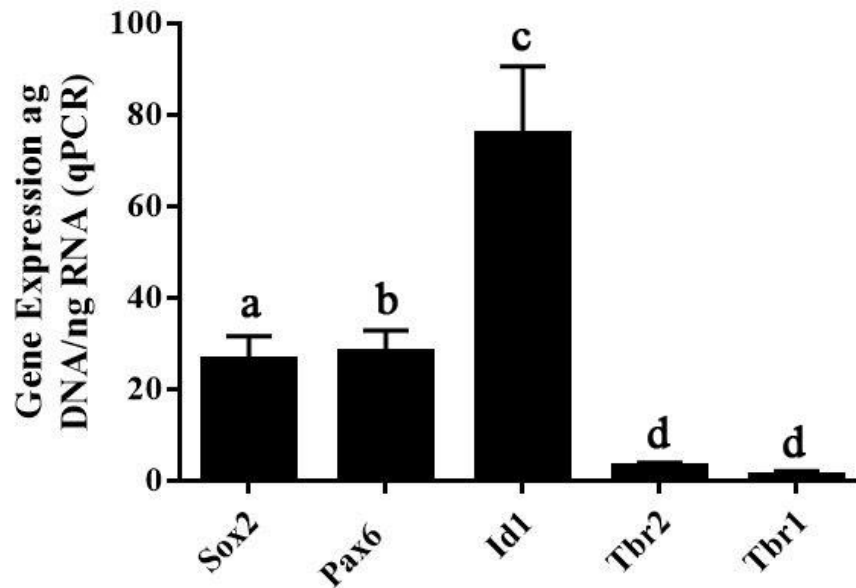


Figure 9: Wild type immortalized neural epithelial cell populations consist primarily of neural stem cells. Total RNA was isolated from WT immortalized SSEA-1-enriched neural epithelial cells and reverse transcribed to cDNA. Quantitative real time PCR was conducted to assess gene expression for critical neural stem cell and differentiation genes. Pax6, Sox2, and Id1 transcription factors were used to assess the presence of neural stem cells. Tbr2 (neural progenitor cells) and Tbr1 (post-mitotic neural cells) reflect the presence of early differentiating neuronal lineages. The expression levels of genes associated with neural stem cells were significantly higher than those associated with neuronal differentiation (One way ANOVA; $p < 0.0001$). Statistical difference between specific gene pairs were assessed with a Tukey's *post hoc* test and indicated by lower case letters, where a similar letter between genes reflects a non-statistical difference between the given pair. Statistical analysis were conducted on values normalized to 18S, which was used as a reference gene, and log transformed with an $n=7$.

consists of neural stem cells with very few neural progenitor cells and minimal detection of differentiated neurons.

An *in vitro* heterotypic (involving more than one cell type) culture system was developed to study the effects of vascular cells on native and immortalized neural epithelial cell morphology. In order to determine if immortalized neural epithelial cells exhibit different cell morphology when exposed to vascular cells compared to native neural cells, we developed a Transwell™ membrane-based coculture model. The coculture system involved plating WT neural epithelial cells alone (SOLO) in contacting (CON) and non-contacting (NON) coculture with vascular cells (MEFs and BAEs) (Figure 10, upper diagram). Neural epithelial cells were cultured for 3 days. Native neural epithelial cells cultured in solo condition display cell aggregate morphology with a common diameter of ~50µm (Figure 10). In contrast, immortalized neural epithelial cells display polarized morphology with extension of cellular processes similar to previously seen morphology (black arrow: compare Figures 8 and 10). Neural epithelial cells, native and immortalized, in contacting coculture with vascular cells form similar cell aggregate morphology (~50µm). Native neural epithelial cells exhibit a similar morphology when cultured in non-contacting coculture by forming aggregates of neural cells. The cell aggregates have not appeared to increase in size indicating either no proliferation, the cells are compacting, or the rate of proliferation and apoptosis are balanced. Immortalized neural epithelial cells in non-contacting coculture form cell aggregates structures. These aggregates appear smaller in size than native neural epithelial cells in contacting coculture (~50µm) but other cell aggregates can form that display sizes varying from 30-

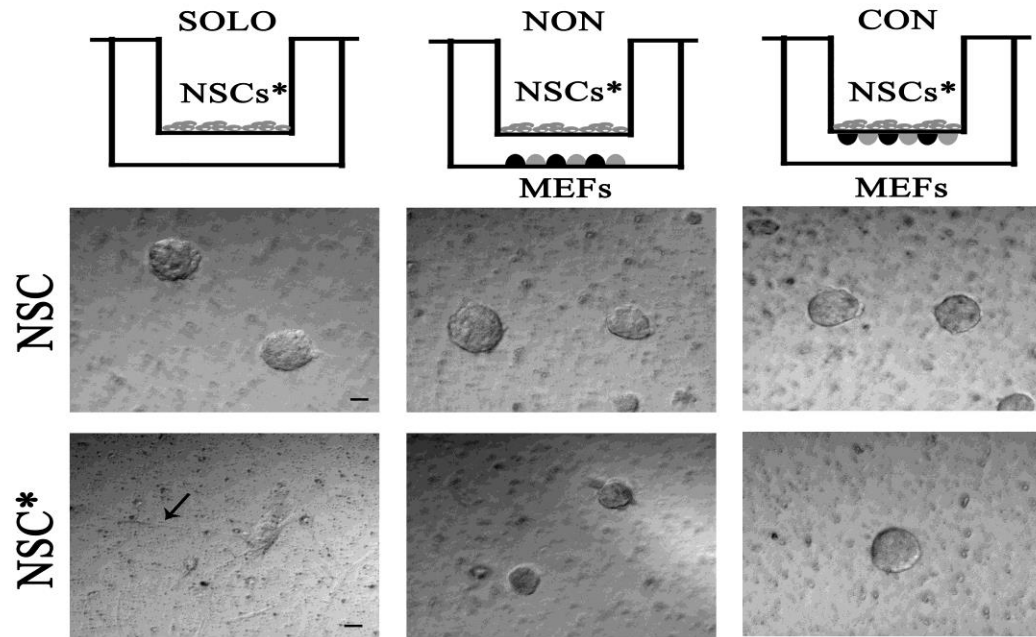


Figure 10: SSEA-1-enriched neural epithelial cells exhibit a similar morphology to native neural epithelial cells in coculture with MEFs. Native and immortalized neural epithelial cells were cocultured either in solo, contacting, or non-contacting coculture with MEFs. Native neural epithelial cells formed aggregates of cells regardless of the culture conditions. In contrast, immortalized neural epithelial cells displayed a flattened morphology (black arrow) when cultured solo indicating that the SSEA-1-enriched neural cells have polarized. Immortalized neural epithelial cells formed cell aggregates when cultured in the presence of MEFs, a similar morphology exhibited by native neural epithelial cells. Scale bar = 25 μ m.

50 μ m in diameter (data not shown). Overall, these results indicate that immortalized neural epithelial cells do not exhibit different morphology than native cells when cultured in the presence of vascular cells.

Before determining the specific influence of vascular cells on neural epithelial cells, we needed to address the possibility of cellular contact through a porous membrane. To accomplish this, native neural epithelial cells were cultured in contact with vascular cells (Figure 11). The neural cells were then fixed and labeled with nestin (neural precursor cell) and DAPI (nuclear DNA). Neural epithelial cells have a smaller, rounder nucleus (~14 μ m in diameter) compared to that of MEFs (~37 μ m in diameter, long way), are clearly in the plane of focus compared to the larger, oval shaped nucleus of the MEFs which are out of the plane of focus. The difference in the plane of focus shows that the neural epithelial cells and MEFs are present on the opposite side of the membrane, indicating that there is no cell migration through the pores by either cell type. Neural epithelial cells cocultured with MEFs formed cell aggregates (>75 μ m in diameter, Figure 11A). Cells within the aggregate extend processes toward other neural epithelial cells (white arrowhead, Figure 11A) indicating contact between neural epithelial cells within aggregates and individual cells. Neural cells also extend processes which pass through the pores on the membrane (white arrows, Figure 11B) and establish contact with MEFs (yellow arrowhead, Figure 11C). Based on these results cellular communication through contact is possible between neural epithelial cells and MEFs. Contact is only established through cell processes and not due to migration of either neural epithelial cells or MEFs. Due to the Transwell™ porous membrane allowing communication between neural and vascular cells we wanted to investigate the influence of vascular cells on neural epithelial

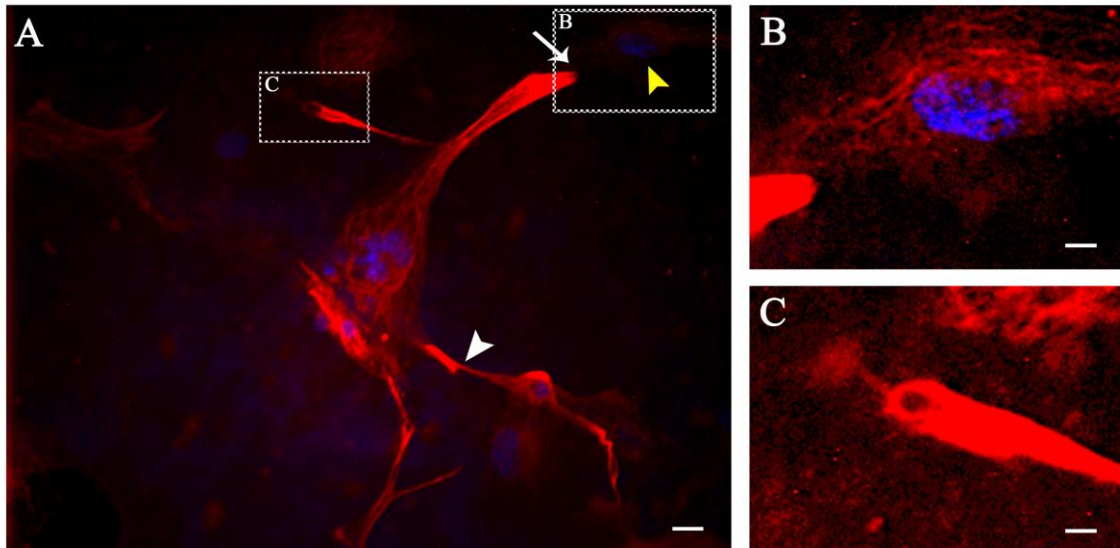


Figure 11: Neural stem cells extend processes through porous membrane and can establish contact with MEFs. Native SSEA-1-enriched neural epithelial cells were cultured on a porous Transwell™ membrane in contact with MEFs. Cultures were fixed and immunolabeled to identify neural epithelial cells (nestin, red) and nuclei (DAPI, blue). (A) Neural epithelial cells formed cell aggregates which produced cellular processes extending toward single neural epithelial cells (white arrowhead) or through pores in the membrane. The dashed box areas labeled B and C in panel A are shown in higher magnification to the right. Panel (B) shows cellular processes passing through a pore and establishing contact with a nucleus from an MEF (yellow arrowhead, panel A). Note the larger nucleus is associated with the MEF. Panel (C) highlights a cellular process passing through a pore on the membrane. In order to increase the signal to noise present on both sides of the membrane in panels (B) and (C), the plane of focus was shifted and images were over exposed for contrast. Scale bar is 25 μm .

cell fate choice.

Vascular cells influence gene expression pattern in immortalized neural epithelial cells

The presence and proximity of vascular cells to the developing neural epithelial cells may potentially influence gene expression patterns in neural epithelial cells. In order to assess the impact of vascular cells on neural cell development, neural epithelial cells were cultured in either solo (S), contacting (+CC), or non-contacting (-CC) coculture with vascular cells. Changes in neural epithelial cell gene expression patterns were assessed (Figure 12). The small ribosomal subunit gene, 18S, was used as a reference gene and showed a similar intensity for solo and contacting coculture compared with a slightly higher intensity in non-contacting coculture. Transcription factors associated with neural stem cells (Pax6, Sox2, and Id1) exhibited similar band intensity across coculture conditions but not among the different transcription factors. The similarity in band intensity indicates that the population of neural stem cells is comparable in all three coculture treatments. This type of qualitative expression pattern assessment confirms that all the appropriate genes are expressed, but there are likely differences in expression pattern associated with the presence of vascular cells in the system.

To further assess the influence of vascular cells on neural epithelial cells, the mitotic profile of neural epithelial cells cultured in solo, contacting, and non-contacting coculture was determined (Figure 13A). Neural epithelial cells cultured in these conditions were labeled with tracking dyes prior to fixation and were labeled with DAPI to visualize the nuclei after fixation. Five representative images from each condition were

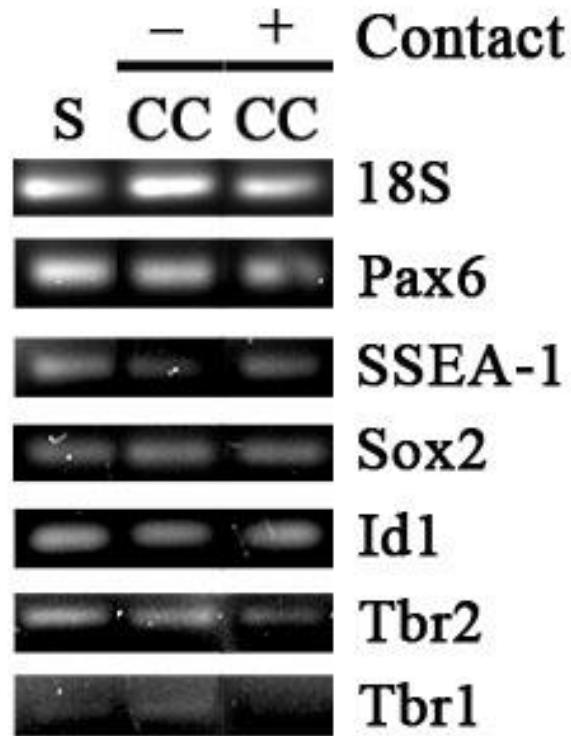


Figure 12: Immortalized SSEA-1-enriched neural epithelial cells display a shift in gene expression patterns when cocultured with vascular cells. WT neural epithelial cells were cultured either in solo, contacting, or non-contacting coculture with MEFs and BAEs (vascular cells) for 5 days. Total RNA was collected from neural epithelial cells and reverse transcribed to cDNA. Standard PCR was used to determine qualitative gene-specific expression. Small ribosomal subunit 18S was used as a reference gene. Pax6, SSEA-1, and Sox2 reflect the presence of neural stem cell populations within each treatment. Id1, neural stem and progenitor cell marker, and Tbr2, neural progenitor cell marker, were also detected in each treatment. Expression of Tbr1, a transcription factor, that identifies post-mitotic neural lineages was present in all culture conditions, although the band intensity was brightest in non-contacting coculture. This experiment was repeated 2X with similar results.

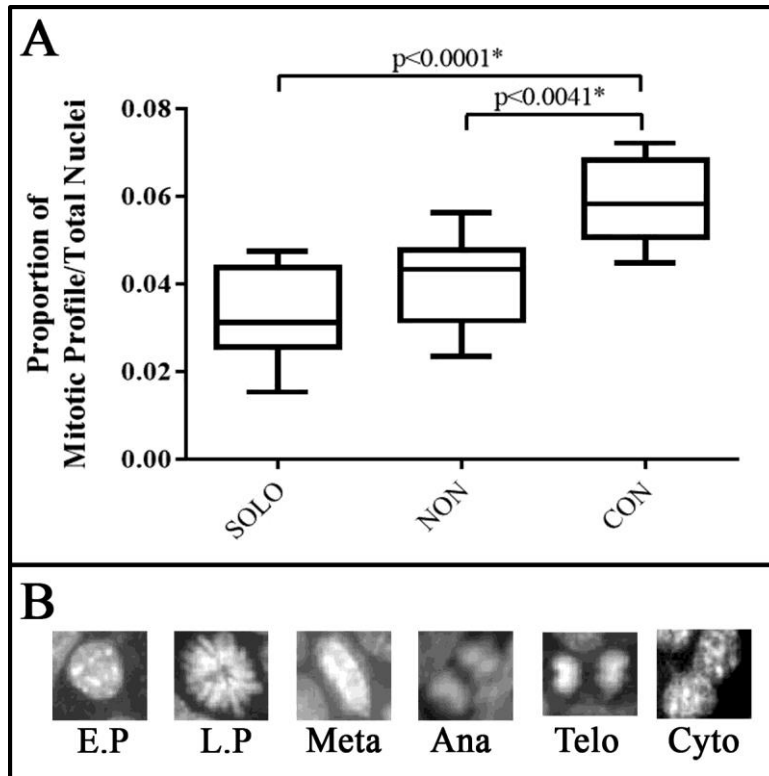


Figure 13: The presence of vascular cells leads to an increase in the mitotic profile displayed by neural epithelial cells. WT immortalized SSEA-1-enriched neural epithelial cells (NSCs*) were labeled with PKH dye prior to being cultured in either solo, contacting, or non-contacting coculture with MEFs (pericytes precursors) and endothelial cells. Cultures were fixed after 5 days in culture and were labeled with DAPI to visualize nuclei. Five representative images were captured at 40X for each coculture treatment. A 5x5 grid was laid over each image and nuclei scored according to the phases shown. The values represent the mean total +/- standard deviation for each of the 5 fields of view. (A) Images were used to assess the proportion of the mitotic profiles (relative to total cell number) in parallel solo and coculture conditions. The NSCs* in direct contact with vascular cocultures exhibited a significantly higher number of mitotic cells compared to

NSCs* in solo and non-contacting coculture ($p < 0.0001$ and $p = 0.0008$, respectively; One way ANOVA with Tukey's *post-hoc* test). (B) Images depict representative mitotic profiles used for classification. This experiment was repeated 2X and the results for each experiment were scored by 2 independent investigators to ensure consistency across the samples. Abbreviations are as followed E.P=Early Prophase, L.P=Late Prophase, Meta=Metaphase, Ana=Anaphase, Telo=Telophase, and Cyto=Cytokinesis.

taken and used to determine the proportion of mitotic profiles relative to total number of nuclei. Classifications of mitotic profiles selected are indicated in Figure 13B along with representative images associated with those stages. Neural epithelial cells cultured with vascular cells display a higher proportion of mitotic profiles compared to cells cultured in the absence of the vascular cells. Indicating that the presence of vascular cells leads to a higher proportion of mitotic profiles exhibited by neural epithelial cells. The proximity of vascular cells leads to a difference in mitotic profiles, where neural epithelial cells cultured in contact with vascular cells exhibited a significantly higher proportion of mitotic profiles than non-contacting coculture (One-way ANOVA, $p < 0.0001$). These results demonstrate that the presence and proximity of vascular cells to neural epithelial cells can lead to an increase in their mitotic profiles possibly correlated with an increase in neural epithelial cell proliferation.

The change in neural epithelial cell proliferation due to the presence of vascular cells could be a result of shifts in gene expression associated with cell fate determination. To assess gene expression, WT SSEA-1-enriched immortalized neural epithelial cells were cultured either in solo, contacting, or non-contacting coculture with vascular cells. Total RNA was isolated from neural cells and reverse transcribed to cDNA. Quantitative PCR was used to determine Pax6 (neural stem cells), Tbr2 (neural progenitor cells), and Tbr1 (early lineage neuronal cells) expression (Figure 14). Neural epithelial cells cocultured with vascular cells displayed a decreasing trend in Pax6 expression indicating a possible decrease in neural stem cells within those populations (One way ANOVA $p = 0.6411$). In contrast, Tbr2 expression exhibited an increasing trend in neural epithelial

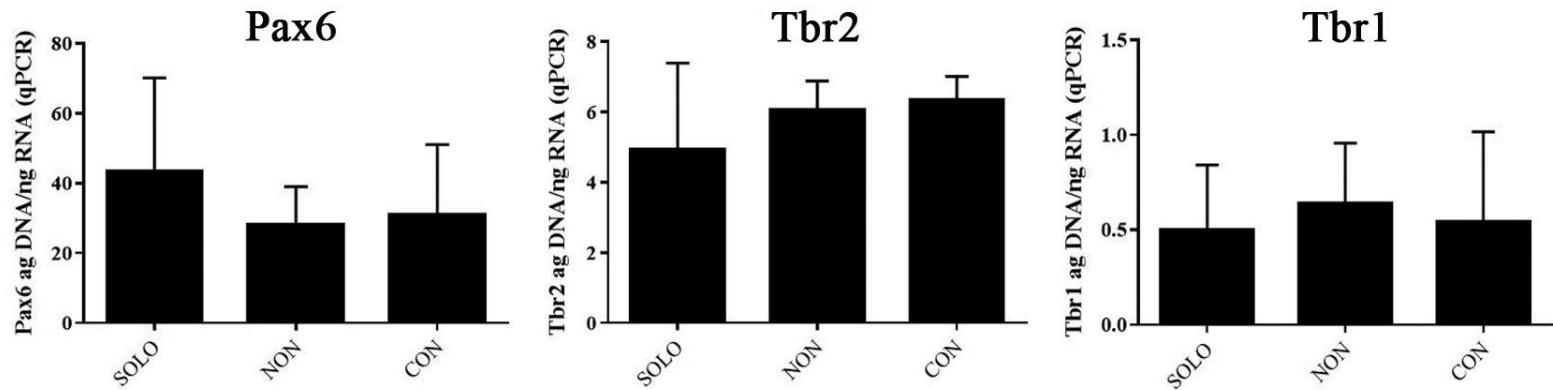


Figure 14: Wild type SSEA-1-enriched neural epithelial cocultured with vascular cells display shifts in expression of genes associated with neural stem cell fate choice. WT immortalized SSEA-1-enriched neural epithelial cells were cultured either in solo, contacting, or non-contacting coculture with vascular cells. Neural cells were isolated and RNA was collected and reverse transcribed to cDNA. Qualitative PCR was utilized to assess expression of Pax6 (neural stem cells), Tbr2 (neural progenitor cells), and Tbr1 (early lineage neuronal cells). Neural epithelial cells exhibit a non-significant decrease in Pax6 expression when cocultured with vascular cells (One way ANOVA $p=0.6411$). Tbr2 expression increase in neural epithelial cells with the presence of vascular cells (One way ANOVA $p=0.3475$). In contrast, neural epithelial cells exhibited a slight increase in Tbr1 expression (One way ANOVA $p=0.8674$). This experiment was repeated 3 times with an $n=3$.

cells when cultured with vascular cells (One way ANOVA $p=0.3475$). Neural epithelial cells in coculture with vascular cells also displayed a slight increase in Tbr1 (One way ANOVA $p=0.8674$). The results for Tbr2 and Tbr1 indicate that neural epithelial cells in coculture with vascular cells are expressing more genes associated with differentiation. Combining this with the Pax6 results, it shows that the presence of vascular cells influences expression of genes associated with neural stem cell differentiation in our neural epithelial cell populations. One thing to take into account with these results is that there is a difference in scale among the genes.

Given the low sample number and the statistical trends (without significance) observed with the qPCR, we wanted to determine if any of the genes shifts in concert. To test this, immortalized SSEA-1-enriched WT neural epithelial cells were cultured either solo, or in contacting or non-contacting coculture with vascular cells. Total RNA was collected from neural cells, reverse transcribed to cDNA, and gene expression was assessed by qPCR. An analysis of covariance was conducted comparing Pax6 (neural stem cells) against expression of Sox2 (stem cells), ID1 (neural stem and progenitor cells), and Tbr2 (neural progenitor cells; Figures 15-17), respectively. Expression of Pax6 in WT neural epithelial cells grown in solo culture exhibits a strong, negative correlation with Sox2 ($R^2=0.978$; Figure 15) indicating that as Pax6 expression increases the expression of Sox2 decreases. The opposite correlation relationship is seen with Id1 ($R^2=0.929$; Figure 16) and Tbr2 ($R^2=0.967$; Figure 17) when plotted against Pax6 expression. This pattern changed when neural epithelial cells were cultured in contact with vascular cells. Pax6 and Sox2 displayed a weak correlation ($R^2=0.011$) as well as Pax6 with Id1 ($R^2=0.0007$) and Tbr2 ($R^2=0.004$). This shows that as Pax6 expression

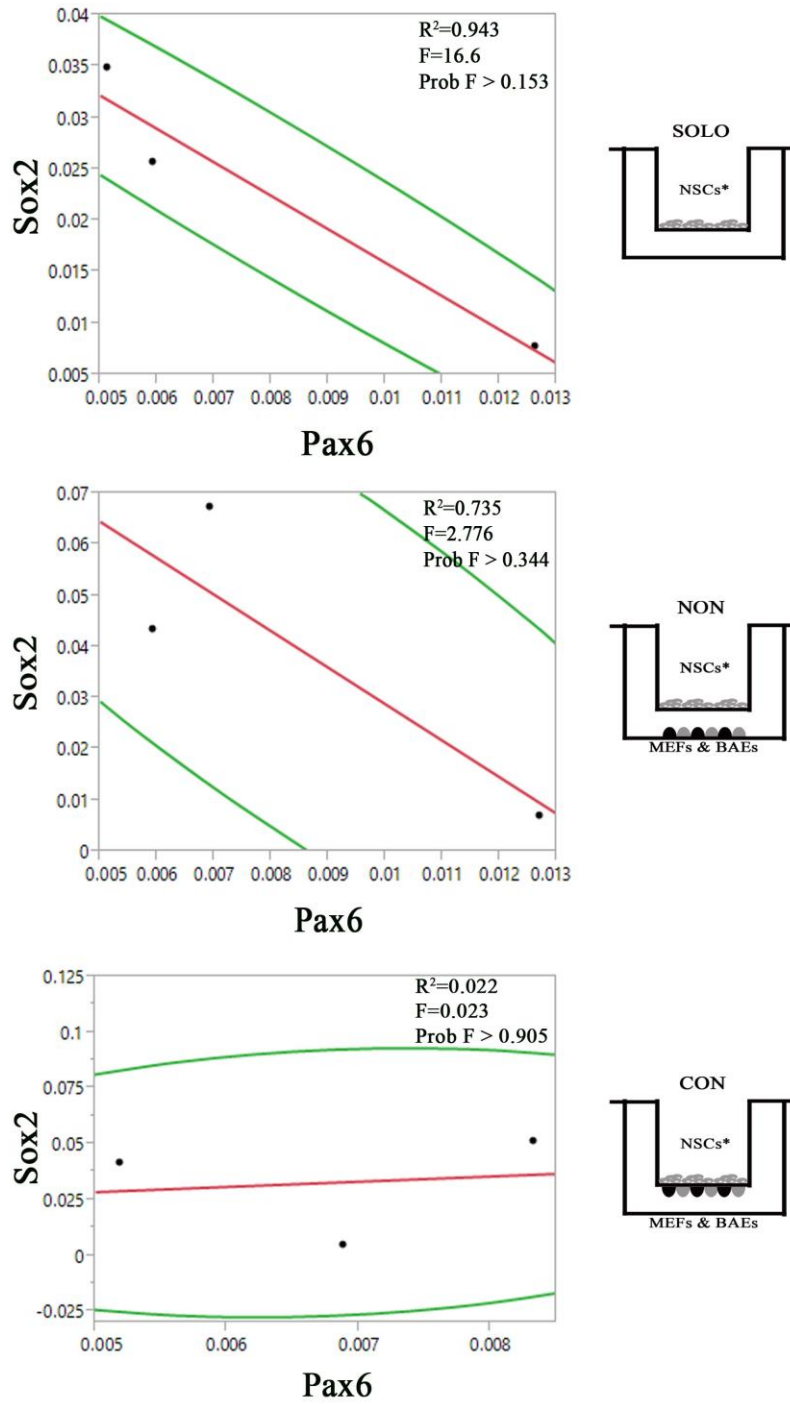


Figure 15: Wild type neural epithelial cells cultured in contacting coculture display no correlation between Pax6 and Sox2 gene expression. SSEA-1-enriched WT neural

epithelial cells were cultured either in solo, contacting, or non-contacting coculture with vascular cells for 5 days. Total RNA was isolated from the neural epithelial cells and reverse transcribed into cDNA. Gene expression for Pax6 (neural stem cells) and Sox2 (neural progenitor cells) was assessed using qPCR. A correlation analysis indicated a positive correlation between Pax6 and Sox2 in both solo and non-contacting coculture with vascular cells ($R^2=0.978$ and $R^2=0.999$, respectively). Neural epithelial cells cultured in contacting coculture displayed no correlation between Pax6 and Sox2 expression ($R^2=0.011$). Linear fit (red line) and bivariate normal ellipse at 95% (green line) are indicated on the graph. The experiment was repeated 3 times with an $n=3$ for each genotype. Table 4 in appendix includes all statistical values for reference.

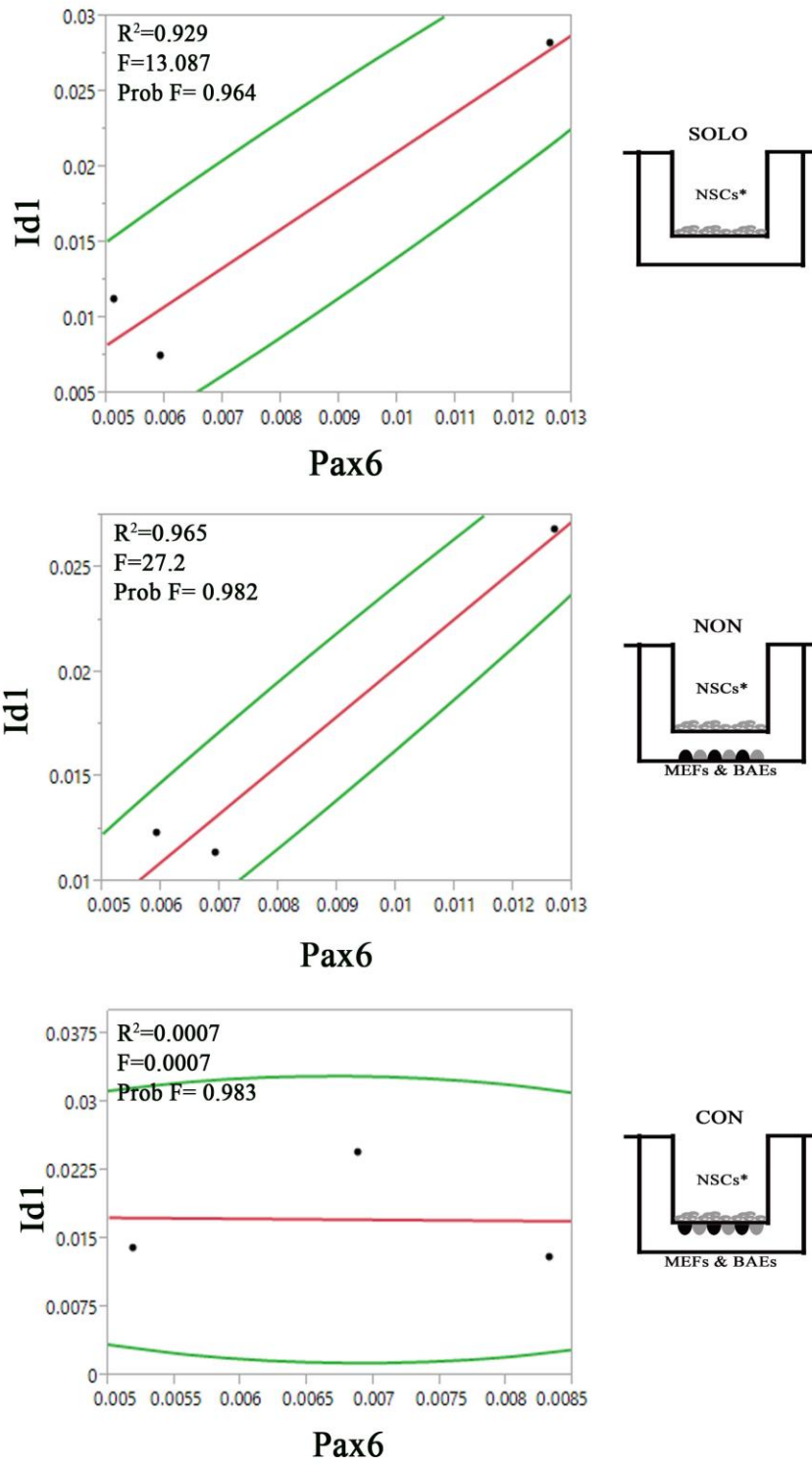


Figure 16: Contact with vascular cells disrupts the correlation of Pax6 and Id1 in WT neural epithelial cells in contacting coculture. For 5 days WT immortalized

SSEA-1-enriched neural epithelial cells were cultured either in solo, contacting, or non-contacting coculture with vascular cells. Neural epithelial cells were isolated and total RNA was collected and reverse transcribed to cDNA. Quantitative PCR was used to determine gene expression of Pax6 (neural stem cells) and Id1 (neural progenitor cells). Neural stem cells in both solo and non-contacting coculture displayed a positive correlation in Pax6 and Id1 gene expression ($R^2=0.929$ and $R^2=0.965$, respectively). No correlation was seen between Pax6 and Id1 gene expression in neural epithelial cells cultured in contacting coculture with vascular cells ($R^2=0.0007$). Linear fit (red line) and bivariate normal ellipse at 95% (green lines) are indicated on the graphs. The experiment was repeated 3 times with an $n=3$ for each genotype. All statistical values are provided in appendix Table 5 for reference.

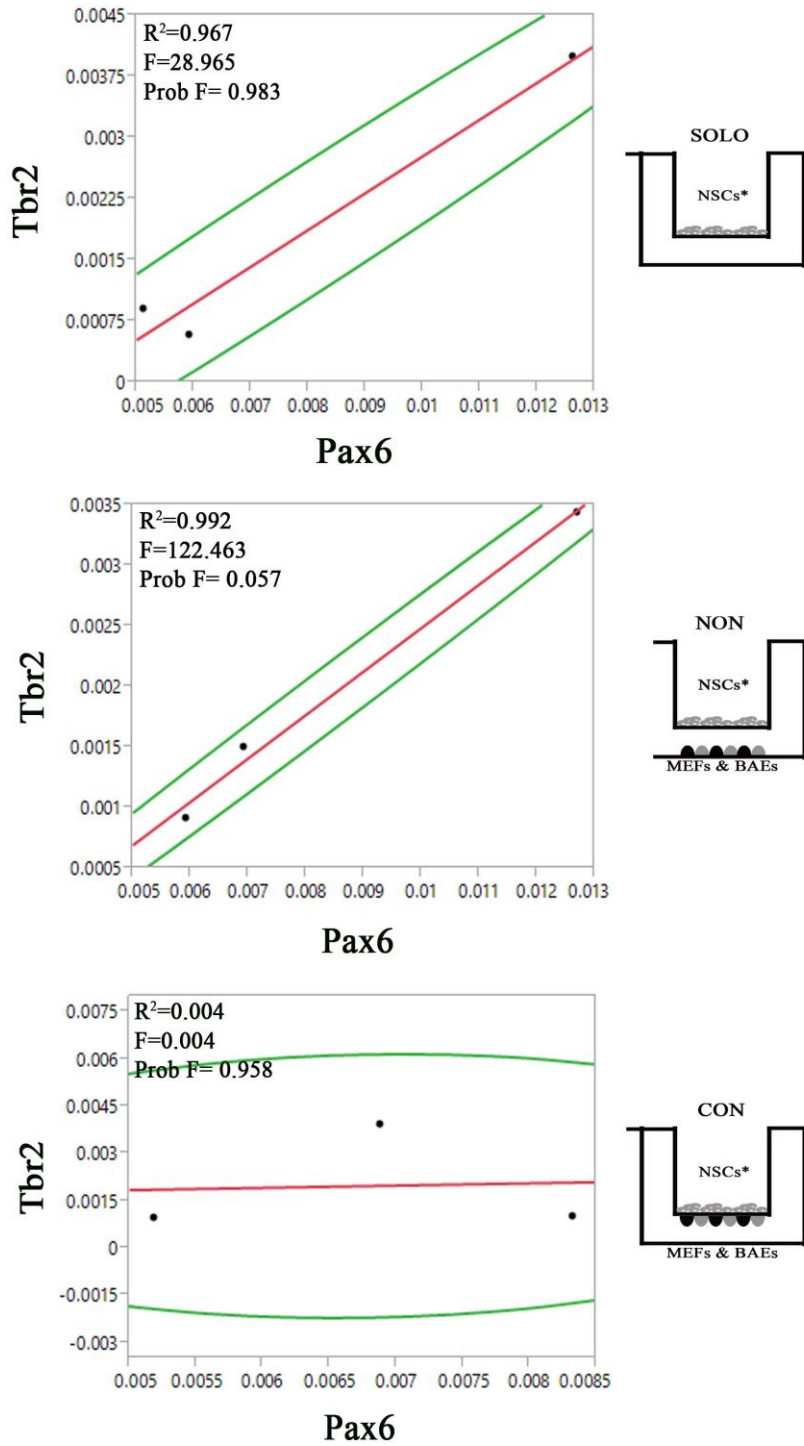


Figure 17: Wild type neural epithelial cells cultured in contacting coculture display a disruption in correlation between Pax6 and Tbr2 gene expression. WT

immortalized SSEA-1-enriched neural epithelial cells were cultured for 5 days in either solo, contacting or non-contacting coculture with vascular cells. Total RNA was isolated from neural cells and reversed transcribed to cDNA which was utilized with qPCR to assess gene expression. A correlation analysis was conducted with Pax6 (neural stem cell maker) against Tbr2 (neural progenitor cells). Pax6 expression in neural epithelial cells cultured solo exhibited strong correlations with Tbr2 ($R^2=0.967$). The same correlation pattern was also displayed in non-contacting cultures. Neural epithelial cells in contacting coculture did not exhibit a correlation between Pax6 and Tbr2 ($R^2=0.004$). Linear fit (red line) and bivariate normal ellipse at 95% (green lines) are indicated on the graphs. This experiment was repeated 3 times with all values depicted on the graph for an n=3 for each genotype. All statistical values are provided in appendix Table 6 for reference.

increased, the expression of Sox2, Id1, and Tbr2 expression did not display a correlated shift in expression patterning. In contrast, when vascular cells are in non-contact with neural epithelial cells there is significant correlation between Pax6 and Sox2 expression ($R^2=0.999$ and $\text{Prob}>F=0.0153$). Strong correlations are also noted with Id1 and Tbr2 against Pax6 expression ($R^2=0.965$ and $R^2=0.992$, respectively). The correlations displayed by non-contacting neural epithelial cells resemble the correlation pattern seen with neural cells in solo culture. The results for solo and non-contacting coculture suggests that there is a directional shift in gene expression that occurs within the neural epithelial populations.

Based off the shifts in neural epithelial cell gene expression in the presence of vascular cells, we wanted to assess whether a similar shift occurs with Vegf isoform production. To test this idea, WT SSEA-1-enriched neural epithelial cells were cultured either in solo, contacting coculture, or non-contacting coculture with vascular cells. A qualitative assessment of shifts in Vegf isoform production was conducted using PCR and gel electrophoresis. Neural epithelial cells cultured solo exhibited a higher intensity of Vegf164 followed by Vegf120, and Vegf188 displayed the weakest intensity (Figure 18). The pattern displayed by neural cells cultured solo resembles what is seen in vivo at E9.5⁶⁹. This pattern changes when neural epithelial cells are cultured with vascular cells. Neural cells in contact with vascular cells had a higher intensity of Vegf164, but unlike the solo condition, Vegf188 intensity was greater than Vegf120. These results indicate that Vegf188 expression may increase when neural epithelial cells are in contact with vascular cells. Neural epithelial cells cultured in non-contacting coculture with vascular cells exhibited a similar intensity for all three Vegf isoforms. The intensity of Vegf164

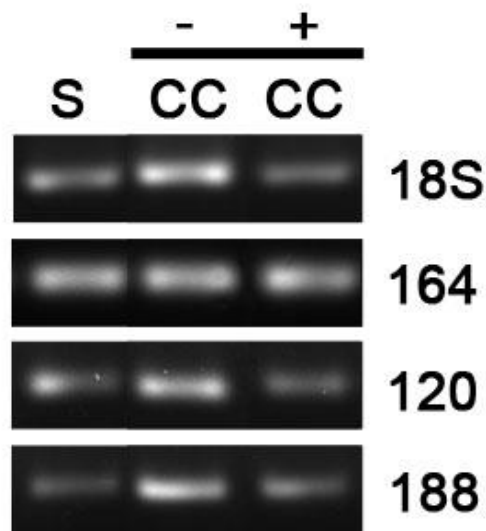
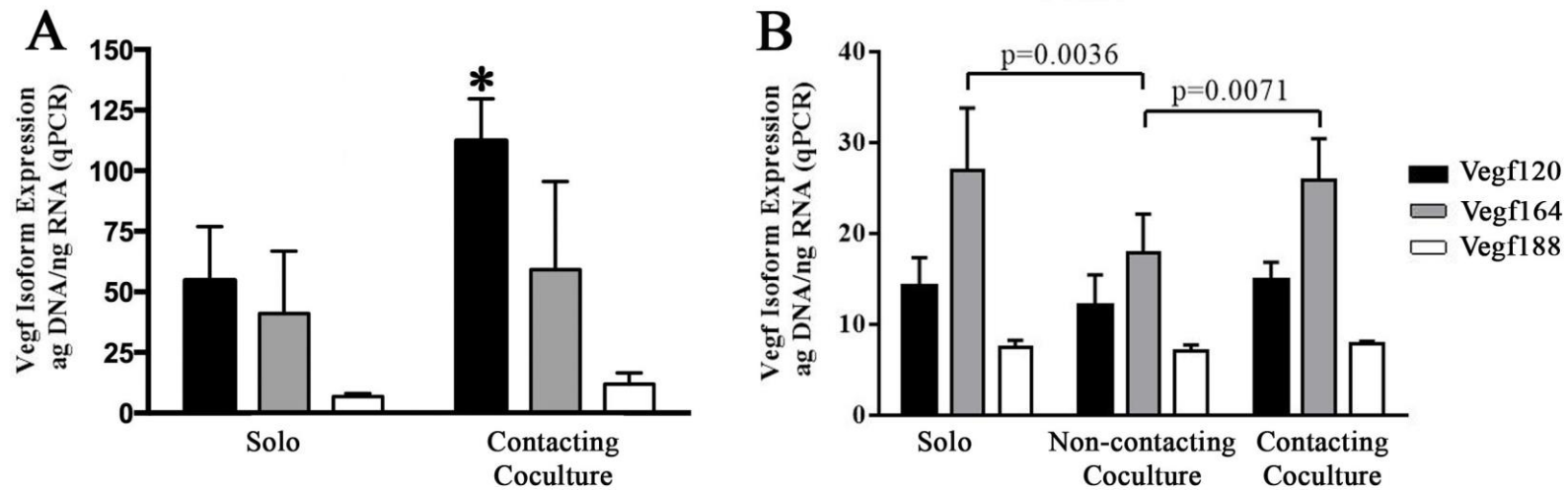


Figure 18: Wild type neural epithelial cells cocultured with MEFs express all three Vegf isoforms. WT immortalized SSEA-1-enriched neural epithelial cells were cultured in solo (S), contacting (CC+), or non-contacting (CC-) coculture with MEFs. Total RNA was isolated from WT neural epithelial cells, and used in standard reverse-transcription PCR to generate a qualitative comparison of Vegf isoform expression across culture conditions. The 18S small ribosomal subunit was used as a reference gene for comparison. Vegf isoforms are expressed in all three culture conditions. Vegf164 band intensity was uniform in all three culture treatments. In contrast, the band intensity for both Vegf120 and Vegf188 was higher in non-contacting coculture compared to solo and contacting coculture. The relative proportion of each specific Vegf isoform band intensity differs in neural epithelial cells in solo and contact while the band intensity of Vegf isoforms in non-contacting coculture appears uniform across isoforms.

remained the same as the other conditions but the intensity of Vegf120 and Vegf188 both increased indicating that soluble factors produced by vascular cells may lead to a shift in Vegf isoform production. Overall, these results show that the intensity of Vegf164 remains relatively similar across the treatments, and the only shifts in Vegf isoform expression occurs with Vegf120 and Vegf188 when in the presence of vascular cells.

While neural epithelial cells as well as vascular cells (specially MEFs) express Vegf isoforms during development, the composition of the isoforms they produce differs from one another. In order to determine the predominant Vegf isoforms produced by each cell source in the heterotypic cell culture model, we cultured pericytes and neural epithelial cells separately in coculture conditions. The first coculture condition consisted of culturing pericytes in contacting coculture with endothelial cells. Pericytes are the primary source of Vegf in the culture where as endothelial cells do not express significant amounts of Vegf ⁹. The second condition entailed plating WT immortalized neural epithelial cells in either solo, contacting, or non-contacting coculture with vascular cells (pericytes and endothelial cells). Total RNA was isolated from pericytes and neural epithelial cells, reverse transcribed to cDNA, and utilized with qPCR to assess Vegf isoform expression. Pericytes cultured alone expressed all three Vegf isoforms with Vegf120 exhibiting the highest expression followed by Vegf164 and Vegf188 (Figure 19A). Pericytes in contacting coculture with endothelial cells exhibited an increase in Vegf isoform expression with a significant increase in Vegf120 expression (asterisks indicates $p < 0.005$; Dunnett's *post-hoc* test). These results indicate that pericytes increase Vegf isoform production when in the presence of endothelial cells ⁹. Similar to pericytes,



70

Figure 19: Vascular cells and immortalized neural epithelial cells display distinct Vegf isoform expression when cocultured. Vascular pericytes (A) and SSEA-1-enriched neural epithelial cells (B) were isolated and total RNA was collected. RNA was reverse transcribed into cDNA and Vegf isoform expression was assessed by qPCR. (A) Pericytes exhibited a significant increase in Vegf120 expression when cocultured with endothelial cells (asterisks indicates $p < 0.005$; Dunnett's post-hoc test). A slight increase in pericytes' expression of Vegf164 and Vegf188 isoforms in coculture was also noted, although not statistically significant. (B) In contrast, immortalized neural epithelial cells displayed higher expression of Vegf164 compared to the other Vegf isoforms in culture. Expression levels of Vegf isoforms do not appear to shift drastically between the different coculture conditions. Both experiments were repeated 3 times with an $n=3$.

neural epithelial cells also express all three Vegf isoforms but the predominant isoform is Vegf164 followed by Vegf120 and Vegf188 (Figure 19B). Expression of Vegf isoforms by neural epithelial cells exhibit small shifts when cultured with vascular cells. Neural epithelial cells in solo and contacting coculture produced significantly more Vegf164 than neural cells in non-contacting coculture (Holm-Sidak *post hoc* $p=0.0036$ and $p=0.0071$, respectively). Vegf120 and Vegf188 expression do not appear to change between solo and coculture treatments. These results indicate that neural epithelial cells decrease Vegf164, when cocultured with vascular cells, with no significant change in the other 2 isoforms. In addition Vegf164 is the predominant Vegf isoform expressed by neural epithelial cells, regardless of culture conditions.

The influence of vascular cells on neural epithelial cells differs with an altered Vegf isoform profile

In order to test the effects of an altered Vegf isoform profile on neural epithelial cell fate, we first had to determine the cell composition, based on gene expression profile, of immortalized SSEA-1-enriched neural epithelial populations derived from Vegf isoform forebrains. To assess the cell composition, RNA was collected from immortalized SSEA-1-enriched neural epithelial cells, was reverse transcribed to cDNA, and then gene expression was quantified using qPCR, targeting lineage-specific genes. Figure 20 shows that the isolated SSEA-1-enriched neural epithelial cells exhibit a similar pattern in gene expression with regard to neural stem, progenitor, and differentiated cells. The most predominant gene expressed in both WT and Vegf isoform cells was Id1 followed by Sox2 and Pax6. These three genes, which are associated with rapidly proliferating neural stem cells, had a significantly higher rate of expression

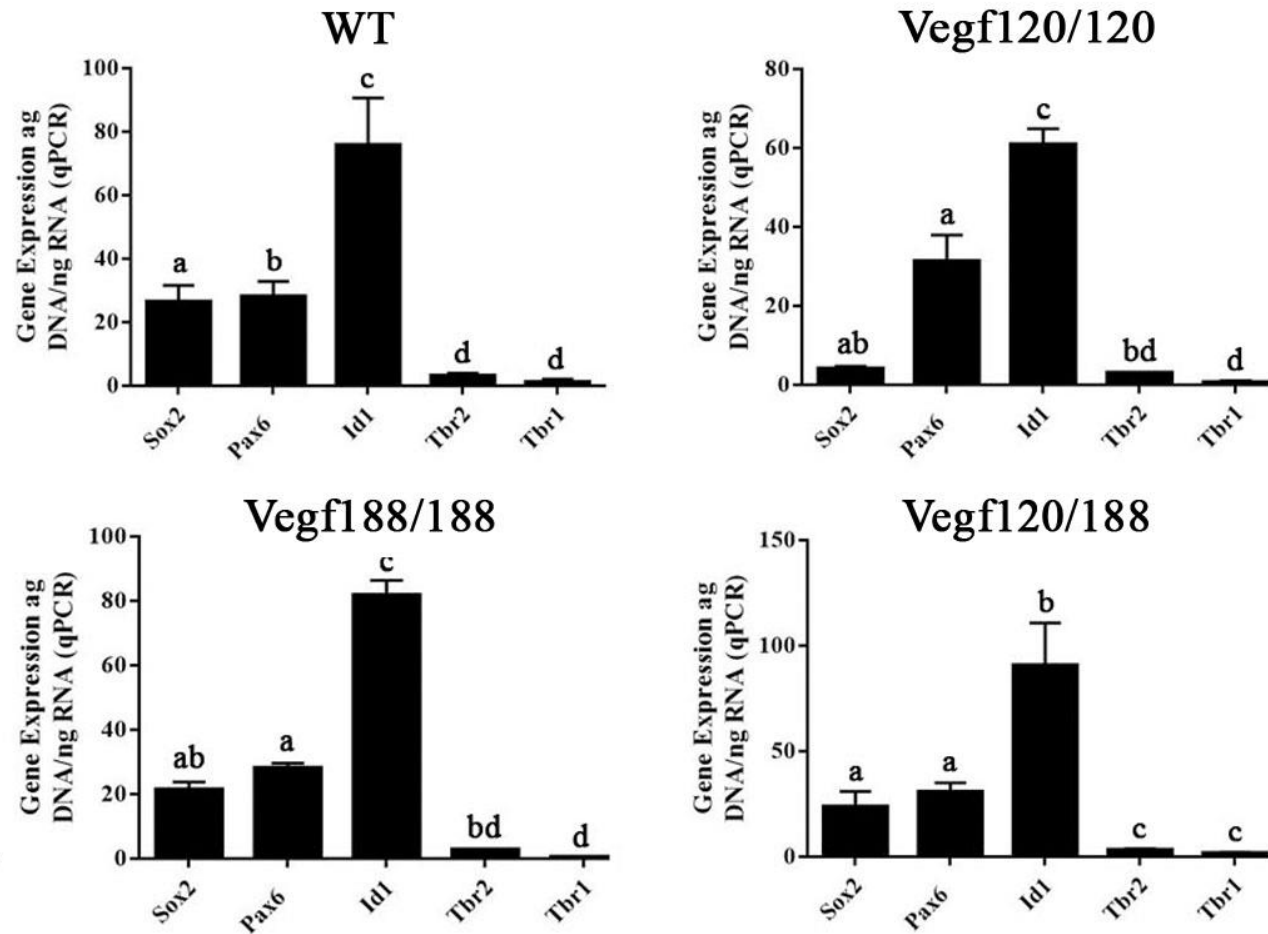


Figure 20: Immortalized neural epithelium derived from Vegf isoform mice show a similar neural stem cell gene expression profile compared to WT. Total RNA was isolated from WT and Vegf isoform immortalized neural epithelial

cells and reverse transcribed to cDNA. Quantitative PCR was used to assess gene expression patterns. Expression of Pax6, Sox2, and Id1 reflect the presence of neural stem cells in the populations. Differentiating neural cells were detected with Tbr2 (progenitor cells) and Tbr1 (post mitotic neural cells) expression. Immortalized neural epithelial cells isolated from WT and Vegf isoform forebrains display significant differences in gene expression patterns associated with neural stem, progenitor, and differentiating neurons (One way ANOVA; $p < 0.0001$ respectively for each genotype). Differences between specific genes indicated with lower case letters between genes reflecting a non-statistical difference between a given pair. The significantly higher expression levels present for neural stem cell markers in both WT and Vegf isoform neural epithelial cells indicates these populations consist primarily of neural stem cells. Note that the y axis differs between WT and Vegf isoform neural epithelial populations. This experiment was repeated 2 X with an n of 5-7 for ≥ 3 independent litter sources.

compared to neural progenitor gene (Tbr2) and differentiated neural cells (Tbr1; Figure 19)^{41, 70, 71}. These results indicate that the population of SSEA-1-enriched neural epithelial cells isolated from the forebrains of WT and Vegf isoform embryos consists primarily of neural stem cells. Expression of Tbr2 and Tbr1 varied depending on the presence of specific Vegf isoforms. Most notable is the fact that Tbr2/Tbr1 expression levels were significantly lower than neural stem cell genes (note difference in y-axis scale). The low expression levels of Tbr2 and Tbr1 suggest that a few progenitor and differentiated neural cells are possibly present in SSEA-1-enriched populations. These cells may arise due to being isolated during the reverse panning process or arose due to differentiation of neural stem cells after isolation.

While the pattern in gene expression is similar across the different neural epithelial populations, there is a difference in gene expression between the WT and Vegf isoform neural epithelial cells (Figure 21). Expression of Pax6 varies slightly between WT and Vegf isoform neural epithelial cells by a non-significant increase in expression levels in Vegf120 and Vegf 120/188 neural cells (One way ANOVA $p=0.6794$). Expression of a neural progenitor gene, Tbr2, also exhibits slight variations between WT and Vegf isoform neural epithelial cells but the difference is not significant (One way ANOVA $p=0.9782$), largely due to the variation in the WT and Vegf120/188 populations which could have resulted in type II error. A more noticeable variation in gene expression between WT and Vegf isoform cells is seen with a significant difference in Tbr1 expression and a non-significant difference with Id1 (One way ANOVA, $p=0.0095$ and $p=0.3361$, respectively). Both genes exhibit a similar pattern where Vegf120 and Vegf188 neural epithelial cells display a decrease in Id1 and Tbr1 compared to WT and

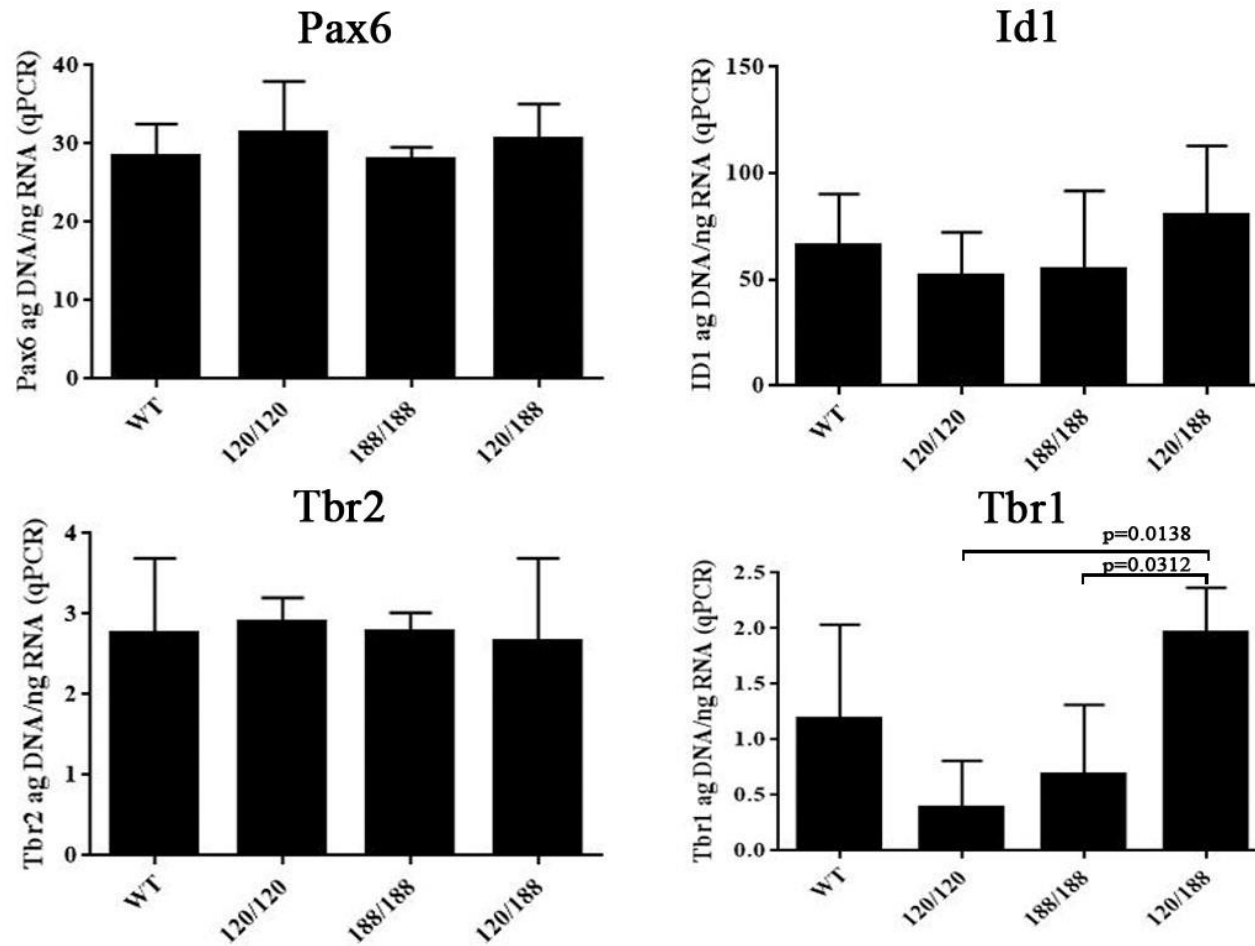


Figure 21: Comparison of a gene-specific perspective reveals clear patterns of NSC genes across genotypes.

Immortalized SSEA-1-enriched neural epithelial cells were cultured between 2-3 weeks before total RNA was isolated.

RNA was reverse transcribed to cDNA which was used to determine expression of genes associated with neural stem cell fate choice with qPCR. Pax6 and Id1 (neural stem cell transcription factors) and Tbr2 (neural progenitor cells) did not significantly differ between WT and Vegf isoform neural epithelial populations (One way ANOVA; $p=0.6794$, $p=0.3361$, and $p=0.9782$ respectively). A significant difference was noted within the neural epithelial populations for post mitotic neural cells (Tbr1; One way ANOVA; $p=0.0095$). A Tukey's *post hoc* determined that Vegf120/188 neural cells significantly differed from both Vegf120 and Vegf188 neural epithelial cells ($p=0.0138$ and $p=0.0312$, respectively). The difference in y axis scale reflects differences in expression levels of specific gene expression, based on internal standard curves. Each experiment is $n=5-7$ with individuals from 3 independent litters.

Vegf120/188 cells. Expression of Tbr1 showed a significant difference in mean values via One-way ANOVA, but a Tukey's *post hoc* indicated that there was no significant difference in Tbr1 expression between WT and Vegf isoform neural epithelial cells. These results indicate that while neural epithelial cells express the desired neural associated genes, the concentration of these transcripts varies with an altered Vegf profile.

Neural epithelial cells isolated from WT and Vegf isoform forebrains express the expected Vegf isoform profile associated with the genotype of the cell source. This was assessed by first establishing the Vegf isoform profile *in vivo* at E9.5 (Figure 22A). E9.5 WT forebrain neural epithelium express all three Vegf isoforms in varying concentrations with Vegf164>Vegf120>>>Vegf188. Forebrains isolated from Vegf isoform mice express only their expected isoform and do not express any additional Vegf isoforms, thereby confirming that the inheritance pattern of the modified alleles has been consistently maintained in the transgenic mouse lines. Second, Vegf isoform profile was assessed in immortalized SSEA-1 enriched neural epithelial cells isolated from WT and Vegf isoform mice (Figure 22B). WT Immortalized neural epithelial cells express all three Vegf isoforms. While Vegf120, Vegf188, and Vegf120/188 neural epithelial cells all express the expected Vegf isoforms. These results indicate that WT and Vegf isoform immortalized neural epithelial cells maintain expression of the expected Vegf isoform profile even after lenti-virus SV40 immortalization.

In order for neural epithelial cells to be influenced by vascular cells they have to be able to respond to factors released by vascular cells, whether juxacrine or paracrine. In addition, neural stem and progenitor cells need to migrate effectively to form cortical

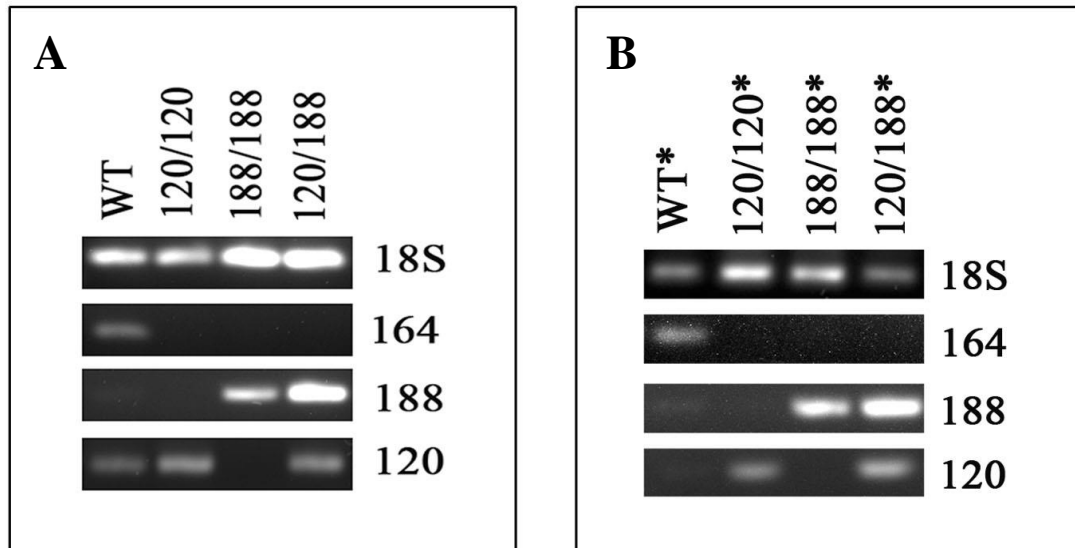


Figure 22: Native and immortalized neural epithelial cells exhibit distinct Vegf isoform expression profiles. Total RNA was isolated from native and immortalized neural epithelial cells (indicated by asterisk). RNA was reverse transcribed into cDNA and Reverse Transcription-PCR was conducted to validate Vegf isoform expression. Expression of 18S was used as a reference gene. WT native and immortalized neural epithelial cells express all three Vegf isoforms with varying intensity between each genotype. Both native and immortalized neural epithelial cells derived from Vegf isoform mice express the expected Vegf isoform profile appropriate for each individual genotype.

layers⁴⁵. To assess neural cell response, a migration assay was conducted to determine (1) if soluble factors released by vascular cells can induce migration of neural epithelial cells to the signal source and (2) if Vegf neural epithelial cells migration differs from WT. Neural epithelial cells were plated on Transwell™ membranes (no cellular contact) that allow cellular migration with or without MEFs plated on the bottom of the well. After 5 days in cultures the neural epithelial cells were fixed and labeled to determine the number of migrated neural epithelial cells on the underside of the membrane. WT and Vegf isoform neural epithelial cells migrated when MEFs were not present indicating immortalized neural epithelial cells are capable of migration (Figure 23). It also suggest that neural epithelial cells can migrate without soluble cues from vascular cells or neural epithelial cells release their own soluble cues. The migration exhibited by WT and Vegf isoform neural epithelial cells without MEFs present did not differ significantly from one another. When MEFs are present in the coculture system, WT and Vegf isoform neural epithelial-derived cells display statistically significant variation in the number of migrated cells (Two way ANOVA, $p < 0.0001$). Since MEFs were on the bottom of the well and not able to physically contact neural epithelial cells, it indicates that MEFs are producing a soluble factor into the media that influences neural epithelial cell migration. While a trend toward increased migration is demonstrated in both WT and Vegf isoform cells, only WT neural epithelial cells show a significant increase in migration when MEFs are present (blue asterisk, Tukey's *post hoc* $p = 0.0001$). In addition, WT neural epithelial cells displayed a significantly higher number of migrated cells compared to Vegf isoform neural cells (red asterisks, Tukey's *post hoc*, Vegf120 $p = 0.0024$, Vegf188

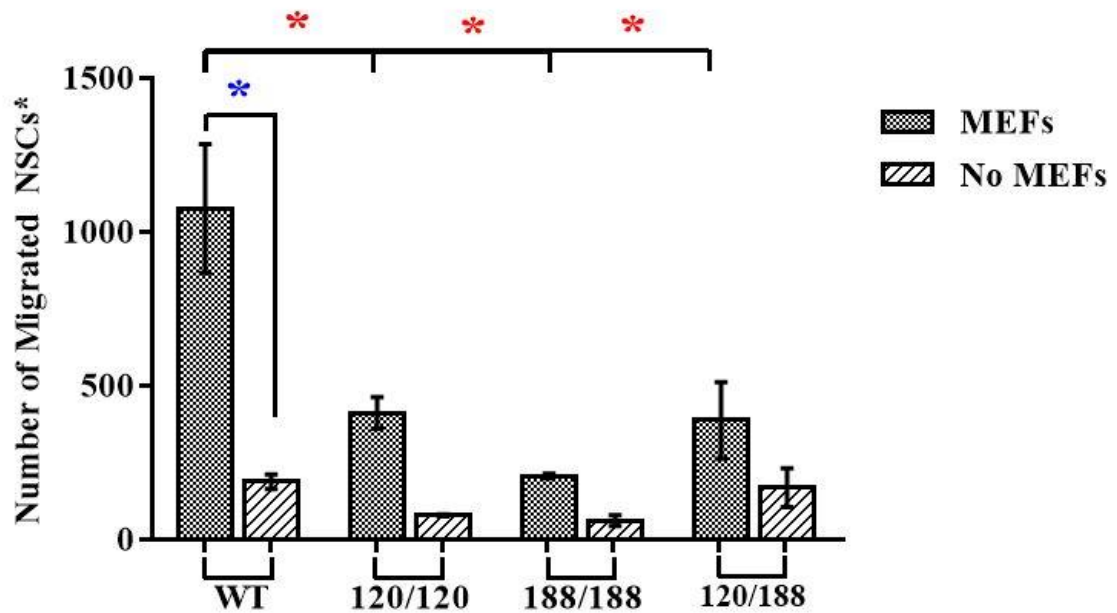


Figure 23: Wild type and Vegf isoform NSCs* exhibit increased migration when cocultured with MEFs. Immortalized SSEA-1-enriched WT and Vegf isoform neural epithelial cells (NSCs*) were cultured for 4 days in either solo or non-contacting coculture with MEFs. NSCs* were fixed and labeled with Phalloidin (filamentous actin) and DAPI (nuclei) to visualize NSCs*. A counting paradigm was designed by dividing the membrane into 8 radial sections with a random point selected in each section to count. The presence of MEFs leads to an increase in NSCs* migration (Two way ANOVA; $p < 0.0001$). WT NSCs* cultured with MEFs had a significant increase in migration compared to WT NSCs* in solo (blue asterisk, Tukey's *post hoc* $p = 0.0001$) as well as Vegf isoform NSCs* cultured with MEFs (red asterisks, Tukey's *post hoc* Vegf120 $p = 0.0024$, Vegf188 $p = 0.0002$, and Vegf120/188 $p = 0.0017$). This experiment was repeated three times and a representative experiment is shown with an $n = 3$ for each sample set. Statistical tests were conducted with values normalized to expression of 18S.

p=0.0002, and Vegf120/188 p=0.0017). The decrease in migration by Vegf isoform could be a result of the neural epithelial cells not being able to produce all three Vegf isoforms. This suggests that neural epithelial cells may need to produce all three Vegf isoforms in order for proper migration.

Due to the nature of neural stem cells during cortical development the migrational response exhibited by neural epithelial cells may be connected to a change in cellular proliferation. To test this, WT and Vegf isoform immortalized SSEA-1-enriched neural epithelial cells were cultured solo, in contacting, and in non-contacting coculture with vascular cells. Neural cells were labeled with tracking dyes and fixed to assess total nuclei. WT neural epithelial cells exhibited a significant difference in total nuclei between solo and coculture (Figure 24, One way ANOVA, $p < 0.0001$). Contacting WT had a significantly larger number of cells compared to both solo and non-contacting coculture (Tukey's *post hoc*; $p < 0.0001$ for both). This indicates that the close proximity of vascular cells to WT neural epithelial cells leads to an increase in cell proliferation or survival. The assay was conducted for a long enough period of time that survival could have had an impact. Vegf120 neural epithelial cells did not show a significant difference in total nuclei between the different culture treatments (One way ANOVA, $p = 0.4035$) and overall the cell numbers were low. In addition, Vegf188 neural cells did not show a statistical difference (One way ANOVA, $p = 0.1833$). The number of total nuclei between cultures resulted in high standard deviation that may have resulted in a Type II error. There was a significant difference in total nuclei between solo and cocultures with Vegf120/188 neural epithelial cells (One way ANOVA, $p = 0.0008$). Neural epithelial

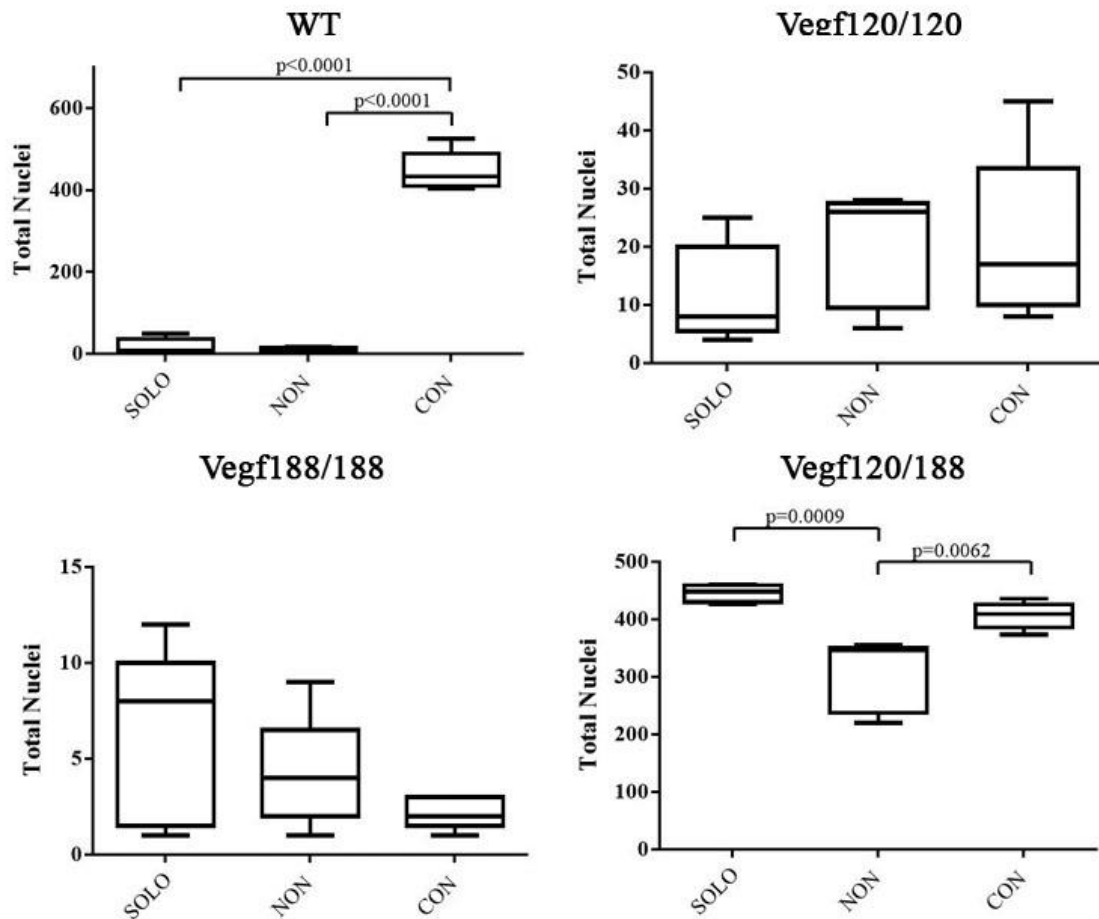


Figure 24: Coculture with MEFs leads to a difference in NSCs* total nuclei profiles that varies with Vegf isoform profiles. WT and Vegf isoform neural epithelial cells were labeled with an intracellular fluorescent dye and cocultured with MEFs either in solo, contacting or non-contacting coculture for 4 days. Cells were fixed and labeled with DAPI to visualize nuclei and 5 images representing 20% of the total membrane area were captured. Images were used to determine the total number of nuclei. WT neural epithelial cells display a significant increase in nuclei in contacting coculture compared to solo and non-contacting cultures ($p < 0.0001$ for both). A lower number of total nuclei is seen with Vegf120 and Vegf188 neural epithelial cells and these cells exhibited no significant

difference between solo, contacting, and non-contacting coculture (One way ANOVA; $p=0.4035$ and $p=0.1833$ respectively). Vegf120/188 exhibited a comparable y axis range of total nuclei to WT neural epithelial cells with a significant difference in total nuclei of neural epithelial cells in solo, contacting, and non-contacting cocultures (One way ANOVA; $p=0.0008$).

cells cultured solo and in contacting coculture displayed no significant difference between each other (Tukey's *post hoc*, $p=0.364$) but both were significantly different than non-contacting coculture (Tukey's *post hoc*, $p=0.0009$ and $p=0.0062$, respectively). The range of total nuclei for WT and Vegf120/188 neural epithelial cells was significantly higher than the range for Vegf120 and Vegf188 neural cells (WT:Vegf120 $p=0.0067$, WT:Vegf188 $p=0.0025$, and Vegf120/188:Vegf120 and Vegf188 $p<0.0001$). This suggests that more than one Vegf isoform is needed for either a higher amount of proliferation in neural epithelial cells or is required for an increase in survival rate.

The migrational and proliferation response exhibited by neural epithelial cells, due to the presence of vascular cells, may be a result of shifts in gene expression within the neural epithelial cells that results in cell fate changes (i.e. differentiation vs. proliferation). To assess this, WT and Vegf isoform neural epithelial cells were cultured with and without vasculature in solo, contacting, or non-contacting conditions and assessed for correlations in gene expression between Pax6 and Sox2, Id1, and Tbr2. Solo and non-contacting cocultures exhibited similar patterns in correlation against Pax6 expression between WT and Vegf isoform neural epithelial cell (Tables 4-6 in Appendix). A difference in correlation was noted between WT and Vegf isoform neural epithelial cells when vascular cells were in contact with neural cells (Table 1 and Figure 25). WT neural epithelial cells displayed a low correlation between Pax6 and Sox2 ($R^2=0.022$) as well as Pax6 and Tbr2 ($R^2=0.004$). A low negative correlation was noted with Pax6 and Id1 ($R^2=0.0007$; $r= -0.027$; Table 1). These results indicate that in WT neural epithelial cells, Pax6 expression is either being maintained or slightly increased,

Table 1: WT and Vegf isoform neural epithelial cells grown in contacting coculture with vascular cells display expression correlation between Pax6 and genes associated with neural stem and progenitor cells. SSEA-1-enriched immortalized WT and Vegf isoform neural epithelial cells were cultured in contacting coculture with vascular cells for 5 days. Vascular cells were removed and total RNA was isolated from neural cells. RNA was reverse transcribed to cDNA and used with qPCR to assess gene expression. A correlation analysis was conducted for Pax6 against Sox2, Id1, and Tbr2 gene expression. Vegf isoform neural epithelial cells displayed correlations between Pax6 and all three neural progenitor gene markers (Sox2, Id1, and Tbr2). In contrast, WT neural epithelial cells did not display any correlation between Pax6 paired with Sox2, Id1, and Tbr2. This experiment was repeated 3 times with an n=3 for each genotype.

Genotype	Treatment	Gene	R²	F	Prob > F	Correlation
WT	CON	Sox2	0.022	0.023	0.905	0.148
WT	CON	Id1	0.0007	0.0007	0.983	-0.027
WT	CON	Tbr2	0.004	0.0043	0.958	0.066
Vegf120/120	CON	Sox2	0.97	31.856	0.112	-0.985
Vegf120/120	CON	Id1	0.993	146.64	0.0525	0.997
Vegf120/120	CON	Tbr2	0.734	2.763	0.345	0.857
Vegf188/188	CON	Sox2	0.119	0.135	0.776	-0.345
Vegf188/188	CON	Id1	0.916	10.853	0.188	0.957
Vegf188/188	CON	Tbr2	0.987	77.486	0.072	0.994
Vegf120/188	CON	Sox2	0.259	0.349	0.66	-0.509
Vegf120/188	CON	Id1	0.94	15.673	0.158	0.97
Vegf120/188	CON	Tbr2	0.998	456.65	0.03*	0.999

while genes associated with differentiation have low expression. There is a shift in the correlation pattern previously seen with WT neural epithelial cells when these cells have an altered Vegf isoform profile. Vegf120 neural cells display a strong correlation between Pax6 and Sox2, Id1, and Tbr2 in all three culture treatments (Table 1). The same correlation trend is seen with both Vegf188 and Vegf120/188 neural epithelial cells (Table 1), indicating that as Pax6 expression increases so does the expression of genes associated with neural progenitor cells. Focusing on the correlation of gene expression between Pax6 (y-axis) and Tbr2 (x-axis), it is clear that the Vegf isoform-derived neural epithelial cells display a stronger correlation pattern than do the WT cells (Figure 25). Vegf120 and Vegf188 neural epithelial cells differ in their Pax6-Tbr2 correlation compared to Vegf120/188 and WT neural cells. In Vegf120 and Vegf188, Pax6 expression has a higher correlation compared to the amount of Tbr2 expression. This differs from Vegf120/188 neural epithelial cells where the difference between Pax6 and Tbr2 expression is not as pronounced. These results suggest that the Vegf isoform neural epithelial cells display a directional shift in gene expression compared to WT neural cells. Where the WT neural epithelial cells maintain a steady Pax6 expression regardless of changes in Tbr2 expression as well as predicts that genes shift in concert as cell fates change.

In contrast, WT and Vegf isoform neural epithelial cells display a similar correlation pattern between neural stem cell and early lineage neuronal genes. WT and Vegf neural epithelial cells that were cultured in solo exhibited a negative correlation in expression (Figure 26). This means that when Pax6 expression is higher there is lower expression of Tbr1 for all WT and Vegf isoform-derived neural epithelial cells ($r=0.478$).

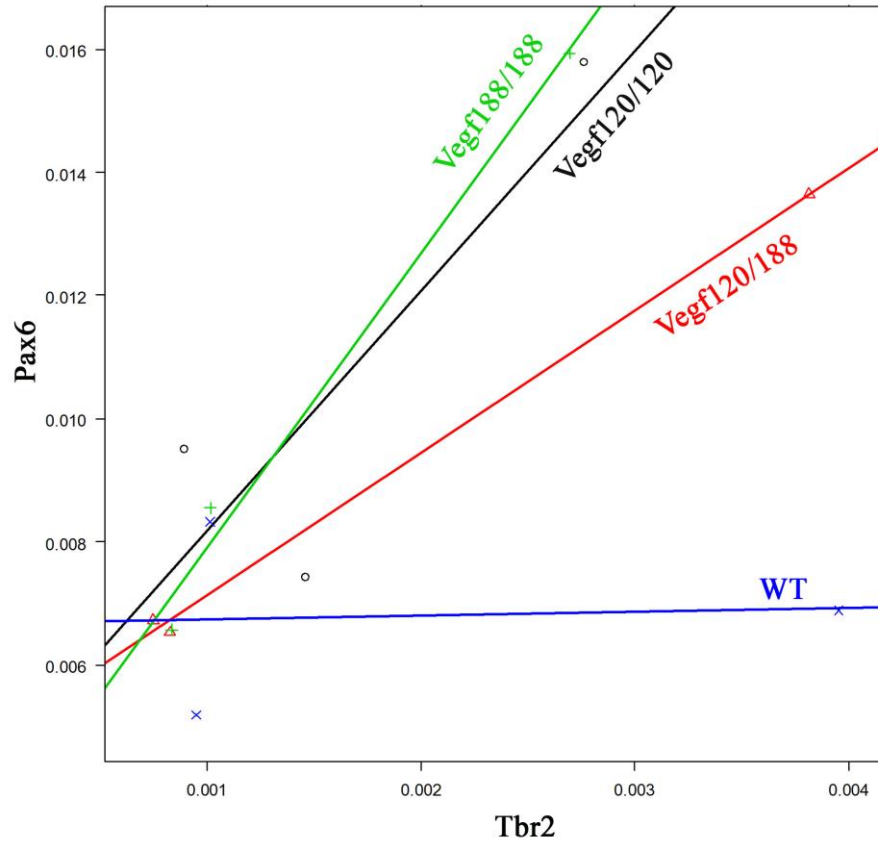


Figure 25: Expression of Pax6 and Tbr2 correlates in Vegf isoform neural epithelial cultures grown in contact with vascular cells. Immortalized SSEA-1-enriched WT and Vegf isoform neural epithelial cells were cultured in contact with vascular cells for 5 days. Vascular cells were removed and total RNA was extracted from neural cells and reverse transcribed to cDNA. Quantitative PCR was utilized to determine gene expression of Pax6 (neural stem cells) and Tbr2 (neural progenitor cells). An analysis of correlation was conducted between Pax6 and Tbr2 for both WT and Vegf isoform neural epithelial cells. Vegf isoform neural epithelial cells have a high correlation between Pax6 and Tbr2 expression. In contrast, Tbr2 expression in WT-derived neural epithelial cells remains low independent of Pax6 expression. This experiment was repeated 3 times with a total sample size of 3.

This indicates that there is a directional shift in gene expression towards neural stem cell fate in neural epithelial cells cultured in solo. Culturing WT and Vegf isoform neural epithelial cells with vascular cells leads to a positive correlation in both contacting and non-contacting cocultures ($R^2=0.264$ and $R^2=0.593$, respectively). The positive correlation shows that a higher expression of Pax6 is associated with a higher expression of Tbr1. This suggests that the presence of vascular cells influences neural epithelial cells to balance a neural stem cell population as well as small differentiated neural populations or low consistent Tbr1 throughout all cells.

DNA methylation in neural stem cell fate choice in vivo and in vitro

While vascular cells are able to influence shifts in neural epithelial cell gene expression, the exact mechanism responsible for these shifts could be DNA methylation. Methylation is a form of epigenetic control of transcription utilized by cells to alter changes in gene expression without causing permanent changes to the DNA sequence. The attachment of a methyl or hydroxymethyl group to a cytosine within the DNA can prevent transcription regulatory complexes from binding to the DNA, thus preventing transcription and gene expression^{72, 73}. To determine if this is the case we first wanted to determine if DNA methylation and hydroxymethylation is actually occurring *in vivo* in E9.5 embryonic forebrains. DNA methylation and hydroxymethylation were assessed using EpiGentek MethylFlash and HydroxymethylFlash kits. The results from both kits indicated that DNA methylation and hydroxymethylation are detectable in vivo at E9.5 (Figure 27). There is a non-significant difference in the proportion of methylated DNA between WT and Vegf isoform forebrains (One way ANOVA, $p=0.4881$). WT and Vegf120 forebrains exhibit similar proportion of DNA methylation, around 0.005

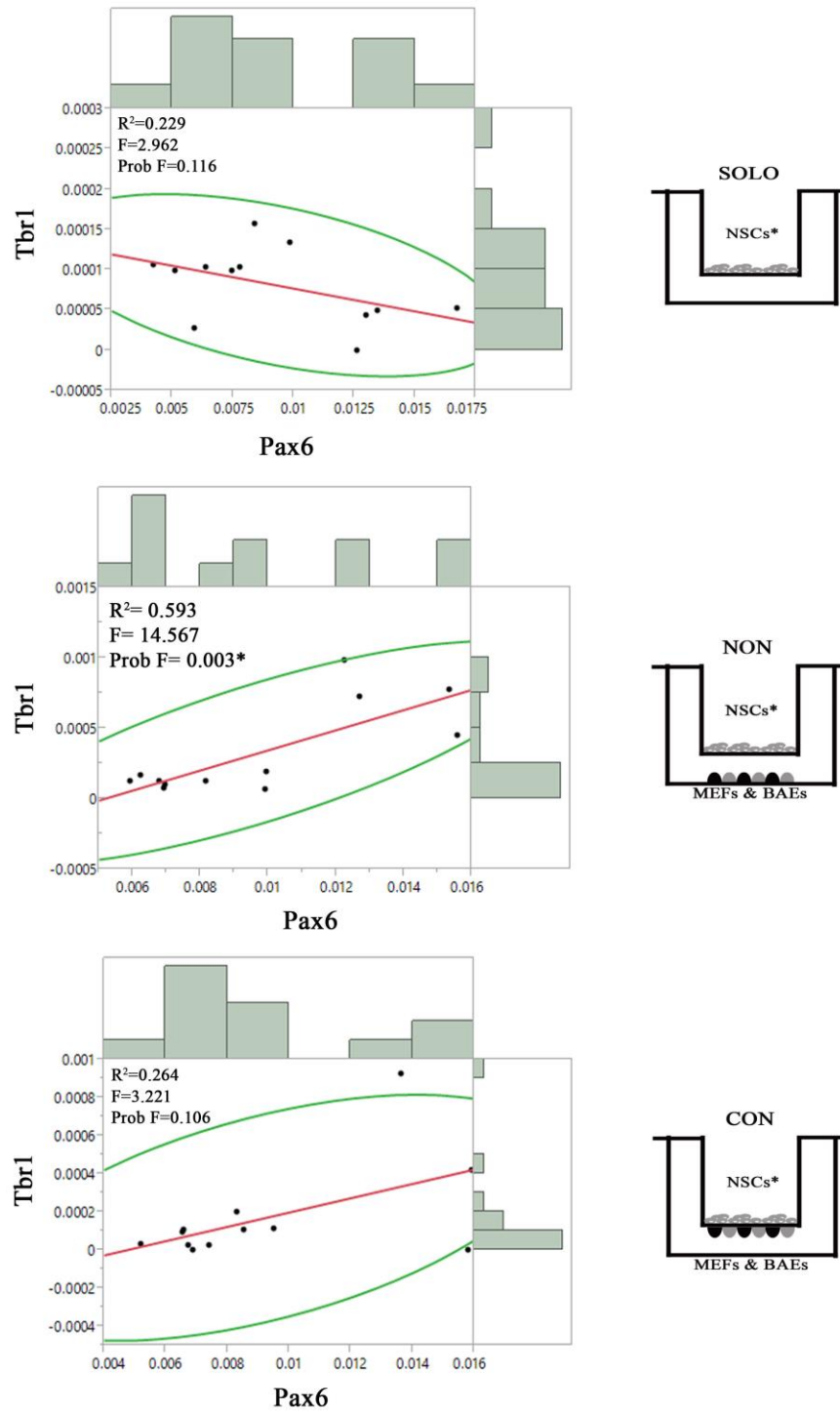


Figure 26: Wild type and Vegf isoform neural epithelial cells cultured with vascular cells display a positive correlation between Pax6 and Tbr1 gene expression.

Immortalized SSEA-1-enriched WT and Vegf isoform neural epithelial cells were cultured in either solo, contacting, or non-contacting coculture with vascular cells for 5 days. Neural epithelial cells were isolated and total RNA was collected and reverse transcribed to cDNA. Quantitative PCR was conducted to assess Pax6 and Tbr1 gene expression. A correlation analysis indicated a negative correlation between Pax6 and Tbr1 expression in neural epithelial cells cultured solo ($R^2=0.229$; $r= -0.478$). In contrast, a positive correlation was noted in WT and Vegf isoform neural epithelial cells cultured in contacting and non-contacting with vascular cells ($R^2=0.264$; $r=0.533$ and $R^2=0.593$; $r=0.77$, respectively). Linear fit (red line) and bivariate normal ellipse at 95% (green line) are indicated on the graphs. WT and Vegf isoform samples are plotted together and distribution of samples is indicated by histogram bar plots. This experiment was repeated 3 times with all values depicted on the graph for an $n=3$ for each genotype. All statistical values are provided in appendix Table 7 for reference.

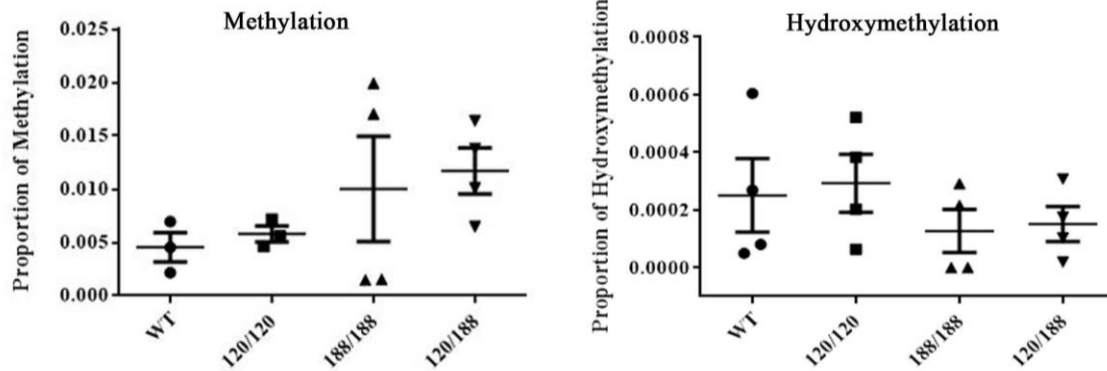


Figure 27: The proportion of methylation and hydroxymethylation differs in embryonic forebrains with an altered Vegf profile *in vivo*. Genomic DNA was extracted from E9.5 forebrains from WT and Vegf isoform mice (n=4 per genotype). DNA was utilized in EpiGentek™ MethylFlash and HydroxymethylFlash Kits to determine the proportion of DNA methylation and hydroxymethylation. (A) WT mice exhibit a lower proportion of overall DNA methylation compared to Vegf188 and Vegf120/188 isoform mice. Slight changes in methylation pattern are noted in the Vegf isoform mice with polarized variation in the Vegf188 mice. (B) Hydroxymethylation occurs on a smaller scale than DNA methylation. ANOVA analysis indicates that there are no significant differences between WT and Vegf isoform mice with regard to methylation (p=0.4881) and hydroxymethylation (p=0.6780). Four independent litters represented for each genotype with an n=4.

of the DNA carries a methylation signature. In contrast to this, Vegf120/188 forebrains have a non-significant increase in the proportion of DNA methylation compared to WT forebrains (Tukey's *post hoc* $p=0.4736$). Vegf188 forebrain samples exhibited a split in their distribution of proportion of DNA methylation, independent of litter origin, within the sample set. Two samples have an average proportion of 0.0015 while the other two samples have an average proportion of 0.185. Previous results have also displayed splits in data from Vegf188 isoform forebrains suggesting that this may be a feature of Vegf188 mice due to penetrance variability. Hydroxymethylation differed from methylation due to the fact that there was very little detectable hydroxymethylation (One way ANOVA, $p=0.678$). While there was no difference in the proportion of hydroxymethylation, that does not rule out the role of hydroxymethylation on gene expression.

Hydroxymethylation could have more of an influence on gene expression during a later stage in development.

Shifts in methylation pattern between WT and Vegf isoform forebrains could indicate that DNA methylation is being utilized to regulate gene expression *in vivo*. Genes that were assessed for DNA methylation were Pax6, Id1, and Suz12, were selected bases on the shifts in gene expression in WT and Vegf isoform forebrains at E9.5⁶⁹ as well as their role in neural stem cell fate choice (reviewed in ⁴⁵). In order to assess methylation, genomic DNA was isolated from *in vivo* E9.5 forebrains and used in the EpiTect kit to assess DNA promoter methylation for Pax6, Id1, and Suz12 using promoter region specific primers targeting CpG island clusters previously identified as methylation regulation targets (Qiagen). DNA promoter methylation for Pax6 (Figure 28A). WT and Vegf120 forebrains revealed no difference between these genotypes. In

contrast, Vegf188 and Vegf120/188 forebrains which showed a slightly higher proportion of promoter methylation relative to WT and Vegf120 samples. In order to possibly link DNA methylation to regulating gene expression a qPCR was conducted for Pax6 to assess changes in mRNA expression. The expression of Pax6 in E9.5 forebrains there is a significant decrease in Pax6 in all Vegf isoforms compared to WT (Tukey's *post hoc*, Vegf120 $p=0.0109$, Vegf188 $p=0.0434$, and Vegf120/188 $p=0.0024$). The lower expression of Pax6 correlates with a higher proportion of DNA methylation indicating that Pax6 expression may be regulated through promoter methylation. Id1 differs from Pax6 promoter methylation by having a lower proportion of methylation (Figure 28B). WT and Vegf120 forebrains have a similar proportion of methylation compared to one another but exhibit a higher proportion of methylation than both Vegf188 and Vegf120/188 forebrains. Linking DNA methylation to possibly shifts in mRNA expression, it was found that Id1 mRNA expression for Vegf120 forebrains does not significantly differ from WT (Tukey's *post hoc*, $p=0.1379$). Id1 expression in Vegf188 forebrains was significantly decreased (Tukey's *post hoc* $p=0.0033$) and in Vegf120/188 it was significantly increased (Tukey's *post hoc* $p=0.0090$). The results for Id1 indicate that a decrease in DNA promoter methylation leads to a significant change in Id1 expression. Suz12 is part of the polycomb complex that is involved with regulating methylation⁷⁴. When examining the promoter methylation for Suz12 it was found there was a very small proportion of methylation, and that methylation did not differ between WT and any of the Vegf isoform forebrains (One way ANOVA, $p=0.2592$). Suz12 mRNA expression was assessed with no significant difference in expression found across

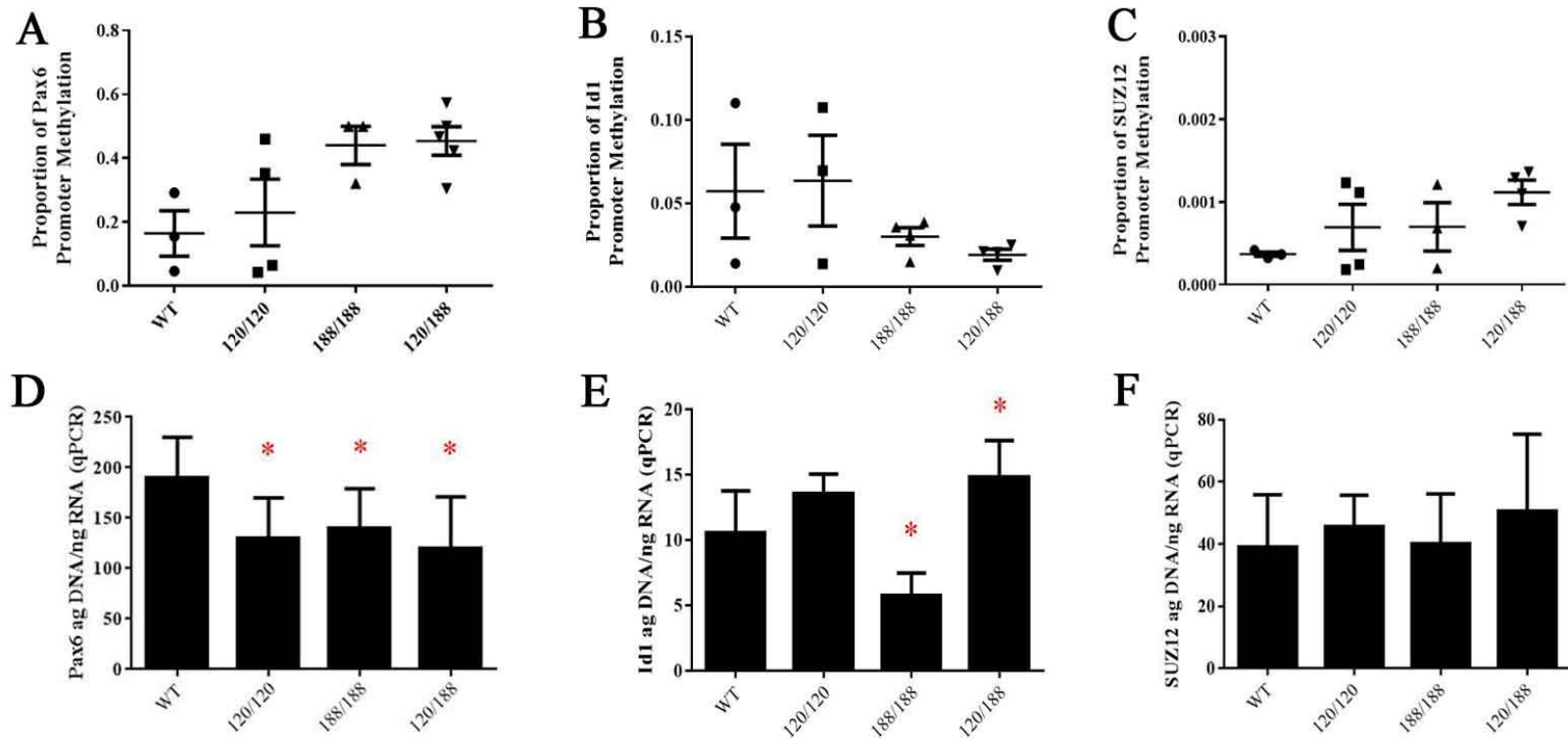


Figure 28: *In vivo* Pax6 and Id1 gene expression correlates with changes in DNA promoter methylation. Genomic DNA and total RNA were isolated from E9.5 embryonic forebrains. Genomic DNA was used with the EpiTect™ promoter methylation kit to assess promoter methylation (upper panel, n=4 per genotype). Total RNA was used to determine gene expression for Pax6, Id1, and Suz12 (lower panel, n=6-11 per genotype). Pax6, Id1, and Suz12 were selected based on shifts in gene expression between wild type

and Vegf isoform mice detected by a microarray analysis, (A) Pax6 promoter methylation increases with an altered Vegf isoform profile and correlates with a significant decrease in Pax6 mRNA expression (D; One way ANOVA; $p=0.0022$). (B) In contrast, Id1 promoter methylation decreases in Vegf188 and Vegf120/188 forebrains. This correlated with significant shifts in Vegf188 and Vegf120/188 Id1 mRNA expression compared to WT forebrains (E; Tukey's *post hoc*; $p<0.0001$). (C&F) Suz12 promoter methylation is barely detectable (note y-axis) and there is no statistical difference across genotypes for either promoter methylation (C) or gene expression (F).

genotypes. These results indicate that Suz12 may not be regulated by DNA promoter methylation (One way ANOVA, $p=0.6042$). This does not rule out the possibility that Suz12 is involved with DNA methylation, particularly with regard to its role as part of the polycomb complex. Others have shown that the polycomb complex is involved with regulating genes associated with embryonic stem cells (Sox2, Oct4, etc...) ⁷⁵. Due to the potential role of the polycomb complex in regulating embryonic stem cells genes, we wanted to assess whether this may be the case with genes associated with neural stem cells. In order to assess the potential role of the polycomb complex in regulating neural stem cells genes we decided to examine expression of Suz12 *in vivo*.

During cortical development there is rapid neural epithelium expansion that occurs between E9.5 and E13.5 which could be influenced by DNA promoter methylation causing shifts in gene expression. To assess whether methylation is potentially involved in the expansion of the neural epithelium, we decided to compare Suz12 expression in WT and Vegf isoform mice at E11.5, which is a transitional stage during the critical E9.5 to E13.5 window. At this time point, the neural cortex is still primarily neural stem cells but Tbr2⁺ neural progenitor cells are starting to be generated. Embryos from E11.5 WT and Vegf isoform were sectioned and labeled with Suz12, lectin, and DAPI. Suz12 was used to determine if DNA methylation was occurring due to its role in the polycomb complex. In the WT there are Suz12 positive cells located near the ventricular zone in the telencephalon (Figure 29, upper panel, white arrows). Suz12 positive cells are present in the ventricular zone which correlates with the location of proliferating neural stem cells, indicating that Suz12 may be expressed in neural stem cells. This differed in the Vegf120 cortex where Suz12 expression was not detected at

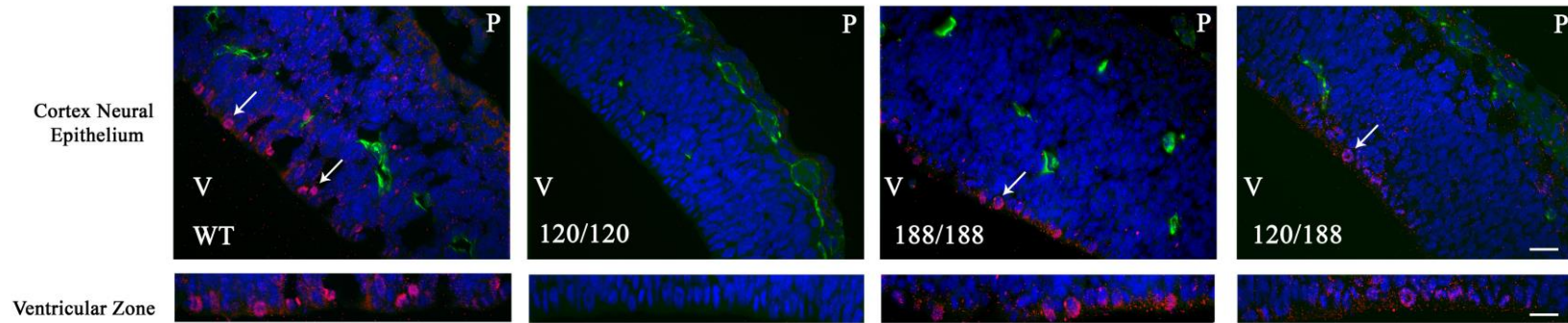


Figure 29: Wild type mice display an expanded range of Suz12 positive cells compared to Vegf isoform mice *in vivo*.

97

Forebrain sections from E11.5 embryos were cut and labeled with Suz12 (a polycomb protein, red), lectin (blood vessels, green), and DAPI (nuclei, blue). Suz12 positive cells (white arrows) are primarily located at the ventricular surface (V; upper panel), while blood vessels are located at the pial surface (P) with some branching into the neural epithelium. The thin band of the ventricular zone for each genotype is shown in the lower panels (scale bars = 25 μ m). An increased range of Suz12-positive cells are present in WT forebrains. A smaller range was noted with Vegf188 and Vegf120/188, while no Suz12-positive cells were detected in Vegf120 forebrain (bottom panel).

E11.5. This differs from E9.5 *in vivo* and E13.5 *in vitro* transcript data. In contrast, Suz12 positive cells were present in both Vegf188 and Vegf120/188 cortices. Vegf188 and Vegf120/188 mice exhibited fewer Suz12 positive cells compared to the WT but Vegf188 more closely resembled WT forebrains than did the Vegf120/188 forebrains. These results indicate that Suz12 is expressed during the transition stage at E11.5 leading to the idea that methylation could be occurring at this point. In addition, we see noticeable differences in the number of Suz12 positive cells between WT and Vegf isoforms indicating that there may be a difference in methylation when the Vegf isoform profile is shifted.

To further explore the role of DNA methylation in cortical development we examined DNA methylation and hydroxymethylation in an *in vitro* system at E13.5. At this time point, multiple neural cell populations are undergoing shifts in gene expression related to neural stem cell fate which makes this a critical time to assess patterns in DNA methylation. Global methylation and hydroxymethylation were determined as previously described, however, this time genomic DNA was collected from SSEA-1-enriched neural epithelial cells (NSC*). DNA methylation showed a significant difference between WT and Vegf isoform neural epithelial cells (Figure 30; One way ANOVA, $p=0.0299$). This first indicates that DNA methylation can be detected within the *in vitro* neural epithelial samples and second it shows that DNA methylation differs with an altered Vegf isoform profile. The proportion of DNA methylation was similar between WT and Vegf120 cells (Tukey's *post hoc*, $p=0.9547$). Both Vegf188 and Vegf120/188 displayed a decrease in the proportion of DNA methylation (Tukey's *post hoc*, Vegf120/188 $p=0.0607$). The only significant difference detected was between Vegf120 and Vegf120/188 (Tukey's *posthoc*;

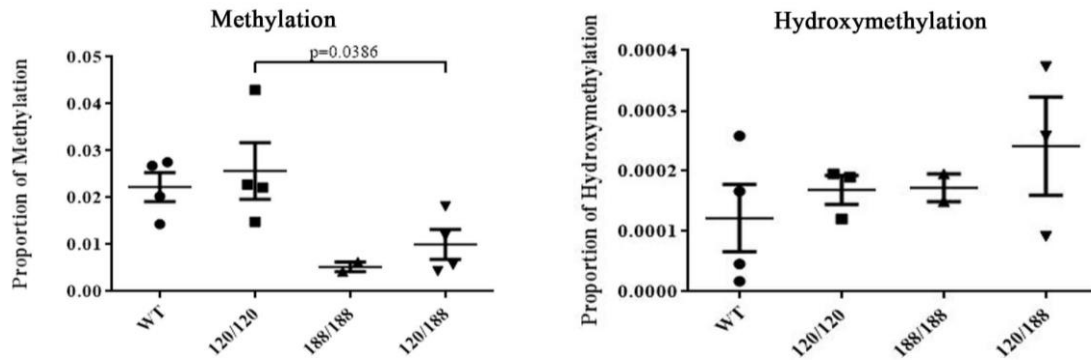


Figure 30: Global methylation and hydroxymethylation was detected *in vitro* utilizing E13.5 immortalized SSEA-1 enriched neural epithelial cells. Genomic DNA was isolated from WT and Vegf isoform immortalized SSEA-1-enriched neural epithelial cells (n=4 per genotype except n=2 for Vegf188) cultured between 3-4 weeks. DNA was utilized in EpiGenetek MethylFlash and HydroxymethylFlash kits to determine global methylation and hydroxymethylation. Global methylation patterns differed between WT and Vegf isoform neural epithelial cells (One way ANOVA; $p=0.0299$) with a significant decrease in the proportion of DNA methylation between Vegf120 and Vegf120/188 ($p=0.0386$). The proportion of hydroxymethylation remains relatively similar between WT and Vegf isoform neural epithelial cells (One way ANOVA; $p=0.3617$). Vegf188 samples were excluded from both methylation and hydroxymethylation statistical comparison. Differences in culture times before DNA sample collection could account for some variation noted between samples.

p=0.0386). In contrast to the methylation results, hydroxymethylation did not differ significantly between WT and Vegf isoform neural epithelial cells (Figure 30, One way ANOVA, p=0.3617). The proportion of hydroxymethylation noted in WT and Vegf neural cells was less than what was observed for methylation; but even so these results indicate that hydroxymethylation still occurs *in vitro*, albeit at a much lower level than methylation.

Changes in gene expression noted in the *in vitro* system may be a result of shifts in DNA promoter methylation of genes associated with neural stem cell fate choice. In order to assess this possibility, we determined DNA promoter methylation for Pax6, Id1, and Suz12 in SSEA-1-enriched neural epithelial cells collected from E13.5 forebrains. Genomic DNA was collected from SSEA-1-enriched neural epithelial cells and used in the Epitect DNA Digest Kit. Only results from WT, Vegf120, and Vegf120/188 neural epithelial cells are presented due to only having two samples for Vegf188 cells of sufficient quality. DNA promoter methylation for Pax6 did not significantly differ between WT, Vegf120, and Vegf120/188 neural epithelial cells (Figure 31A; One way ANOVA, p=0.1603). Even though the difference is not significant there is a trend in Pax6 promoter methylation where Vegf120 and Vegf120/188 have a lower proportion of methylation than WT neural epithelial cells. This decrease in Pax6 promoter methylation correlates to an increase in Pax6 expression *in vitro*, indicating that Pax6 expression may be regulated by DNA promoter methylation *in vitro*. Results for Id1 promoter methylation show that there is no significant difference between WT and Vegf isoform cells (Figure 31B; One way ANOVA, p=0.5867). In contrast to the trend seen with Pax6, analyses, although they are shown in the graph for Id1 promoter methylation

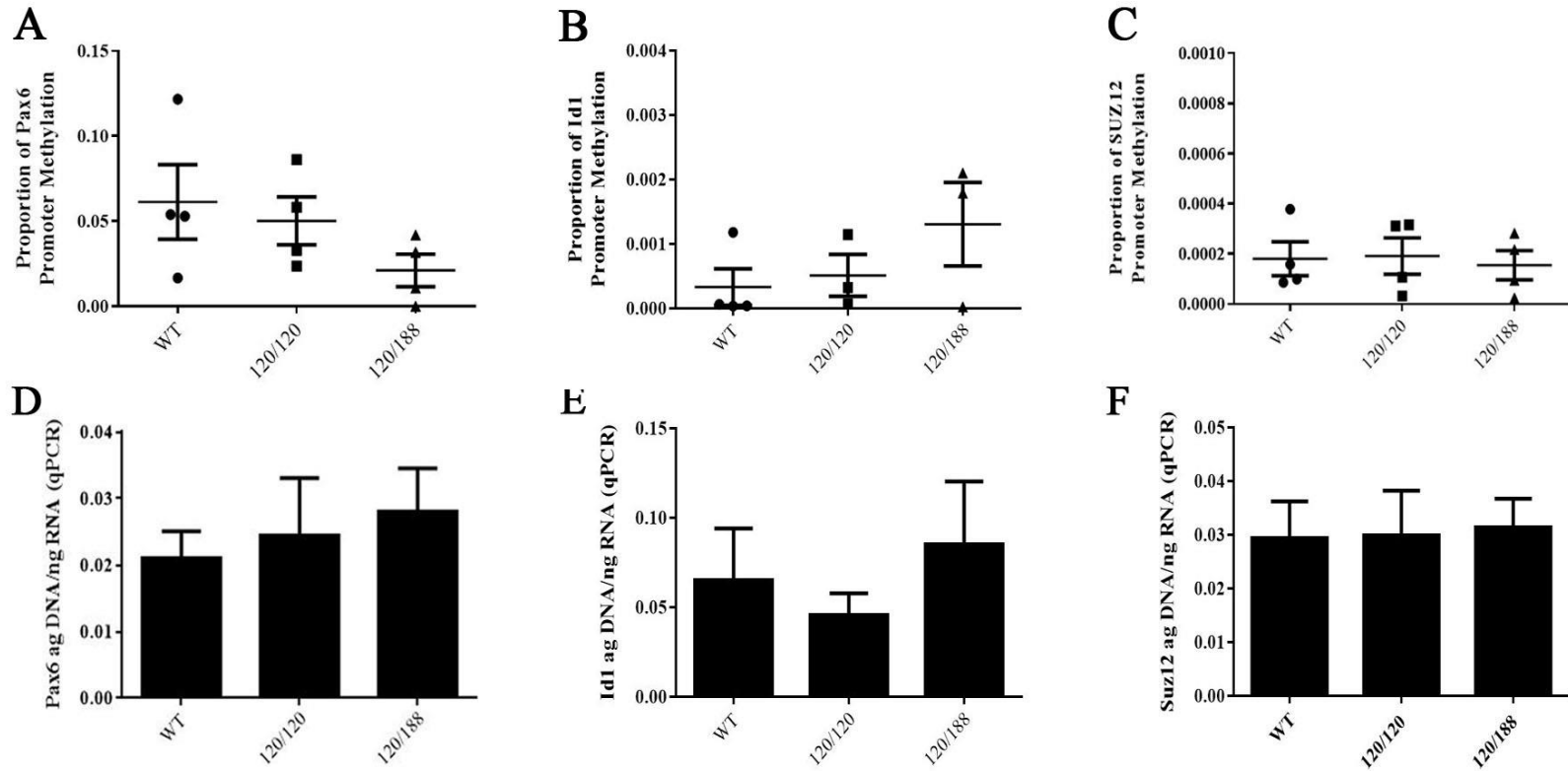


Figure 31: Changes in DNA promoter methylation correlate with Pax6 and Id1 gene expression *in vitro*. Genomic DNA and total RNA were extracted from WT and Vegf isoform immortalized SSEA-1-enriched neural epithelial cells. Genomic DNA was used with the EpiTect kit (A-C) to determine DNA promoter methylation while RNA was utilized to assess Pax6, Id1 and Suz12 mRNA

expression (D-F). (A) DNA promoter methylation for Pax6 exhibited a decrease in Vegf120/188 neural cells compared to WT and Vegf120, which were relatively similar to one another. This correlates with an increase in Pax6 expression in Vegf120/188 cells (D). (B) In contrast, an increase in DNA promoter methylation was noted with Id1 in Vegf120/188 isoform neural epithelial cells with a slight increase in Id1 mRNA expression (E). Both Suz12 promoter methylation (C) and mRNA expression (F) did not differ between WT and Vegf isoform neural epithelial cells. Transcript data was collected for Vegf188 neural epithelial cells but was not included due to low number of quality genomic DNA samples required for promoter methylation assessment.

increases in Vegf120 and Vegf120/188 neural epithelial cells. When examining Id1 mRNA expression *in vitro* there are slight differences noted in Vegf120 and Vegf120/188 neural epithelial compared to WT cells, but they do not match what would be predicted for transcription based on the methylation state. While these differences are not significant, it does not rule out the possibility that DNA promoter methylation is involved in Id1 regulation. When examining the proportion of DNA promoter methylation for Suz12 it was found that there was no significant difference between WT and Vegf isoform neural epithelial cells (Figure 31C; One way ANOVA, $p=0.8918$). Also, Suz12 mRNA expression did not significantly differ between WT and Vegf isoform neural epithelial cells (One way ANOVA, $p=0.8314$). These results indicate that Suz12 expression may not be regulated through DNA promoter methylation at this site.

The shifts in Pax6 DNA methylation and expression could be associated with changes in Suz12 expression. To address this question, an analysis of covariance was conducted examining Pax6 and Suz12 mRNA expression from WT and Vegf isoform immortalized neural epithelial cells. WT neural epithelial cells showed a significant correlation between Pax6 and Suz12 expression, indicating that when Pax6 expression increased, so did the expression of Suz12 (Figure 32, $R^2=0.6694$). Vegf isoform neural epithelial cells display a similar correlation between Pax6 and Suz12. A weaker correlation was noted with Vegf120 and Vegf120/188 neural cells ($R^2=0.3238$ and $R^2=0.2719$, respectively) where as Vegf188 cells displayed a stronger correlation ($R^2=0.5849$) with Pax6 and Suz12 expression. These results indicate that when Pax6 expression increases in WT and Vegf isoform neural epithelial cells there is an increase in Suz12 expression.

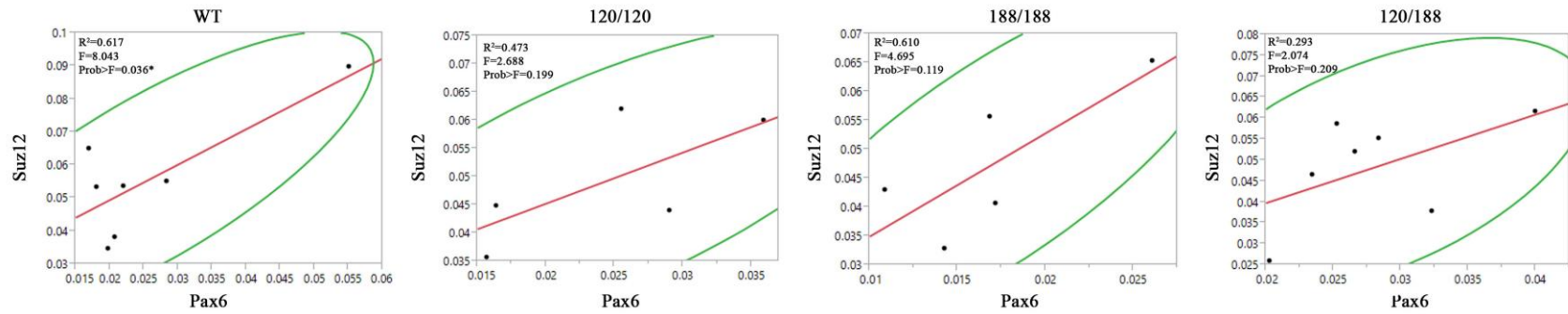


Figure 32: A positive correlation was noted between Pax6 and Suz12 in Wild type and Vegf isoform neural epithelial cells. Total RNA was isolated from WT and Vegf isoform immortalized neural epithelial cells and reversed transcribed to cDNA which was used with qPCR to assess gene expression. Correlation analysis indicated a positive correlation between Pax6 and Suz12 expression for both WT and Vegf isoform neural epithelial cells. The correlation shows an increase in Pax6 corresponds to an increase in Suz12 expression. Linear fit (red line) and bivariate normal ellipse at 95% (green lines) are indicated on the graphs and n=5-7 for each genotype.

CHAPTER IV

DISCUSSION

Overview

Multiple organ systems require the presence of vasculature for proper development. While the same is true for cortical development, what is still unclear is the exact relationship between the vasculature and neural epithelium. This leads to the following question, what influence does the vasculature have on neural epithelium development and function? How integrated or interdependent is this relationship? When addressing these question in terms of development of organ systems (such as the cortex), one is also assessing the question of what extrinsic and intrinsic cues are involved with stem cell fate decisions. This study aimed to address these ideas by using a heterotypic tri-coculture system to recapitulate the developing cortical microenvironment. Mimicking the early neural epithelium provided the opportunity to determine the specific influence that vascular cells may have on neural stem cell fate choice. In addition, it allows the ability to assess whether extrinsic or intrinsic cues are involved in switching cell fate decisions by neural stem cells. To further gauge the relationship between these systems, the Vegf isoform profile was shifted within the coculture system. This provided the opportunity to determine how a specific growth factor within the microenvironment can alter neural stem cell development. As neural stem cells differentiate they undergo shifts in gene expression (influenced by extrinsic and intrinsic cues) which can correlate to

specific cell fates. A major question currently being asked in the neural development field is what mechanisms are being used to cause these shifts in expression? This project aims to address this question by assessing DNA promoter methylation for genes known to be involved with neural stem cell fate decisions as well as the previously mentioned questions.

Can a system be developed to study interactions between neural epithelial and vascular cells that occur during cortical development?

The ability to study *in vivo* systems using *in vitro* methods has been paramount in biology, but there are both strengths and limitations associated with using an *in vitro* system. Potential issues are culturing long term primary cell lines, maintaining specific characteristics associated with cell lines, and developing an *in vitro* model that recapitulates the *in vivo* system. The problem with maintaining long term primary cell cultures is often due to the cells undergoing early senescence. Cellular senescence is a cell's programmed response to exposure to stress, which can result in a shortened lifespan for some primary cells. Stressors that can trigger senescence are oxidative stress, DNA damage, oncogene activity, telomere uncapping/shortening, and many others (reviewed in ⁷⁶). While all these stressors can result in senescence, the main candidate mechanism for early senescence is the shortening of telomeres (telomere end stability). This can occur in cells undergoing multiple divisions due to the cells inability to maintain telomerase activity which is responsible for telomere length. It has been demonstrated that human fibroblasts cultured for multiple passages display shorter telomere lengths compared to younger fibroblasts ⁷⁷. This suggests that the shortened telomeres within human fibroblasts acts as a biomarker for aging cells ⁷⁸. Unstable telomeres have also been observed in

fibroblasts that were collected from Hutchinson-Gilford progeria donors; the patient's fibroblasts display a reduced rate of proliferation, a characteristic of aging cells, which corresponded to shortened telomeres⁷⁸. The correlation between a shorter telomere and an aging cell can be reversed by preventing telomere shortening. Transfection of human retinal pigmented epithelial cells and foreskin fibroblasts with the human telomerase catalytic subunit results in an increase in cell division and a decrease in cellular senescence⁷⁹. For these two examples, maintaining telomere length resulted in an increase lifespan, lending further support to the idea that shortening telomeres can result in cellular senescence.

One method used to overcome this issue of cellular senescence via telomere instability is to generate immortalized cell lines by using Simian vacuolating virus 40 T antigen (SV40). SV40 has been used to generate long term cell lines from primary cells that display a limited lifespan. Mouse embryonic fibroblasts (MEFs) immortalized with SV40 exhibited long-term cell proliferation at the same time that they maintained their multipotency⁸⁰. While no studies have directly indicated exactly how SV40 induces an increase in proliferation and lifespan, it is postulated that SV40 is either increasing or restoring telomerase activity (reviewed in⁸¹). The primary neural epithelial cells utilized within the current research exhibited the same limitations as seen with human fibroblast cells, a limited lifespan. By immortalizing the neural epithelial cells with SV40 there was an increase in cell lifespan and proliferation. This indicates that SV40 can produce long term cultures, most likely through regulating telomerase activity.

A parallel concern with SV40 immortalized, in general, is whether or not incorporation of large T antigen alters the capacity of features of the immortalized line. In

several studies using SV40 large T antigen immortalization, the stability and differentiation potential have been explored. Mouse osteoclast precursor cells immortalized with SV40 large T antigen maintained the ability to reabsorb bone, which is a function of native mouse osteoclasts⁸². In addition, the immortalized cells were still able to differentiate into mature osteoclasts after several months in culture. Similar results were noted with the immortalization of immature and mature astrocytes where they displayed similar stellate and flat morphology as well as growth patterns comparable to native astrocytes⁸³. The ability of immortalized cells to retain similar morphological features suggests that gene expression patterns are also similar. Immortalized MEFs retained the ability to differentiate into osteogenic, chondrogenic, and adipogenic lineages which suggests that the immortalization process did not interfere with gene expression normally attributed to native MEFs⁸⁰. We observed similar morphological and transcript-level features in our immortalized vs non-immortalized neural epithelial cells. In fact, the neural epithelial cells continued to express genes associated with neural stem, progenitor, and early lineage cells. The presence of cells expressing neural stem cell genes (Pax6 and Sox2) suggests that the immortalization process did not alter characteristics associated with SSEA-1-positive cells (i.e. neural stem cells). In addition, neural progenitor (Tbr2) and early lineage (Tbr1) cells were present, based on positive gene expression. While it is possible that Tbr2 and Tbr1 positive cells must have been isolated during SSEA-1-enrichment, but the most likely scenario is that these population arose from neural stem cell differentiation as SSEA-positive stem cells do not normally co-express Tbr2 and certainly not Tbr1⁸⁴. The presence of Tbr2 and Tbr1 expression in the SSEA-1-enriched cultures, therefore, suggests that the immortalized neural epithelial

cells still have retained the ability to differentiate into neural lineage cells. This ability to retain differentiation potential over time is consistent with the results for other SV40 immortalized lines^{80, 82, 83} (and reviewed in⁸¹). The results obtained from the current study, in conjunction with published work with other cell lineages, suggests that the immortalized neural epithelial cells retain their neural stem cell characteristics. As a result, these cells can be used as the foundation for an *in vitro* system designed to mimic the developing cortical microenvironment.

An *in vitro* system geared to recapitulating the developing cortical microenvironment needs to have the capability to incorporate multiple factors present *in vivo*. A critical element present in the cortical epithelium is the basement membrane. The basement membrane is comprised of multiple components, but a major player is laminin (reviewed in⁸⁵). Neural epithelial cells can bind to laminin through laminin-integrin interactions. The importance of neural epithelial-laminin interactions has been demonstrated in early postnatal day 1 mouse forebrains. When laminin- β 1 integrin interactions were inhibited by generation of conditional β 1-integrin mutant mice, neural precursor cell death was dramatically increased relative to cortical cultures⁶⁰. This suggests that laminin plays a role in neural epithelial cell survival. In addition to regulating cell survival laminin is required for proper formation of cortical layers. Mice that have a mutation in laminin production exhibited a disruption in lamination and characterized by a proportion of radial glial cells not establishing contact between the basement membrane and their endfeet. As a result, ectopic clusters of neural precursor cells formed, with a corresponding failure in upper layer neuron migration⁶². Similar results were noted in a study conducted by Halfter et al. where the endfeet of glial cells

did not establish contact with the basement membrane. In this latter study, lack of glial cell contact with the laminin of the basement membrane inhibited normal migration of Cajal-Retzius cells and, in some cases, a complete absence of Cajal-Retzius cells ⁶³. These studies show that neural epithelial cells require laminin during cortical development to mediate cell survival, attachment, and migration. To provide this vertical substrate in our coculture system, we coated the permeable membrane with poly-lysine and laminin, thereby provides the neural epithelial cells with a basement membrane. Given the fact that neural epithelial cells require other potential signaling sources during development, we took advantage of the fact that the Transwell™ system allows communication between different cell sources in one culture condition. Previous studies have used the Transwell™ system to mimic the neurovascular environment. Chou et al. cultured human neural stem cells with adult human brain endothelial cells using a Transwell™ system ⁶⁵. The results from this study showed that the endothelial cells were able to form vascular like structures only when cultured with the neural stem cells ⁶⁵. The author did not include a fibroblast-like pericytes precursor cell in their system, however. Endothelial cells, in conjunction with pericytes, form the vascular cell foundation for capillary beds, including those present in the developing cortical neuroepithelium. This indicates that multiple cell sources cultured using the Transwell™ system are able to communicate with one another. By combining the Transwell system that has a coated poly-lysine/laminin membrane with both neural epithelial and vascular cells it produces an *in vitro* system that recapitulates the microenvironment present during cortical development. The current thesis work provides the 1st demonstration of this multi-cell type system linking vascular cells and neural stem cell fate choice.

Do neural epithelial and vascular cells display an interdependent relationship during cortical development?

Neural epithelial cells within the developing cortex are exposed to multiple signaling cues, present in the microenvironment, which can influence cell fate choice. These cues can be derived from different cell sources or extracellular components within the environment. A potential, major contributor to these cues is vascular cells. Vascular cells develop in concert with neural epithelial cells which suggests the notion that there could be an interdependent relationship between these cell sources. In order to assess the dynamic of this relationship, it is necessary to examine neural epithelial cell fate choice in the context 1) neural epithelial cell autocrine signaling, 2) paracrine signaling from vascular cells, and 3) juxtacrine signaling from vascular cells.

Neural epithelial cells can utilize autocrine signaling to promote a neural stem cell fate choice. Stem cells have the ability to release cues into the microenvironment which can influence their own cell fate choice (i.e. autocrine signaling). This is the case with human multipotent adipose-derived stem cells that produce and export Fibroblast Growth Factor (FGF) 2 to the cell surface, which triggers a self-renewal response in the stem cells⁸⁶. The expression and release of FGF in neurons has been detected in the adult rat brain and leads to a similar autocrine signaling mechanism could occur in developing neural epithelial cells⁸⁷. A study by Gensburger et al. (1987) proposed that neural precursor cells, isolated from P13 day old rats, can use FGF2 in an autocrine fashion to promote cellular proliferation⁸⁸. Another potential autocrine cue, produced by neural epithelial cells, is Vegf. The neural epithelial cells that were isolated in the current study were shown to produce all three Vegf isoforms. Vegf has been shown to increase proliferation

of neural precursor cells within the subventricular zone within the adult rat brain ⁵⁸. These effects are not limited to *in vivo* studies but have also been documented using *in vitro* systems. Schanzer et al. (2004) demonstrated that Vegf was produced by adult rat neural stem cells *in vitro* and that a majority of these cells express VEGFR2. When Vegf164 levels within the cultures were increased it led to an increase in proliferation of the rat neural stem cells through activation of VEGFR2 ⁵⁵. A similar response occurs in E16 cortical neural precursor cells, where cell proliferation is activated by Vegf/VEGFR2 signaling ⁵⁸. These results suggest that neural epithelial cells could be using Vegf in an autocrine fashion to promote cellular proliferation, which is a defining characteristic of a neural stem cells.

In addition to producing autocrine signals, neural epithelial cells could be regulating cell fate decisions through preprogrammed, intrinsic cues. As an example, primary neural epithelial cells isolated from embryonic mice E13.5 cortex retained the expression of Pax6 after 6 passages in culture ⁸⁹. In contrast, cells isolated from the medial ganglion eminence (MGE) did not express Pax6, due to the fact that Pax6 expression is restricted to neural epithelial cells present in the dorsal telencephalon ⁸⁹. This indicates that neural epithelial cells isolated from specific regions within the cortex can maintain their region specification characteristics in culture. Collectively, these data suggest that neural epithelial cells have the capability to retain their stem cell fate within an *in vitro* system. This appears to be the case with our primary, immortalized neural epithelial cells cultured in solo condition. These cells were able to exhibit a neural stem cell fate, possibly due to pre-programmed intrinsic cues, established prior to their isolation, which may have been maintained/supported through autocrine signaling. Similarly, neural

epithelial cells present *in vivo* at E9.5 may utilize this proposed signaling scenario during cortical development. At this earlier developmental stage there is no vascular investment in the cortex, which implies that neural epithelial cells are most likely relying on intrinsic and autocrine signals to promote a neural stem cell fate and sustain the population. The microenvironment changes dramatically when neural epithelial cells are exposed to paracrine signals from vascular cells.

We are utilizing our heterotypic cell culture system to test the idea that vascular cells can influence neural epithelial cell fate choice through paracrine signaling during cortical development. One potential mechanism is via vascular cells causing a shift in the proportion of soluble factors present within the microenvironment. It has been established that neural epithelial cells express both Vegf as well as FGF2⁹⁰. By culturing neural epithelial cells with vascular cells it could lead to a shift in the proportion of these growth factors available within the microenvironment. When the concentration of FGF2 is increased in cultures consisting of bovine aortic endothelial cells, it leads to an increase in Vegf production by the endothelial cells⁹¹. The increase presence of Vegf within the microenvironment can lead to the formation and stabilization of vascular structures consisting of endothelial cells and pericytes (reviewed in⁹²). An increase in the presence of Vegf in the microenvironment via changes in endothelial cell or pericytes growth factor expression, could be a significant impact on neural epithelial cells. As an example, when Vegf concentration is up-regulated through adenovirus vector mediated gene transfection in postnatal day 3 rat brains, it results in an increase in nestin-positive neural stem cells as well as astrocytes and oligodendrocytes⁹³. This suggests that by shifting the concentration of available Vegf it could induce neural epithelial cell proliferation

followed by differentiation. In addition to Vegf, there could be a slight increase of soluble FGF or EGF in the microenvironment. Both FGF and EGF bind to heparan sulfate proteoglycans in the ECM. Uchimura et al demonstrated using an ELISA system, that remodeling of the ECM with sulfatase 2 (HSulf-2) leads to heparan sulfate proteoglycan-associated Vegf and FGF being released into the microenvironment ⁹⁴. This idea is further supported by the presence of HSulf-2 in E15.5 dorsal telencephalon, where it is involved with extracellular signaling through remodeling heparan sulfate in the ECM ⁹⁵. Remodeling the ECM of neural and vascular cells can cause an increase in the presence of soluble FGF and EGF in the microenvironment. The increase in these growth factors could impact neural epithelial cell fate. For example, FGF2 can promote proliferation of adult rat cortical progenitor cells followed by differentiation of these cells into neurons ⁹⁶. A similar result is seen with E14 mouse striatal progenitor cells, where exposure to EGF led to an increase in proliferation that preceded differentiation into neurons and astrocytes ⁹⁷. Shifting the concentration of soluble factors (i.e. Vegf, EGF, and FGF) in the microenvironment may lead to subsequent changes in neural epithelial cell fate. A shift in the growth factors in the microenvironment may be one explanation for the results seen with the neural epithelial cells cultured in non-contacting coculture with vascular cells. The presence of the vascular cells could have caused a shift in soluble cues in the microenvironment. Altering the proportion of soluble cues within the non-contacting coculture condition could have resulted in an increase in neural epithelial cell proliferation as well as differentiation into early lineage neural cells via paracrine signaling. While a subset of the neural epithelial cells within the non-contacting coculture were differentiating, another subset of cells appeared to maintain their neural stem cell

fate. This could be due to autocrine signals having a stronger effect on the neural epithelial cells compared to the paracrine signals. The response of neural epithelial cells in non-contacting coculture with vascular cells resembles the shift in cell fate decisions seen during rapid expansion of the cortex beginning around E11.5 (Figure 33). While vascular cells can signal to neural epithelial cells using paracrine cues, they can also signal through a juxtacrine mechanism via establishing direct contact with neural epithelial cells.

The combination of autocrine signals from neural epithelial cells with paracrine and juxtacrine signals from vascular cells may lead to the generation of multiple neural epithelial cell populations in one microenvironment. As previously described with regard to paracrine signaling, vascular cells can release soluble factors (Vegf, EGF, and FGF) into the microenvironment. The concentration of these growth factors that neural epithelial cells are exposed too can increase with the establishment of direct contact with vascular cells. This is due to FGF being present in the ECM of neural epithelial cells such as has been observed in embryonic rat cortical neural epithelial cells⁹⁰ and the ECM of bovine aortic endothelial cells⁹⁸. Due to having a similar structure as FGF, EGF is also located in the ECM generated by bovine endothelial cells⁹⁹. Through establishing contact it leads to an increase in growth factor presence, not necessarily production, in the ECM between neural epithelial and vascular cells. This increase in growth factor presence can trigger juxtacrine signaling between these cells which could influence neural epithelial cell fate. The influence of EGF and FGF can have two different impacts on neural epithelial cell fate. The first is that EGF and FGF can promote an increase in neural epithelial cell proliferation followed by differentiation. The second is that those autocrine

factors can promote self-renewal of neural epithelial cells. EGF has been shown to stimulate an increase in symmetric division of mouse E8.5 embryonic neural epithelial cells resulting in a self-renewing stem cell population ¹⁰⁰. Likewise, if undifferentiated human embryonic stem cells are cultured with FGF2 beads that release a stable concentration of FGF2 (10ng/ml), this generates an increase in self-renewing stem cells with a decrease in spontaneous differentiation ¹⁰¹. These studies indicate that neural epithelial and vascular cells do not use EGF and FGF in a strictly paracrine or juxtacrine manner but rather a combination of the two. This suggests that by combining these signaling mechanisms the result may be a mixed population (neural stem, progenitor, and early lineage neural cells) which is exactly the situation observed in mouse embryonic forebrain at E13.5 ⁴⁵ (Figure 33).

In addition to growth factors, vascular cells may be inducing and/or altering signaling pathways within the neural epithelial cells through juxtacrine signaling. One signaling pathway that has been shown to influence cell fate decisions during development is the Notch pathway. Human umbilical vein endothelial cells express Notch ligands on their membrane, and when cocultured with cancer stem-like cells (CSLC), stimulate an increase in growth and self-renewal of the stem cell population ¹⁰². Notch activation elicits a similar response in neural epithelial cells. This is seen in embryonic E15.5 neural stem cells which require the activation of Notch in order to maintain a neural stem cell population ¹⁰³. Activation of Notch in mouse E13.5 embryonic neural stem cells increases their survival ¹⁰⁴. These results suggest that by establishing direct contact between vascular and neural epithelial cells juxtacrine

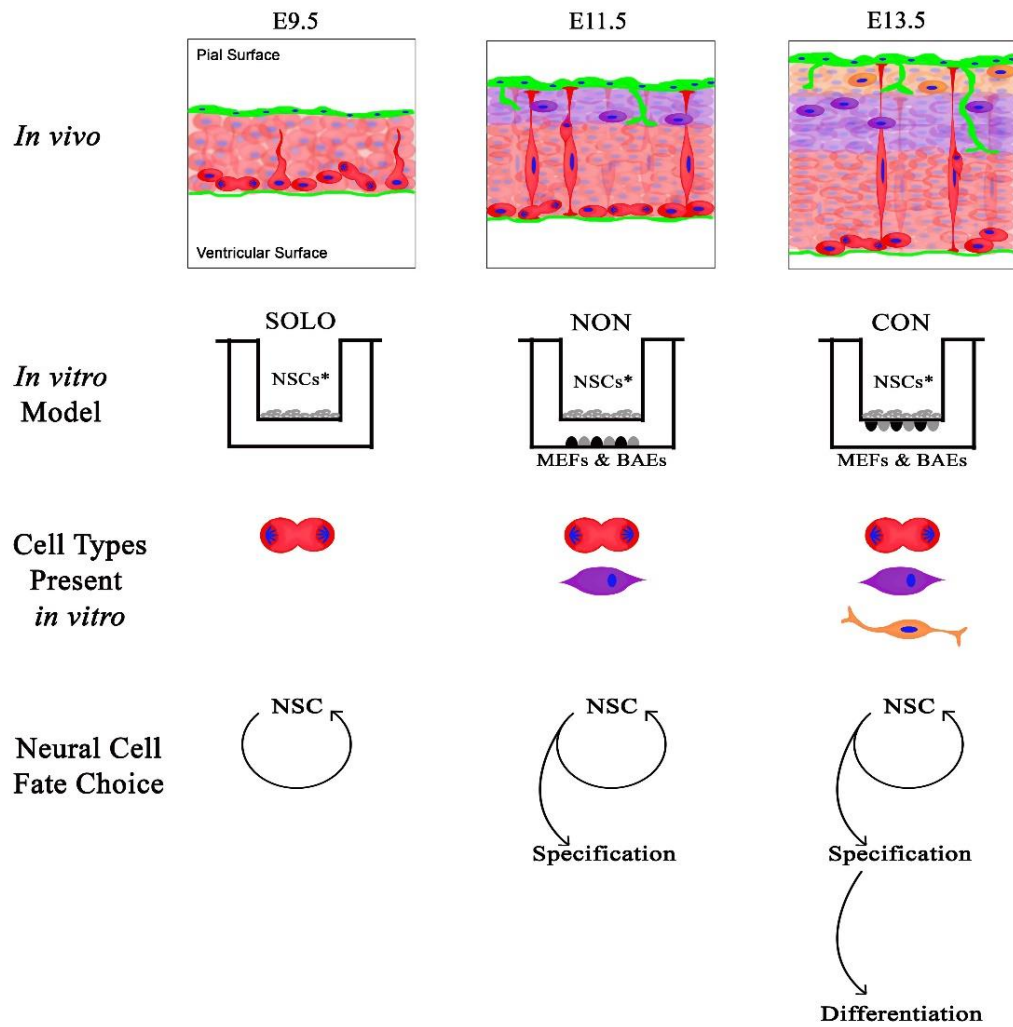


Figure 33: The *in vitro* system recaptured the microenvironment present during different stages in cortical development. At the developmental stage of E9.5 the neuroepithelium consists primarily of neural stem cells. This environment was mimicked *in vitro* by culturing immortalized SSEA-1-enriched neural epithelial cells by themselves (solo). This condition produced mainly self-renewing neural stem cells, which is consistent with E9.5 *in vivo* neural epithelium. At E11.5 *in vivo*, there is an increase in the neuroepithelium due to the generation of neural progenitor cells through asymmetric

division by neural stem cells. Also the initial stages of vascular investment of the cortex is occurring. By culturing neural epithelial cells in non-contacting coculture with vascular cells, the *in vivo* microenvironment was recapitulated in an *in vitro* system. This system generated a cell population consisting of primarily of neural stem and progenitor cells which are the cell populations present *in vivo* neuroepithelium at E11.5. At E13.5 the *in vivo* neural epithelium consists of neural stem, progenitor, and early lineage neural cells. Also, during this time the vascular investment has increased in the cortical tissue. In order to recapitulate this developmental time point, neural epithelial cells were cultured in contacting coculture with vascular cells. This condition produced and maintained all three cell populations (neural stem, progenitor, and early lineage neural cells) which correlates to *in vivo* neural epithelium at E13.5.

signaling pathways such as the Notch signaling pathway may directly impact cell fate decisions. During cortical development, Juxtacrine signaling does not occur by itself due to the fact that neural epithelial cells in direct contact with vascular cells can still utilize autocrine and paracrine signaling. This is most likely the case for neural epithelial cells cultured in contacting coculture with vascular cells. The neural epithelial cells can be receiving autocrine signals from themselves that promote neural stem cell fate. In parallel, paracrine and juxtacrine signals from the vascular cells can promote maintenance of a neural stem cell population, which also generating an early lineage neural cell population within the same microenvironment. This scenario has been shown in E13.5 forebrains where cell fate-specific transcription factor expression has been tracked (reviewed in ⁴⁵). While the contribution of the vasculature was not explored by Hevner and colleagues, close examination of the Pax6, Tbr2, and Tbr1 positive layers shows anatomical divisions running along vascular plexus breaks in the tissue (reviewed in ⁴⁵). Based on published literature and our own results, it appears that the proximity of the vasculature to neural epithelial cells can elicit varying responses during cortical development, and that the vasculature is critical for more than just delivering oxygen and nutrients.

Do neural epithelial cells require cues from extrinsic sources, intrinsic sources, or both in order to progress through cell differentiation during cortex development?

Neural epithelial cells within the developing cortex are exposed to signaling cues from within the cell themselves (intrinsic) as well as from the microenvironment (extrinsic) which can influence cell fate decisions. Extrinsic cues present in the cortical microenvironment can be derived from multiple sources such as neural epithelial cells,

vascular cells, the ECM, etc. Through altering the proportion or distribution of extrinsic cues in the environment may result in changes to neural epithelial cell fate. An extrinsic cue present within the developing cortex is Vegf, which is produced by both neural epithelial cells and vascular cells. When the concentration of Vegf (5ng/ml-100ng/ml) is increased within a culture condition consisting of bovine endothelial cells (BAE), it leads to a dose-dependent increase in FGF2 generated by the BAEs ¹⁰⁵. FGF2 has been shown to promote slow expansion of neural precursor cells isolated from adult striatal tissue. However, when these neural precursor cells are exposed to FGF and EGF it promotes faster expansion of the culture ¹⁰⁰. This suggests that by altering the Vegf concentration, or potentially Vegf isoform profile, it could affect the concentration of other growth factors. Thereby, demonstrating that by altering one extrinsic factor (i.e. Vegf) can have a compounding effect, leading to a change in growth factor composition within the microenvironment that could influence shifts in neural epithelial cell fate.

While neural epithelial cells can be influenced by extrinsic cues, they are also able to rely on intrinsic cues to determine cell fate. Neural epithelial cells from specific regions in the brain have been shown to retain regional identity in an *in vitro* system. Klein et al (2005) demonstrated this by showing that neural stem cells isolated from E14.5 lateral and medial ganglion eminence were able to differentiate into GABA-ergic neurons, astrocytes, and oligodendrocytes after being cultured for 7-10 days ¹⁰⁶. This intrinsic regional identity in neural epithelial cell cultures also applies to cells isolated from the cortex. Cortical E14.5 mouse neural epithelial cells continue to express region specific genes (empty spiracles homeobox 1;Emx1 and orthodenticle homeobox 2;Otx2) after being cultured for 7 days ¹⁰⁷. These studies suggest that neural epithelial cells

contain intrinsic cues that are 1) programmed for a specific cell lineage and 2) can be retained when cells are cultured within an *in vitro* system. The programmed intrinsic cues can be altered by exposure to extrinsic cues from the microenvironment. For example, taking E14.5 mouse neural stem cells from the dorsal forebrain (DB), midbrain (MB), and hindbrain (HB) and culturing them with cues from ventral forebrain tissue, it results in late-expression ventral forebrain genes (Dlx4 and Dlx6) in DB, MB, and HB neural stem cells¹⁰⁷. This suggests that by changing the microenvironment neural epithelial cells are cultured in (extrinsic) may alter intrinsic mechanisms that result in a change in cell fate. The use of this information as well as the results obtained in this study, suggest that neural epithelial cells require both intrinsic and extrinsic cues for cell fate decisions. The alteration of Vegf isoform production within neural epithelial cells, in the current study, may have caused changes in extrinsic and intrinsic cues. Extrinsic cues could have been shifted by having a different proportion and distribution of Vegf isoforms within the culture conditions which may have impacted other growth factors present. Also, the intrinsic cues appeared to be altered due to the fact that Vegf isoform neural epithelial cells did not act in the same manner when cocultured with vascular cells compared to wild type neural epithelial cells. The results seen with both wild type and Vegf isoform neural epithelial cells in coculture conditions brings to mind a question regarding what potential intrinsic cues may be regulating shifts in expression of genes associated with neural epithelial cell fate.

DNA methylation is required for proper development of an organism through regulating shifts in gene expression. When an organism is unable to regulate changes in DNA methylation patterns it can lead to death. Li et al (1992) demonstrated this by

preventing changes in DNA methylation in murine embryonic stem cells through inhibiting DNA methyltransferase (Dnmt) activity which led to prenatal death at mid-gestation ¹⁰⁸. While preventing DNA methylation in embryonic stem cells showcases the large impact of methylation, it does not highlight the fact that these changes are occurring within populations of cells. This is seen when Dnmt inhibition is restricted to central nervous system precursor cells which result in impaired function of neurons within the respiratory system ¹⁰⁹. Regulating gene expression using DNA methylation provides cells with an intrinsic mechanism to regulate timing of cellular differentiation.

Neural epithelial cells have been shown to utilize DNA methylation to regulate both timing of differentiation during cortical development. Tissue samples collected from the cortex of E12-18 Dnmt knockout mice displayed an increase in the number of astrocytes due to a decrease in DNA methylation ¹¹⁰. This suggests that DNA methylation is involved in regulating astrocyte differentiation. In order to assess this idea, Takizawa et al. (2001) examined DNA methylation in the glial fibrillary acidic protein (GFAP) in neural epithelial cells at E11.5 and at E14.5. These time points were selected due to astrocytes not being present within the cortex until E14.5. The study showed that at E11.5 the GFAP promoter region was highly methylated whereas at E14.5 there was a decrease in promoter methylation ¹¹¹. This suggests that the timing of astrocyte differentiation is regulated by DNA methylation. DNA methylation regulates shifts in cell fate through altering gene expression. When DNA methylation is decreased by using BrdU in murine embryonic stem cells it leads to a decrease in Pax6 and Sox2 (neural stem cell markers) expression ¹¹². The decrease in Pax6 and Sox2 expression results in an increase in astrocyte differentiation. These results indicate that DNA methylation is involved with

regulating specific genes, such as Pax6 and Sox2, which can impact neural epithelial cell fate. Salem et al demonstrated that Pax6 expression was regulated by DNA methylation in human bladder and colon cancer cell lines ¹¹³. They did this by using a methylation-sensitive single nucleotide primer extension assay to assess DNA promoter methylation before and after treatment with 5-aza-2-deoxycytidine ¹¹³. The results indicated that Pax6 expression was inhibited by methyl groups binding to the Pax6 promoter region ¹¹³. A similar result was obtained from the work done by this study which also suggests that DNA methylation regulates Pax6 expression. A decrease in Pax6 DNA promoter methylation correlated with an increase in Pax6 expression in both the *in vivo* (E9.5 forebrains) and *in vitro* (E13.5 neural epithelial cells) samples.

The correlation between Pax6 expression and DNA methylation brought the question to mind of what mechanism could be responsible for Pax6 promoter methylation. A complex that is present with the developing neural tissue that has been linked to regulating DNA methylation is the polycomb repressive complex 2 (PRC2; reviewed in ¹¹⁴). The PRC2 is comprised of 4 subunits: Eed (embryonic ectoderm development), Ezh1 (enhancer of zeste homolog 1), Ezh2 (enhancer of zeste homolog 2), and Suz12 (suppressor of zeste homolog 12). A study conducted by Viré et al showed that Ezh2 acts in a recruiting manner with Dnmt within human bone osteosarcoma cells (U2OS cell line) to facilitate DNA methylation ¹¹⁵. The activity of Ezh2 within the PRC2 complex does not work alone to regulate methylation. It has been shown that Suz12 is essential for Ezh2 activity ¹¹⁶. This was done by knocking out Suz12 expression in HeLa cells ¹¹⁶. Also decreasing Suz12 expression in human TIG3-Tcells results in a decrease in cell proliferation ¹¹⁶. The change in cell proliferation suggest that PRC2 may be involved

with regulating expression of genes associated with cell fates that exhibit proliferation (i.e. stem cells). The PRC2 was found to regulate expression of NANOG, OCT4, and SOX2 (genes associated with stem cells) using methylation within human embryonic stem cells⁷⁵. The role of PRC2 in regulating genes associated with stem cells presents the idea that PRC2 is potentially regulating DNA methylation of Pax6. The correlation between Pax6 and Suz12 presented within this study suggests that there could be a possibility that Pax6 DNA methylation is regulated by Suz12 and the PRC2.

Summary and Future Directions

This study aimed to provide an answer to the question, what influence does the vasculature have on neural epithelium development? While the results of this study provide a possible idea to this question, it does not provide a concrete answer. The proliferation and migration assay provide clear results that indicate the presence of the vascular cells leads to an increase in neural epithelial cell proliferation and migration. In contrast, when exploring shifts in neural epithelial cell fate choice through examining gene expression, there was no definitive results. Instead these results indicated a possible trend in cell fate decisions due to the presence of the vascular cells. When vascular cells are present it seems to cause a higher proportion of neural epithelial cells to undergo differentiation compared to when neural epithelial cells are cultured by themselves. While the gene expression results were not significant and no conclusive conclusions can be drawn, it does not mean these results are ineffective. What can be drawn from this study is that vascular cells influence neural epithelial cell responses, but whether these responsive are due to changes in cell fate decisions is still not conclusive. In order to provide results that support the idea that vascular cells are influencing neural epithelial

cell fate future experiments will need to be conducted. Experiments utilizing immunohistochemistry to visualize transcription factors (Pax6, Tbr2, and Tbr1) expressed by neural epithelial cells in coculture conditions will provide additional support for the proposed conclusions regarding neural epithelial cell fate decisions previously highlighted in this study. Also, additional coculture experiments should be conducted to increase the number of replicates and then used to quantify gene expression using quantitative real time PCR. These additional replicates can be used to provide a more accurate representation of neural epithelial cell fate decisions in coculture conditions. While this study was not able to provide conclusive results it does provide 1) an *in vitro* system that can be used to study cortical development, 2) results that shown vascular cells impact neural epithelial cell responses, and 3) an idea for how vascular cells are influencing neural epithelial cell fate choice. The results from this study provides a foundation on which others can build upon to further investigate the relationship between vascular and neural epithelial cells during cortical development.

APPENDIX

The Appendix contains supplementary results that were not presented within the body of the text. The data presented in this portion of the document were not required for data interpretation but are used to support the results and conclusions of the current study. Contained within the Appendix are tables presenting primers and PCR protocols used for standard and quantitative PCR. In addition, there are graphs and tables that depict correlation trends and values between genes associated with neural epithelial cell fate in wild type and Vegf isoform neural epithelial cells. Lastly, there are graphs that show the concentration of neural epithelial associated genes, Pax6, Tbr2, and Tbr1, in Vegf isoform neural epithelial cells which was determined by qPCR.

Table 2: Sequence for forward and reverse primers used for genotype, qualitative, and quantitative PCRs. Sequences are indicated 5'→3'. The Vegf A common forward is paired with reverse primers specific to each isoform.

Gene Name	Alternative nomenclature or Acronym(s)	NMZ Access #
MS 18S F:GACACGGACAGGATTGACAGATTGATAG	18S ribosomal	NR_003278.3 R: GTTAGCATGCCAGAGTCTCGTTCGTT
MS 18S Second Primer F:TAACCCGTTCCCATTC	18S ribosomal	NR_003278.3 R:CATCCAATCGGTAGTAGCGAC
Fucosyltransferase 4 F: TGGGTGTGGATGAACTTCGA	SSEA-1	NM_010242.3 R: GCTGTTTCAGTTGGATCGCTC
Paired box 6 F: GCTTGGTGGTGTCTTTGTCA	Pax6	NM_001244200.1 R: TCACACAACCGTTGGATAC
Inhibitor of DNA binding 1 F: AGCAAAGCGTGGCCATCTC	Id1	NM_010495.3 R: AGGACGTTACCTGCTGCTC
Sex determining region Y box 2 F: CTCTGCACATGAAGGAGCAC	Sox2	NM_011443.3 R: CTCCGGGAAGCGTGTACTTA

Table 2. cont.

Gene Name	Alternative nomenclature Or Acronym	NMZ Access #
T-box protein 2/EOMES F: GCAGGCGCATGTTTCCTTTC	Tbr2	NM_010136.3 R: GTGTTAGGAGATTCTGGGTGAACG
T-box protein 1 F: AACAAATGGGCAGATGGTGG	Tbr1	NM_009322.3 R: CCCGTGTAGATCGTGTCATAGT
Supressor of zeste homolog 12 F: AAAGGAAGGATGTAAGTTGTCCA	Suz12	NM_001163018.1 R:CGAGTAGGACTTCACCATATGG
Vegf A Common forward F: GCCAGCACATAGGAGAGATGAGC		NM_001287056.1
Vegf120 Isoform		R: CCTTGGCTTGTCACATTTTTCTGGC
Vegf164 Isoform		R: AACAAAGGCTCACAGTGATTTTTCTGGC
Vegf188 Isoform		R: AACAAAGGCTCACAGTGAACGCT

Table 3: Standard PCR protocol for Vegf120 genotyping. The PCR protocol used to detect the presence of the Vegf 120 isoform.

Step	Temperature	Time
1	94°C	5'
2	94°C	3'
3	56°C	2'30s
4	72°C	3'45s
	Step 2 3X	
5	94°C	3'
6	60°C	2'30s
7	72°C	3'45s
	Step 5 25X	
8	72°C	5'
9	4°C	HOLD

Table 4: Standard PCR protocol for Vegf188 genotyping. The PCR protocol used to detect the presence of the Vegf188 isoform.

Step	Temperature	Time
1	95°C	3'
2	95°C	2'
3	58°C	2'
4	72°C	3'
	Step 2 30X	
5	72°C	10'
6	4°C	HOLD

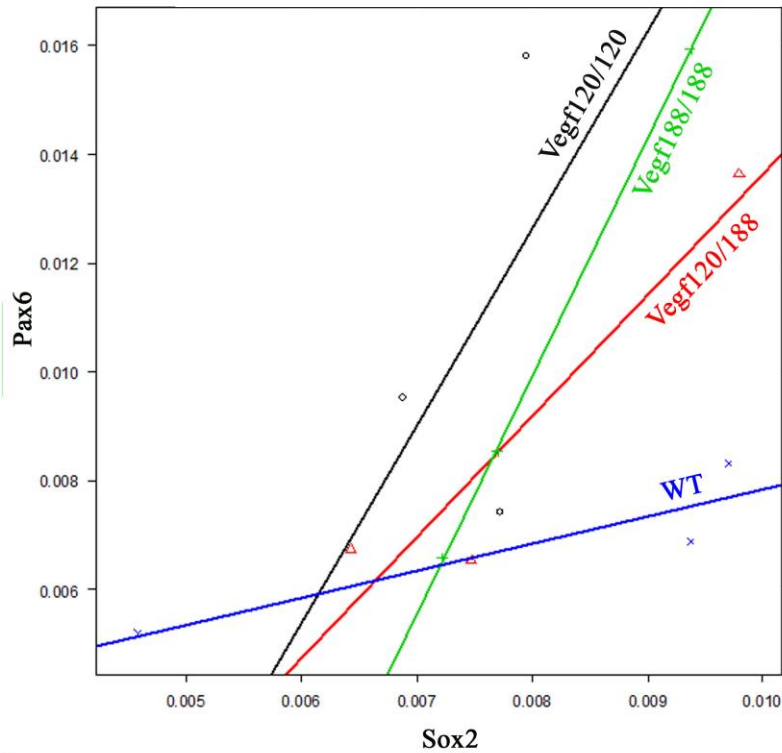


Figure 34: Vegf isoform neural epithelial cells cultured in contact with vascular cells exhibit a correlation between Pax6 and Sox2 gene expression. Immortalized SSEA-1-enriched WT and Vegf isoform neural epithelial cells were cultured for 5 days in contacting coculture with vascular cells. Neural cells were isolated and total RNA was extracted and reverse transcribed into cDNA. Quantitative PCR was used to assess gene expression of Pax6 and Sox2. Vegf120 and Vegf188 neural epithelial cells display a similar correlation pattern ($R^2=0.848$ and $R^2=0.972$) between Pax6 and Sox2 expression compared to Vegf120/188 neural cells ($R^2=0.999$). In contrast WT neural cells do not exhibit a correlation between these two genes. This experiment was conducted 3 times with an $n=3$ for each genotype. All statistical values are included in Appendix Table III for reference.

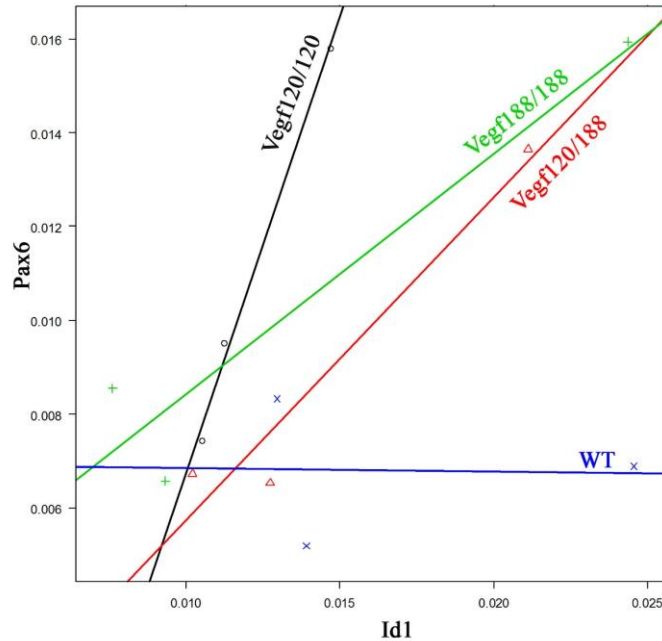


Figure 35: Expression of Pax6 and Id1 correlates in Vegf isoform neural epithelial cells grown in contacting coculture with vascular cells. Immortalized SSEA-1-enriched WT and Vegf isoform neural epithelial cells were cultured for 5 days in contacting coculture with vascular cells. Total RNA was isolated from neural epithelial cells and reverse transcribed to cDNA. Gene expression for Pax6 (neural stem cells) and Id1 (neural progenitor cells) was assessed by qPCR. An analysis of correlation determined that Vegf isoform neural epithelial cells have a high correlation between Pax6 and Id1. Vegf120 has the relatively strongest correlation ($R^2=0.993$) followed closely by Vegf188 ($R^2=0.916$) and Vegf120/188 ($R^2=0.94$). A correlation was not noted with WT neural epithelial cells. This experiment was repeated 3 times with an $n=3$ for each genotype. All statistical values are included in Appendix Table IV for reference.

Table 5: The results of an analysis of correlation between Pax6 and Sox2 for immortalized SSEA-1-enriched WT and Vegf isoform neural epithelial cells.

Immortalized SSEA-1-enriched WT and Vegf isoform neural epithelial cells were cultured in either solo, contacting, or non-contacting coculture with vascular cells. Total RNA was collected, reverse transcribed to cDNA, and qPCR was utilized to assess gene expression. Vegf isoform neural epithelial cells displayed a correlation between Pax6 and Sox2. In contrast, WT neural cells did not have a correlation between Pax6 and Sox2 gene expression. Note that values boxed in blue are graphed as a correlation plot in Figure 15.

Genotype	Treatment	Gene	R²	F	Prob > F	Correlation
WT	SOLO	Sox2	0.943	16.6	0.153	-0.971
Vegf120/120	SOLO	Sox2	0.528	1.119	0.482	-0.727
Vegf188/188	SOLO	Sox2	0.501	0.054	0.855	-0.226
Vegf120/188	SOLO	Sox2	0.123	0.14	0.772	-0.351
WT	CON	Sox2	0.022	0.023	0.905	0.148
Vegf120/120	CON	Sox2	0.97	31.856	0.112	-0.985
Vegf188/188	CON	Sox2	0.119	0.135	0.776	-0.345
Vegf120/188	CON	Sox2	0.259	0.349	0.66	-0.509
WT	NON	Sox2	0.735	2.776	0.344	-0.857
Vegf120/120	NON	Sox2	0.011	0.011	0.934	0.103
Vegf188/188	NON	Sox2	0.538	1.167	0.476	-0.734
Vegf120/188	NON	Sox2	0.0346	0.036	0.881	-0.186

Table 6: The results of an analysis of correlation between Pax6 and Id1 for immortalized SSEA-1-enriched WT and Vegf isoform neural epithelial cells.

Immortalized SSEA-1-enriched WT and Vegf isoform neural epithelial cells were cultured in either solo, contacting, or non-contacting coculture with vascular cells. Total RNA was collected and reverse transcribed to cDNA. Gene expression was assessed using qPCR. Pax6 and Id1 expression did not correlate in WT cells. There was a correlation between Pax6 and Id1 in Vegf isoform neural epithelial cells. Note that values boxed in blue are graphed as a correlation plot in Figure 16. Asterisks indicate significance for the combination of genotype and coculture condition.

Genotype	Treatment	Gene	R²	F	Prob > F	Correlation
WT	SOLO	Id1	0.929	13.087	0.171	0.964
Vegf120/120	SOLO	Id1	0.999	306116.8	0.0036*	0.999
Vegf188/188	SOLO	Id1	0.813	4.335	0.285	0.901
Vegf120/188	SOLO	Id1	0.998	440.54	0.0303*	0.999
WT	CON	Id1	0.0007	0.0007	0.983	-0.027
Vegf120/120	CON	Id1	0.993	146.64	0.0525	0.997
Vegf188/188	CON	Id1	0.916	10.853	0.188	0.957
Vegf120/188	CON	Id1	0.94	15.673	0.158	0.97
WT	NON	Id1	0.965	27.2	0.121	0.982
Vegf120/120	NON	Id1	0.755	3.08	0.33	0.869
Vegf188/188	NON	Id1	0.996	223.563	0.043*	0.998
Vegf120/188	NON	Id1	0.906	9.618	0.199	0.952

Table 7: The results of an analysis of correlation between Pax6 and Tbr2 for immortalized SSEA-1-enriched WT and Vegf isoform neural epithelial cells.

Immortalized SSEA-1-enriched WT and Vegf isoform neural epithelial cells were cultured for 5 days in either solo, contacting, or non-contacting coculture with vascular cells. Neural epithelial cells were isolated and total RNA was collected and reverse transcribed to cDNA. Quantitative PCR was used to assess Pax6 and Tbr2 gene expression. A correlation between Pax6 and Tbr2 expression was not noted with WT neural epithelial cells but a correlation was exhibited in Vegf isoform neural cells. Values boxed in blue are graphed as a correlation plot in Figure 17. Asterisks indicate significance for the combination of genotype and coculture condition

Genotype	Treatment	Gene	R²	F	Prob > F	Correlation
WT	SOLO	Tbr2	0.967	28.965	0.117	0.983
Vegf120/120	SOLO	Tbr2	0.991	112.43	0.06	0.996
Vegf188/188	SOLO	Tbr2	0.773	3.401	0.316	0.879
Vegf120/188	SOLO	Tbr2	0.955	21.29	0.136	0.978
WT	CON	Tbr2	0.004	0.0043	0.958	0.066
Vegf120/120	CON	Tbr2	0.734	2.763	0.345	0.857
Vegf188/188	CON	Tbr2	0.987	77.486	0.072	0.994
Vegf120/188	CON	Tbr2	0.998	456.65	0.03*	0.999
WT	NON	Tbr2	0.992	122.463	0.057	0.996
Vegf120/120	NON	Tbr2	0.782	3.579	0.31	0.884
Vegf188/188	NON	Tbr2	0.988	86.27	0.068	0.994
Vegf120/188	NON	Tbr2	0.944	16.76	0.0153	0.971

Table 8: The results of an analysis of correlation between Pax6 and Tbr1 for immortalized SSEA-1-enriched WT and Vegf isoform neural epithelial cells.

Immortalized SSEA-1-enriched WT and Vegf isoform neural epithelial cells were cultured in either solo, contacting, or non-contacting coculture with vascular cells for 5 days. Neural epithelial cells were isolated and total RNA was collected and reverse transcribed to cDNA. Pax6 and Tbr1 expression were determined using qPCR. Neural epithelial cells cultured solo displayed a negative correlation. In contrast, neural epithelial cells in contacting and non-contacting coculture with vascular cells had a positive correlation between Pax6 and Tbr1 gene expression with the exception of Vegf 120/120 (boxed in blue), regardless of genotype.

Genotype	Treatment	Gene	R²	F	Prob > F	Correlation
WT	SOLO	Tbr1	0.612	1.576	0.428	-0.782
Vegf120/120	SOLO	Tbr1	0.956	21.899	0.134	-0.978
Vegf188/188	SOLO	Tbr1	0.481	0.928	0.512	-0.694
Vegf120/188	SOLO	Tbr1	0.568	1.314	0.457	-0.753
WT	CON	Tbr1	0.56	1.275	0.461	0.749
Vegf120/120	CON	Tbr1	0.237	0.311	0.676	-0.487
Vegf188/188	CON	Tbr1	0.96	24.252	0.128	0.98
Vegf120/188	CON	Tbr1	0.992	121.31	0.058	0.996
WT	NON	Tbr1	0.96	24.128	0.128	0.98
Vegf120/120	NON	Tbr1	0.542	1.182	0.474	0.736
Vegf188/188	NON	Tbr1	0.997	322.33	0.035*	0.998
Vegf120/188	NON	Tbr1	0.924	12.197	0.178	0.961

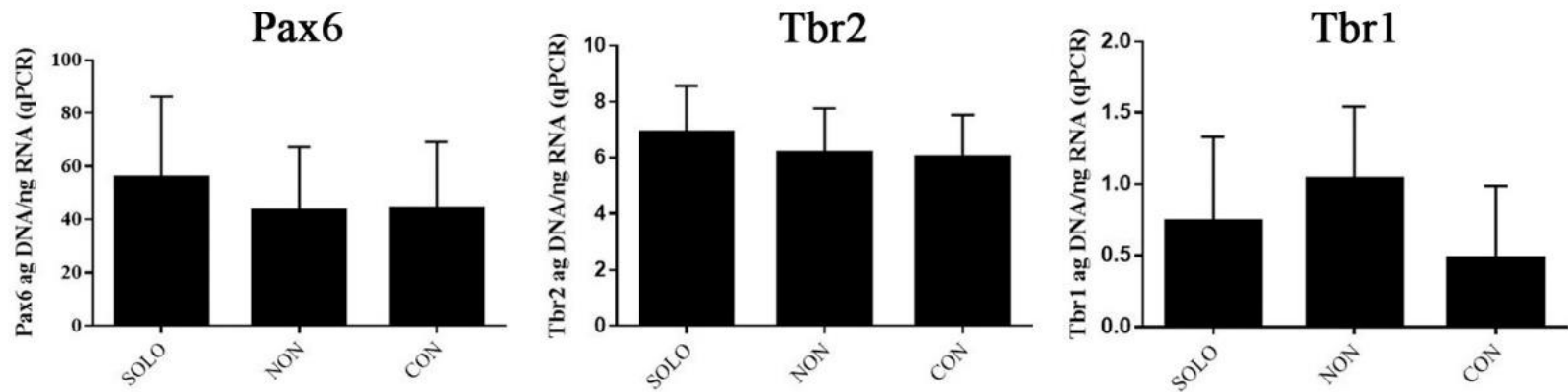


Figure 36: Vegf120 SSEA-1-enriched neural epithelial cells display shifts in expression of genes associated with neural stem cell fate choice when cocultured with vascular cells. Immortalized Vegf120 SSEA-1-enriched neural epithelial cells were cultured either in solo, contacting, or non-contacting coculture with vascular cells. Total RNA was isolated from neural epithelial cells and transcribed to cDNA. Pax6, Tbr2, and Tbr1 expression was quantified with qPCR. Neural epithelial cells exhibit a decreasing trend in Pax6 expression when cocultured with vascular cells (One way ANOVA $p=0.8202$). There was a decreasing trend in Tbr2 expression in neural epithelial cells with the presence of vascular cells (One way ANOVA $p=0.7810$). The expression of Tbr1 exhibited an increasing trend in non-contacting coculture and a decrease in contacting coculture (One way ANOVA $p=0.3121$). This experiment was repeated 3 times with an $n=3$.

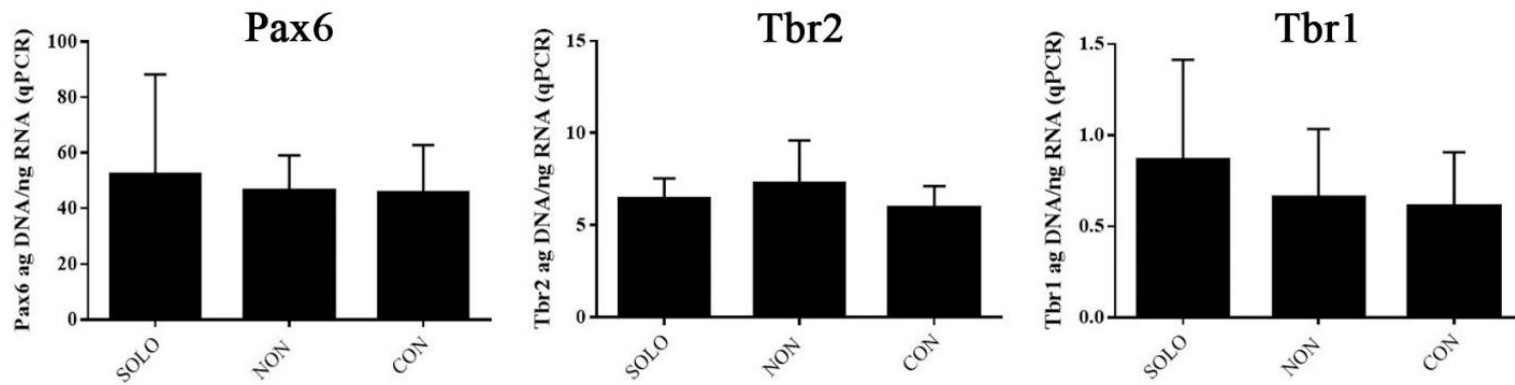


Figure 37: Vegf188 SSEA-1-enriched neural epithelial cells cocultured with vascular cells display shifts in expression of genes associated with neural stem cell fate choice. Vegf188 immortalized SSEA-1-enriched neural epithelial cells were cultured either in solo, contacting, or non-contacting coculture with vascular cells. Neural cells were isolated and RNA was collected and reverse transcribed to cDNA. Qualitative PCR was utilized to assess expression of Pax6, Tbr2, and Tbr1. Neural epithelial cells exhibit a slight decreasing trend in Pax6 expression when cocultured with vascular cells (One way ANOVA $p=0.9383$). Tbr2 expression displayed an increasing trend in neural epithelial cells in non-contacting coculture with vascular cells (One way ANOVA $p=0.5614$). In contrast, neural epithelial cells exhibited a slight increasing trend in Tbr1 expression (One way ANOVA $p=0.6647$). This experiment was repeated 3 times with an $n=3$.

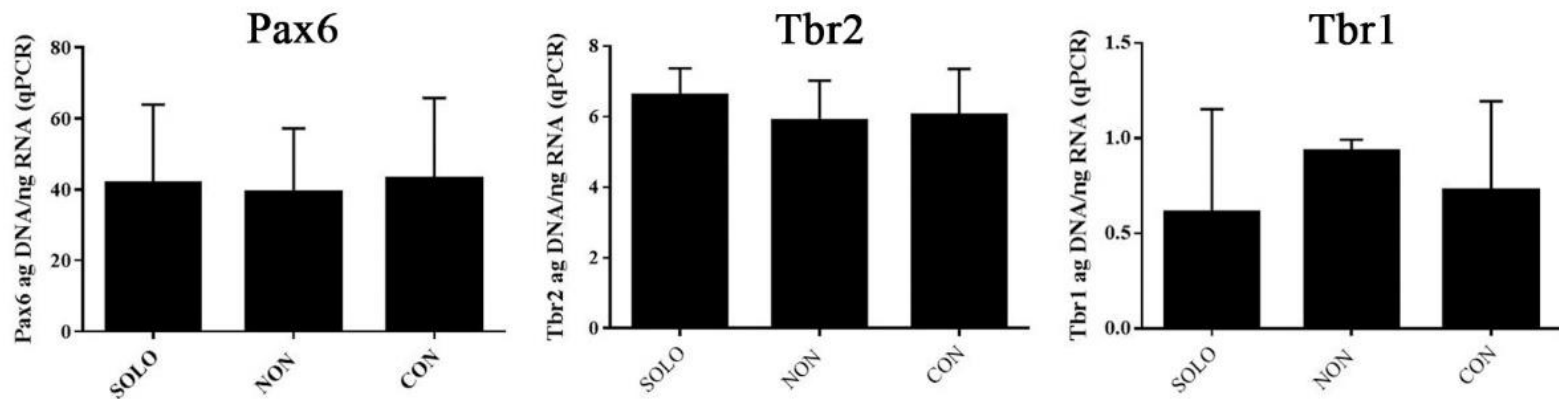


Figure 38: Vegf120/188 SSEA-1-enriched neural epithelial cells cocultured with vascular cells display shifts in expression of genes associated with neural stem cell fate choice. Vegf120/188 immortalized SSEA-1-enriched neural epithelial cells were cultured either in solo, contacting, or non-contacting coculture with vascular cells. Total RNA was collected from neural epithelial cells. RNA was reverse transcribed to cDNA and gene expression assessed by qPCR. Non-significant changes in Pax6 expression were noted in neural epithelial cells cocultured with vascular cells (One way ANOVA $p=0.9761$). Tbr2 expression exhibited a decreasing trend in neural epithelial cells with the presence of vascular cells (One way ANOVA $p=0.7040$). In contrast, neural epithelial cells exhibited a slight increasing trend in Tbr1 expression (One way ANOVA $p=0.6507$). This experiment was repeated 3 times with an $n=3$.

REFERENCES

1. Drake, C. J., *Embryonic and adult vasculogenesis*. Birth Defects Research Part C: Embryo Today: Reviews, 2003. **69**(1): p. 73-82.
2. Vasudevan, A. and Bhide, P. G., *Angiogenesis in the embryonic CNS: a new twist on an old tale*. Cell Adhesion and Migration, 2008. **2**(3): p. 167-169.
3. Schmidt, A., Brixius, K., and Bloch, W., *Endothelial precursor cell migration during vasculogenesis*. Circulation Research, 2007. **101**(2): p. 125-136.
4. Gerhardt, H., Golding, M., Fruttiger, M., Ruhrberg, C., Lundkvist, A., Abramsson, A., Jeltsch, M., Mitchell, C., Alitalo, K., and Shima, D., *VEGF guides angiogenic sprouting utilizing endothelial tip cell filopodia*. The Journal of Cell Biology, 2003. **161**(6): p. 1163-1177.
5. Risau, W., *Differentiation of endothelium*. The FASEB journal, 1995. **9**(10): p. 926-933.
6. Bar, T., Guldner, F. H., and Wolff, J. R., *"Seamless" endothelial cells of blood capillaries*. Cell Tissue Research, 1984. **235**(1): p. 99-106.
7. Hirakow, R. and Hiruma, T., *Scanning electron microscopic study on the development of primitive blood vessels in chick embryos at the early somite-stage*. Anatomy and Embryology, 1981. **163**(3): p. 299-306.
8. Lamalice, L., Le Boeuf, F., and Huot, J., *Endothelial cell migration during angiogenesis*. Circulation Research, 2007. **100**(6): p. 782-794.
9. Darland, D. C., Massingham, L. J., Smith, S. R., Piek, E., Saint-Geniez, M., and D'amore, P. A., *Pericyte production of cell-associated VEGF is differentiation-dependent and is associated with endothelial survival*. Developmental Biology, 2003. **264**(1): p. 275-288.
10. Tischer, E., Mitchell, R., Hartman, T., Silva, M., Gospodarowicz, D., Fiddes, Jc, and Abraham, Ja, *The human gene for vascular endothelial growth factor. Multiple protein forms are encoded through alternative exon splicing*. Journal of Biological Chemistry, 1991. **266**(18): p. 11947-11954.
11. Houck, K. A., Leung, D. W., Rowland, A. M., Winer, J., and Ferrara, N., *Dual regulation of vascular endothelial growth factor bioavailability by genetic and proteolytic mechanisms*. The Journal of Biological Chemistry 1992. **267**(36): p. 26031-26037.
12. Neufeld, G., Cohen, T., Gengrinovitch, S., and Poltorak, Z., *Vascular endothelial growth factor (VEGF) and its receptors*. The FASEB Journal, 1999. **13**(1): p. 9-22.
13. Ruhrberg, C., Gerhardt, H., Golding, M., Watson, R., Ioannidou, S., Fujisawa, H., Betsholtz, C., and Shima, D. T., *Spatially restricted patterning cues provided by heparin-binding VEGF-A control blood vessel branching morphogenesis*. Genes & Development, 2002. **16**(20): p. 2684-2698.

14. Koch, S. and Claesson-Welsh, L., *Signal transduction by vascular endothelial growth factor receptors*. Cold Spring Harbor Perspectives in Medicine, 2012. **2**(7): p. 1-21.
15. Vaisman, N., Gospodarowicz, D., and Neufeld, G., *Characterization of the receptors for vascular endothelial growth factor*. The Journal of Biological Chemistry, 1990. **265**(32): p. 19461-19466.
16. Koch, S., Tugues, S., Li, X., Gualandi, L., and Claesson-Welsh, L., *Signal transduction by vascular endothelial growth factor receptors*. Biochemical Journal, 2011. **437**(2): p. 169-183.
17. Kukk, E., Lymboussaki, A., Taira, S., Kaipainen, A., Jeltsch, M., Joukov, V., and Alitalo, K., *VEGF-C receptor binding and pattern of expression with VEGFR-3 suggests a role in lymphatic vascular development*. Development, 1996. **122**(12): p. 3829-3837.
18. Fong, G. H., Rossant, J., Gertsenstein, M., and Breitman, M. L., *Role of the Flt-1 receptor tyrosine kinase in regulating the assembly of vascular endothelium*. Nature, 1995. **376**: p. 66-70.
19. Claesson-Welsh, L., *Signal transduction by vascular endothelial growth factor receptors*. Biochemical Society Transactions, 2003. **31**(1): p. 20-24.
20. Shalaby, F., Ho, J., Stanford, W. L., Fischer, K. D., Schuh, A. C., Schwartz, L., Bernstein, A., and Rossant, J., *A requirement for Flk1 in primitive and definitive hematopoiesis and vasculogenesis*. Cell, 1997. **89**(6): p. 981-990.
21. Waltenberger, J., Claesson-Welsh, L., Siegbahn, A., Shibuya, M., and Heldin, C. H., *Different signal transduction properties of KDR and Flt1, two receptors for vascular endothelial growth factor*. Journal of Biological Chemistry, 1994. **269**(43): p. 26988-26995.
22. Takahashi, T., Yamaguchi, S., Chida, K., and Shibuya, M., *A single autophosphorylation site on KDR/Flk-1 is essential for VEGF-A-dependent activation of PLC-gamma and DNA synthesis in vascular endothelial cells*. The EMBO Journal, 2001. **20**(11): p. 2768-2778.
23. Lamalice, L., Houle, F., Jourdan, G., and Huot, J., *Phosphorylation of tyrosine 1214 on VEGFR2 is required for VEGF-induced activation of Cdc42 upstream of SAPK2/p38*. Oncogene, 2004. **23**(2): p. 434-45.
24. Gille, H., Kowalski, J., Li, B., Lecouter, J., Moffat, B., Zioncheck, T. F., Pelletier, N., and Ferrara, N., *Analysis of biological effects and signaling properties of Flt-1 (VEGFR-1) and KDR (VEGFR-2) A reassessment using novel receptor-specific vascular endothelial growth factor mutants*. Journal of Biological Chemistry, 2001. **276**(5): p. 3222-3230.
25. Shalaby, F., Rossant, J., Yamaguchi, T. P., Gertsenstein, M., Wu, X. F., Breitman, M. L., and Schuh, A. C., *Failure of blood-island formation and vasculogenesis in Flk-1-deficient mice*. Nature, 1995. **376**(6535): p. 62-66.
26. Meadows, K. N., Bryant, P., and Pumiglia, K., *Vascular endothelial growth factor induction of the angiogenic phenotype requires Ras activation*. Journal of Biological Chemistry, 2001. **276**(52): p. 49289-49298.
27. Kawamura, H., Li, X., Harper, S. J., Bates, D. O., and Claesson-Welsh, L., *Vascular endothelial growth factor (VEGF)-A165b is a weak in vitro agonist for*

- VEGF receptor-2 due to lack of coreceptor binding and deficient regulation of kinase activity.* Cancer Research, 2008. **68**(12): p. 4683-92.
28. Huang, K., Andersson, C., Roomans, G. M., Ito, N., and Claesson-Welsh, L., *Signaling properties of VEGF receptor-1 and -2 homo- and heterodimers.* The International Journal of Biochemistry and Cell Biology, 2001. **33**(4): p. 315-324.
 29. Soker, S., Miao, H. Q., Nomi, M., Takashima, S., and Klagsbrun, M., *VEGF165 mediates formation of complexes containing VEGFR - 2 and neuropilin - 1 that enhance VEGF165 - receptor binding.* Journal of Cellular Biochemistry, 2002. **85**(2): p. 357-368.
 30. Takagi, S., Kasuya, Y., Shimizu, M., Matsuura, T., Tsuboi, M., Kawakami, A., and Fujisawa, H., *Expression of a cell adhesion molecule, neuropilin, in the developing chick nervous system.* Developmental Biology, 1995. **170**(1): p. 207-222.
 31. Koch, S., *Neuropilin signalling in angiogenesis.* Biochemical Society Transactions, 2012. **40**(1): p. 20-25.
 32. Soker, S., Takashima, S., Miao, H. Q., Neufeld, G., and Klagsbrun, M., *Neuropilin-1 is expressed by endothelial and tumor cells as an isoform-specific receptor for vascular endothelial growth factor.* Cell, 1998. **92**(6): p. 735-745.
 33. Cleaver, O. and Melton, D. A., *Endothelial signaling during development.* Nature Medicine, 2003. **9**(6): p. 661-668.
 34. Lammert, E., Cleaver, O., and Melton, D., *Role of endothelial cells in early pancreas and liver development.* Mechanisms of Development, 2003. **120**(1): p. 59-64.
 35. Matsumoto, K., Yoshitomi, H., Rossant, J., and Zaret, K. S., *Liver organogenesis promoted by endothelial cells prior to vascular function.* Science, 2001. **294**(5542): p. 559-563.
 36. Fabris, L., Cadamuro, M., Libbrecht, L., Raynaud, P., Spirli, C., Fiorotto, R., Okolicsanyi, L., Lemaigre, F., Strazzabosco, M., and Roskams, T., *Epithelial expression of angiogenic growth factors modulate arterial vasculogenesis in human liver development.* Hepatology, 2008. **47**(2): p. 719-728.
 37. Ng, Y. S., Rohan, R., Sunday, M. E., Demello, D. E., and D'amore, P. A., *Differential expression of VEGF isoforms in mouse during development and in the adult.* Developmental Dynamics, 2001. **220**(2): p. 112-21.
 38. Ng, Y. S., Rohan, R., Sunday, M. E., Demello, D. E., and D'amore, P. A., *Differential expression of VEGF isoforms in mouse during development and in the adult.* Developmental Dynamics, 2001. **220**(2): p. 112-121.
 39. Gomez, A. R., Norwood, V. F., and Tufro - Mcreddie, A., *Development of the kidney vasculature.* Microscopy Research and Technique, 1997. **39**(3): p. 254-260.
 40. Vasudevan, A., Long, J. E., Crandall, J. E., Rubenstein, J. L., and Bhide, P. G., *Compartment-specific transcription factors orchestrate angiogenesis gradients in the embryonic brain.* Nature Neuroscience, 2008. **11**(4): p. 429-439.
 41. Englund, C., Fink, A., Lau, C., Pham, D., Daza, R., Bulfone, A., Kowalczyk, T., and Hevner, R. F., *Pax6, Tbr2, and Tbr1 are expressed sequentially by radial*

- glia, intermediate progenitor cells, and postmitotic neurons in developing neocortex.* The Journal of Neuroscience, 2005. **25**(1): p. 247-251.
42. Price, M., *Members of the Dlx- and Nkx2-gene families are regionally expressed in the developing forebrain.* Journal of Neurobiology, 1993. **24**(10): p. 1385-1399.
 43. Noctor, S. C., Martínez-Cerdeño, V., Ivic, L., and Kriegstein, A. R., *Cortical neurons arise in symmetric and asymmetric division zones and migrate through specific phases.* Nature Neuroscience, 2004. **7**(2): p. 136-144.
 44. Bayatti, N., Sarma, S., Shaw, C., Eyre, J. A., Vouyiouklis, D. A., Lindsay, S., and Clowry, G. J., *Progressive loss of PAX6, TBR2, NEUROD and TBR1 mRNA gradients correlates with translocation of EMX2 to the cortical plate during human cortical development.* European Journal of Neuroscience, 2008. **28**(8): p. 1449-1456.
 45. Hevner, R. F., *From radial glia to pyramidal-projection neuron: transcription factor cascades in cerebral cortex development.* Molecular Neurobiology 2006. **33**(1): p. 33-50.
 46. Bedogni, F., Hodge, R. D., Elsen, G. E., Nelson, B. R., Daza, R. A., Beyer, R. P., Bammler, T. K., Rubenstein, J. L., and Hevner, R. F., *Tbr1 regulates regional and laminar identity of postmitotic neurons in developing neocortex.* Proceedings of the National Academy Science USA, 2010. **107**(29): p. 13129-13134.
 47. Edmondson, J. C. and Hatten, M. E., *Glial-guided granule neuron migration in vitro: a high-resolution time-lapse video microscopic study.* The Journal of Neuroscience, 1987. **7**(6): p. 1928-1934.
 48. Rakic, P., *Mode of cell migration to the superficial layers of fetal monkey neocortex.* Journal of Comparative Neurology, 1972. **145**(1): p. 61-83.
 49. Noctor, S. C., Flint, A. C., Weissman, T. A., Dammerman, R. S., and Kriegstein, A. R., *Neurons derived from radial glial cells establish radial units in neocortex.* Nature, 2001. **409**(6821): p. 714-720.
 50. Malatesta, P., Hartfuss, E., and Gotz, M., *Isolation of radial glial cells by fluorescent-activated cell sorting reveals a neuronal lineage.* Development, 2000. **127**(24): p. 5253-5263.
 51. Darland, D. C., Cain, J. T., Berosik, M. A., Saint-Geniez, M., Odens, P. W., Schaubhut, G. J., Frisch, S., Stemmer-Rachamimov, A., Darland, T., and D'amore, P. A., *Vascular endothelial growth factor (VEGF) isoform regulation of early forebrain development.* Developmental Biology, 2011. **358**(1): p. 9-22.
 52. Ruiz De Almodovar, C., Coulon, C., Salin, P. A., Knevels, E., Chounlamountri, N., Poesen, K., Hermans, K., Lambrechts, D., Van Geyte, K., Dhondt, J., Dresselaers, T., Renaud, J., Aragones, J., Zacchigna, S., Geudens, I., Gall, D., Stroobants, S., Mutin, M., Dassonville, K., Storkebaum, E., Jordan, B. F., Eriksson, U., Moons, L., D'hooge, R., Haigh, J. J., Belin, M. F., Schiffmann, S., Van Hecke, P., Gallez, B., Vinckier, S., Chedotal, A., Honnorat, J., Thomasset, N., Carmeliet, P., and Meissirel, C., *Matrix-binding vascular endothelial growth factor (VEGF) isoforms guide granule cell migration in the cerebellum via VEGF receptor Flk1.* Journal of Neuroscience, 2010. **30**(45): p. 15052-15066.

53. Sondell, M., Lundborg, G., and Kanje, M., *Vascular endothelial growth factor has neurotrophic activity and stimulates axonal outgrowth, enhancing cell survival and Schwann cell proliferation in the peripheral nervous system*. Journal of Neuroscience, 1999. **19**(14): p. 5731-5740.
54. Long, J. B., Jay, S. M., Segal, S. S., and Madri, J. A., *VEGF-A and Semaphorin3A: modulators of vascular sympathetic innervation*. Developmental Biology, 2009. **334**(1): p. 119-132.
55. Schanzer, A., Wachs, F. P., Wilhelm, D., Acker, T., Cooper-Kuhn, C., Beck, H., Winkler, J., Aigner, L., Plate, K. H., and Kuhn, H. G., *Direct stimulation of adult neural stem cells in vitro and neurogenesis in vivo by vascular endothelial growth factor*. Brain Pathology, 2004. **14**(3): p. 237-248.
56. Ogunshola, O. O., Antic, A., Donoghue, M. J., Fan, S. Y., Kim, H., Stewart, W. B., Madri, J. A., and Ment, L. R., *Paracrine and autocrine functions of neuronal vascular endothelial growth factor (VEGF) in the central nervous system*. The Journal of Biological Chemistry, 2002. **277**(13): p. 11410-11415.
57. Nishijima, K., Ng, Y. S., Zhong, L., Bradley, J., Schubert, W., Jo, N., Akita, J., Samuelsson, S. J., Robinson, G. S., and Adamis, A. P., *Vascular endothelial growth factor-A is a survival factor for retinal neurons and a critical neuroprotectant during the adaptive response to ischemic injury*. The American Journal of Pathology, 2007. **171**(1): p. 53-67.
58. Jin, K., Zhu, Y., Sun, Y., Mao, X. O., Xie, L., and Greenberg, D. A., *Vascular endothelial growth factor (VEGF) stimulates neurogenesis in vitro and in vivo*. Proceedings of the National Academy of Sciences, 2002. **99**(18): p. 11946-11950.
59. Soen, Y., Mori, A., Palmer, T. D., and Brown, P. O., *Exploring the regulation of human neural precursor cell differentiation using arrays of signaling microenvironments*. Molecular Systems Biology, 2006. **2**: p. 1-14.
60. Leone, D. P., Relvas, J. B., Campos, L. S., Hemmi, S., Brakebusch, C., Fassler, R., Ffrench-Constant, C., and Suter, U., *Regulation of neural progenitor proliferation and survival by beta1 integrins*. Journal of Cell Science, 2005. **118**(Pt 12): p. 2589-2599.
61. Freire, E., Gomes, F., Linden, R., Neto, V. M., and Coelho-Sampaio, T., *Structure of laminin substrate modulates cellular signaling for neurite outgrowth*. Journal of Cell Science, 2002. **115**(24): p. 4867-4876.
62. Haubst, N., Georges-Labouesse, E., De Arcangelis, A., Mayer, U., and Gotz, M., *Basement membrane attachment is dispensable for radial glial cell fate and for proliferation, but affects positioning of neuronal subtypes*. Development, 2006. **133**(16): p. 3245-3254.
63. Halfter, W., Dong, S., Yip, Y. P., Willem, M., and Mayer, U., *A critical function of the pial basement membrane in cortical histogenesis*. The Journal of Neuroscience, 2002. **22**(14): p. 6029-6040.
64. Reichardt, L. F. and Tomaselli, K. J., *Extracellular matrix molecules and their receptors: functions in neural development*. Annual Review of Neuroscience, 1991. **14**: p. 531.

65. Chou, C. H., Sinden, J. D., Couraud, P. O., and Modo, M., *In vitro modeling of the neurovascular environment by coculturing adult human brain endothelial cells with human neural stem cells*. PLoS ONE, 2014. **9**(9): p. e106346.
66. Tropepe, V., Sibilia, M., Ciruna, B. G., Rossant, J., Wagner, E. F., and Van Der Kooy, D., *Distinct neural stem cells proliferate in response to EGF and FGF in the developing mouse telencephalon*. Developmental Biology, 1999. **208**(1): p. 166-188.
67. Hellstrom, M., Gerhardt, H., Kalen, M., Li, X., Eriksson, U., Wolburg, H., and Betsholtz, C., *Lack of pericytes leads to endothelial hyperplasia and abnormal vascular morphogenesis*. The Journal of Cell Biology, 2001. **153**(3): p. 543-553.
68. Carmeliet, P., Ng, Y. S., Nuyens, D., Theilmeier, G., Brusselmans, K., Cornelissen, I., Ehler, E., Kakkar, V. V., Stalmans, I., Mattot, V., Perriard, J. C., Dewerchin, M., Flameng, W., Nagy, A., Lupu, F., Moons, L., Collen, D., D'amore, P. A., and Shima, D. T., *Impaired myocardial angiogenesis and ischemic cardiomyopathy in mice lacking the vascular endothelial growth factor isoforms VEGF164 and VEGF188*. Nature Medicine, 1999. **5**(5): p. 495-502.
69. Cain, J. T., Berosik, M. A., Snyder, S. D., Crawford, N. F., Nour, S. I., Schaubhut, G. J., and Darland, D. C., *Shifts in the vascular endothelial growth factor isoforms result in transcriptome changes correlated with early neural stem cell proliferation and differentiation in mouse forebrain*. Developmental Neurobiology, 2014. **74**(1): p. 63-81.
70. Ellis, P., Fagan, M. B., Magness, S. T., Hutton, S., Taranova, O., Hayashi, S., McMahon, A., Rao, M., and Pevny, L., *SOX2, a persistent marker for multipotential neural stem cells derived from embryonic stem cells, the embryo or the adult*. Stem and Progenitor Cells in the Central Nervous System, 2004. **26**(2-4): p. 149-165.
71. Tzeng, S. F. and De Vellis, J., *Id1, Id2, and Id3 gene expression in neural cells during development*. Glia, 1998. **24**(4): p. 372-381.
72. Hahn, M. A., Qiu, R., Wu, X., Li, A. X., Zhang, H., Wang, J., Jui, J., Jin, S. G., Jiang, Y., and Pfeifer, G. P., *Dynamics of 5-hydroxymethylcytosine and chromatin marks in mammalian neurogenesis*. Cell Reports, 2013. **3**(2): p. 291-300.
73. Shyamasundar, S., Jadhav, S. P., Bay, B. H., Tay, S. Sw., Kumar, D. S., Rangasamy, D., and Dheen, T. S., *Analysis of epigenetic factors in mouse embryonic neural stem cells exposed to hyperglycemia*. PloS One, 2013. **8**(6): p. 1-13.
74. Kuzmichev, A., Nishioka, K., Erdjument-Bromage, H., Tempst, P., and Reinberg, D., *Histone methyltransferase activity associated with a human multiprotein complex containing the Enhancer of Zeste protein*. Genes and Development, 2002. **16**(22): p. 2893-2905.
75. Lee, T. I., Jenner, R. G., Boyer, L. A., Guenther, M. G., Levine, S. S., Kumar, R. M., Chevalier, B., Johnstone, S. E., Cole, M. F., and Isono, K., *Control of developmental regulators by Polycomb in human embryonic stem cells*. Cell, 2006. **125**(2): p. 301-313.

76. Ben-Porath, I. and Weinberg, R. A., *The signals and pathways activating cellular senescence*. The International Journal of Biochemistry & Cell Biology, 2005. **37**(5): p. 961-976.
77. Harley, C. B., Futcher, A. B., and Greider, C. W., *Telomeres shorten during ageing of human fibroblasts*. Nature, 1990. **345**(6274): p. 458-460.
78. Allsopp, R. C., Vaziri, H., Patterson, C., Goldstein, S., Younglai, E. V., Futcher, A. B., Greider, C. W., and Harley, C. B., *Telomere length predicts replicative capacity of human fibroblasts*. Proceedings of the National Academy Science USA, 1992. **89**(21): p. 10114-10118.
79. Bodnar, A. G., Ouellette, M., Frolkis, M., Holt, S. E., Chiu, C. P., Morin, G. B., Harley, C. B., Shay, J. W., Lichtsteiner, S., and Wright, W. E., *Extension of life-span by introduction of telomerase into normal human cells*. Science, 1998. **279**(5349): p. 349-352.
80. Wang, N., Zhang, W., Cui, J., Zhang, H., Chen, X., Li, R., Wu, N., Chen, X., Wen, S., Zhang, J., Yin, L., Deng, F., Liao, Z., Zhang, Z., Zhang, Q., Yan, Z., Liu, W., Ye, J., Deng, Y., Wang, Z., Qiao, M., Luu, H. H., Haydon, R. C., Shi, L. L., Liang, H., and He, T. C., *The piggyBac transposon-mediated expression of SV40 T antigen efficiently immortalizes mouse embryonic fibroblasts (MEFs)*. PLoS One, 2014. **9**(5): p. 1-11.
81. Jha, K. K., Banga, S., Palejwala, V., and Ozer, H. L., *SV40-Mediated immortalization*. Experimental Cell Research, 1998. **245**(1): p. 1-7.
82. Chen, W. and Li, Y. P., *Generation of mouse osteoclastogenic cell lines immortalized with SV40 large T antigen*. Journal of Bone and Mineral Research, 1998. **13**(7): p. 1112-1123.
83. Frisa, Ps, Goodman, Mn, Smith, Gm, Silver, J, and Jacobberger, Jw, *Immortalization of immature and mature mouse astrocytes with SV40 T antigen*. Journal of Neuroscience Research, 1994. **39**(1): p. 47-56.
84. Abramova, N., Charniga, C., Goderie, S. K., and Temple, S., *Stage-specific changes in gene expression in acutely isolated mouse CNS progenitor cells*. Developmental Biology, 2005. **283**(2): p. 269-81.
85. Aumailley, M. and Smyth, N., *The role of laminins in basement membrane function*. Journal of Anatomy, 1998. **193**(01): p. 1-21.
86. Zaragosi, Le., Ailhaud, G., and Dani, C., *Autocrine fibroblast growth factor 2 signaling is critical for self - renewal of human multipotent adipose - derived stem cells*. Stem Cells, 2006. **24**(11): p. 2412-2419.
87. Pettmann, B., Labourdette, G., Weibel, M., and Sensenbrenner, M., *The brain fibroblast growth factor (FGF) is localized in neurons*. Neuroscience Letters, 1986. **68**(2): p. 175-80.
88. Gensburger, C., Labourdette, G., and Sensenbrenner, M., *Brain basic fibroblast growth factor stimulates the proliferation of rat neuronal precursor cells in vitro*. FEBS Letters, 1987. **217**(1): p. 1-5.
89. Parmar, M., Skogh, C., Bjorklund, A., and Campbell, K., *Regional specification of neurosphere cultures derived from subregions of the embryonic telencephalon*. Molecular and Cellular Neuroscience, 2002. **21**(4): p. 645-56.

90. Weise, B., Janet, T., and Grothe, C., *Localization of bFGF and FGF-receptor in the developing nervous system of the embryonic and newborn rat*. Journal Neuroscience Research, 1993. **34**(4): p. 442-453.
91. Seghezzi, G., Patel, S., Ren, C. J., Gualandris, A., Pintucci, G., Robbins, E. S., Shapiro, R. L., Galloway, A. C., Rifkin, D. B., and Mignatti, P., *Fibroblast growth factor-2 (FGF-2) induces vascular endothelial growth factor (VEGF) expression in the endothelial cells of forming capillaries: an autocrine mechanism contributing to angiogenesis*. The Journal of Cell Biology, 1998. **141**(7): p. 1659-1673.
92. Darland, D. C. and D'amore, P. A., *Blood vessel maturation: vascular development comes of age*. Journal of Clinical Investigation, 1999. **103**(2): p. 157-8.
93. Sun, J., Sha, B., Zhou, W., and Yang, Y., *VEGF-mediated angiogenesis stimulates neural stem cell proliferation and differentiation in the premature brain*. Biochemical and Biophysical Research Communications, 2010. **394**(1): p. 146-152.
94. Uchimura, K., Morimoto-Tomita, M., Bistrup, A., Li, J., Lyon, M., Gallagher, J., Werb, Z., and Rosen, S. D., *HSulf-2, an extracellular endoglucosamine-6-sulfatase, selectively mobilizes heparin-bound growth factors and chemokines: effects on VEGF, FGF-1, and SDF-1*. BMC Biochemistry, 2006. **7**: p. 1-13.
95. Nagamine, S., Koike, S., Keino-Masu, K., and Masu, M., *Expression of a heparan sulfate remodeling enzyme, heparan sulfate 6-O-endosulfatase sulfatase FP2, in the rat nervous system*. Developmental Brain Research, 2005. **159**(2): p. 135-143.
96. Palmer, T. D., Markakis, E. A., Willhoite, A. R., Safar, F., and Gage, F. H., *Fibroblast growth factor-2 activates a latent neurogenic program in neural stem cells from diverse regions of the adult CNS*. The Journal of Neuroscience, 1999. **19**(19): p. 8487-8497.
97. Reynolds, B. A., Tetzlaff, W., and Weiss, S., *A multipotent EGF-responsive striatal embryonic progenitor cell produces neurons and astrocytes*. Journal of Neuroscience, 1992. **12**(11): p. 4565-4574.
98. Speir, E., Sasse, J., Shrivastav, S., and Casscells, W., *Culture-induced increase in acidic and basic fibroblast growth factor activities and their association with the nuclei of vascular endothelial and smooth muscle cells*. Journal of Cellular Physiology, 1991. **147**(2): p. 362-373.
99. Vlodavsky, I., Folkman, J., Sullivan, R., Fridman, R., Ishai-Michaeli, R., Sasse, J., and Klagsbrun, M., *Endothelial cell-derived basic fibroblast growth factor: synthesis and deposition into subendothelial extracellular matrix*. Proceedings of the National Academy of Sciences, 1987. **84**(8): p. 2292-2296.
100. Gritti, A., Frölichsthal-Schoeller, P., Galli, R., Parati, E. A., Cova, L., Pagano, S. F., Bjornson, C. R., and Vescovi, A. L., *Epidermal and fibroblast growth factors behave as mitogenic regulators for a single multipotent stem cell-like population from the subventricular region of the adult mouse forebrain*. The Journal of Neuroscience, 1999. **19**(9): p. 3287-3297.
101. Lotz, S., Goderie, S., Tokas, N., Hirsch, S. E., Ahmad, F., Corneo, B., Le, S., Banerjee, A., Kane, R. S., Stern, J. H., Temple, S., and Fasano, C. A., *Sustained*

- levels of FGF2 maintain undifferentiated stem cell cultures with biweekly feeding.* PLoS One, 2013. **8**(2): p. 1-10.
102. Zhu, T. S., Costello, M. A., Talsma, C. E., Flack, C. G., Crowley, J. G., Hamm, L. L., He, X., Hervey-Jumper, S. L., Heth, J. A., Muraszko, K. M., Dimeco, F., Vescovi, A. L., and Fan, X., *Endothelial cells create a stem cell niche in glioblastoma by providing NOTCH ligands that nurture self-renewal of cancer stem-like cells.* Cancer Research, 2011. **71**(18): p. 6061-6072.
 103. Imayoshi, I., Sakamoto, M., Yamaguchi, M., Mori, K., and Kageyama, R., *Essential roles of Notch signaling in maintenance of neural stem cells in developing and adult brains.* The Journal of Neuroscience, 2010. **30**(9): p. 3489-3498.
 104. Androutsellis-Theotokis, A., Leker, R. R., Soldner, F., Hoepfner, D. J., Ravin, R., Poser, S. W., Rueger, M. A., Bae, S. K., Kittappa, R., and McKay, R. Dg., *Notch signalling regulates stem cell numbers in vitro and in vivo.* Nature, 2006. **442**(7104): p. 823-826.
 105. Li, D., Zhang, C., Song, F., Lubenec, I., Tian, Y., and Song, Qh., *VEGF regulates FGF-2 and TGF- β 1 expression in injury endothelial cells and mediates smooth muscle cells proliferation and migration.* Microvascular Research, 2009. **77**(2): p. 134-142.
 106. Klein, C., Butt, S. Jb., Machold, R. P., Johnson, J. E., and Fishell, G., *Cerebellum- and forebrain-derived stem cells possess intrinsic regional character.* Development, 2005. **132**(20): p. 4497-4508.
 107. Hitoshi, S., Tropepe, V., Ekker, M., and Van Der Kooy, D., *Neural stem cell lineages are regionally specified, but not committed, within distinct compartments of the developing brain.* Development, 2002. **129**(1): p. 233-244.
 108. Li, E., Bestor, T. H., and Jaenisch, R., *Targeted mutation of the DNA methyltransferase gene results in embryonic lethality.* Cell, 1992. **69**(6): p. 915-926.
 109. Fan, G., Beard, C., Chen, R. Z., Csankovszki, G., Sun, Y., Siniaia, M., Biniszkiwicz, D., Bates, B., Lee, P., and Kühn, R., *DNA hypomethylation perturbs the function and survival of CNS neurons in postnatal animals.* The Journal of Neuroscience, 2001. **21**(3): p. 788-797.
 110. Fan, G., Martinowich, K., Chin, M. H., He, F., Fouse, S. D., Hutnick, L., Hattori, D., Ge, W., Shen, Y., Wu, H., Ten Hoeve, J., Shuai, K., and Sun, Y. E., *DNA methylation controls the timing of astrogliogenesis through regulation of JAK-STAT signaling.* Development, 2005. **132**(15): p. 3345-3356.
 111. Takizawa, T., Nakashima, K., Namihira, M., Ochiai, W., Uemura, A., Yanagisawa, M., Fujita, N., Nakao, M., and Taga, T., *DNA methylation is a critical cell-intrinsic determinant of astrocyte differentiation in the fetal brain.* Developmental Cell, 2001. **1**(6): p. 749-758.
 112. Schneider, L. and D'adda Di Fagagna, F., *Neural stem cells exposed to BrdU lose their global DNA methylation and undergo astrocytic differentiation.* Nucleic Acids Research, 2012. **40**(12): p. 5332-5342.

113. Salem, C. E., Markl, I. Dc., Bender, C. M., Gonzales, F. A., Jones, P. A., and Liang, G., *PAX6 methylation and ectopic expression in human tumor cells*. International Journal of Cancer, 2000. **87**(2): p. 179-185.
114. Corley, M. and Kroll, K., *The roles and regulation of Polycomb complexes in neural development*. Cell and Tissue Research, 2015. **359**(1): p. 65-85.
115. Viré, E., Brenner, C., Deplus, R., Blanchon, L., Fraga, M., Didelot, C., Morey, L., Van Eynde, A., Bernard, D., and Vanderwinden, Jm., *The Polycomb group protein EZH2 directly controls DNA methylation*. Nature, 2006. **439**(7078): p. 871-874.
116. Pasini, D., Bracken, A. P., Jensen, M. R., Denchi, E. L., and Helin, K., *Suz12 is essential for mouse development and for EZH2 histone methyltransferase activity*. The EMBO journal, 2004. **23**(20): p. 4061-4071.